LETTER FROM THE EDITOR

We have mostly longer pieces for you in this issue, with a heavy emphasis on calculus and probability.

Our lead article is a fascinating survey of a very important topic: How do we measure the extent of segregation in a large population? Social scientists have taken a serious interest in this question since at least 1928, when sociologist Ernest Burgess published a seminal study of racial segregation in American cities. A survey of then available indices for quantifying segregation published by Duncan and Duncan in 1955 concluded that none were adequate. The field has progressed since then, as lucidly explained by David Hunter and Chisondi Warioba. Mathematically the paper involves some clever applications of multivariable calculus, and I know I will try to work in some of this material the next time I teach that course.

The multivariable calculus theme continues with Steven Krantz's article. He considers the problem of defining the concept of a "holomorphic function." Introductory texts in complex variables typically define holomophicity in terms of the complex derivative. There is nothing wrong with this, but it is not necessarily the most perspicuous approach with regard to the further development of complex function theory. Krantz suggests an alternative approach based on Green's theorem. I must confess that even after twenty years as a professional mathematician, I still often blanch at an article with too many integral signs. But Krantz's writing is so readable that I positively enjoyed them in this case.

David Burton and John Coleman explore a different question from calculus. Everyone knows that a decreasing exponential function has an invariant half-life. Is this property characteristic of exponential functions, or are there also non-exponential functions with the same property? The answer turns out to be the latter, as Burton and Coleman explain.

With the article by Michael Veatch, we turn to probability and combinatorics. He shows, once again, that topics inspired by games and puzzles often lead to surprisingly rich mathematics. Veatch analyzes the dice-rolling game TENZI, the modeling of which leads to a fascinating use of Markov chains. Kaity Parsons, Peter Tingley, and Emma Zajdela also consider a dice-rolling game, but this time with the intent of modeling poker. Their investigations lead them to questions in game theory.

Finally, Eduardo Sáenz de Cabezón and Juan Luis Varona prove an intriguing result about the sums of the reciprocals of "pandigital numbers." Never heard of pandigital numbers? Neither had I before reading this fascinating note, so do be sure to have a look.

We close with our usual selection of Proofs Without Words, Problems, and Reviews, as well as an article about the 2020 International Mathematical Olympiad. Fun for the whole family, or at least that subset of the family that enjoys mathematics.

Jason Rosenhouse, Editor

Math. Mag. **94** (2021) 162. doi:10.1080/0025570X.2021.1909339

Segregation Surfaces

DAVID J. HUNTER
Westmont College
Santa Barbara, CA 93108
dhunter@westmont.edu

CHISONDI WARIOBA
Westmont College
Santa Barbara, CA 93108
cwarioba@westmont.edu

Over the past half century, social scientists have devised a clever assortment of tools to measure the nature and extent of segregation [6]. Usually, a segregation measurement takes the form of a number, or *index*, which quantifies the isolation and clustering of groups defined by race, income, education, or other factors. Numerical indices are handy because they can give us ways to track changes in a neighborhood over time, and they allow for comparisons among different regions.

However, numerical summary statistics alone are limited when it comes to finding geometric patterns of segregation in two-dimensional data. In this note, we use some familiar ideas from third-semester calculus to extend the machinery behind some commonly used segregation indexes. We will see how segregation patterns can be represented by a surface, and how the geometric properties of these surfaces reveal ways that our cities and towns are divided.

Numerical measures of segregation

In order to define a segregation measure, we assume that we have data describing the population within a particular geographic region, including the locations of where people live. For simplicity, we will regard the population as being split into two sets A and B, where B is the complement of A (e.g., white/nonwhite, above/below median income). Most of the measures we consider below can be extended to more than two groups.

One of the earliest measures of segregation to become widely adopted is the *index of dissimilarity* of Duncan and Duncan [5]. The definition of this index requires a partition of the region in question into k subsets. Typically, this partition is defined by census tracts or block groups. For each subset of this partition, let a_i be the population of group A residing in the subset, and let b_i be the population of group B, where $1 \le i \le k$. Denote the total populations of groups A and B by N_A and N_B, respectively. The index of dissimilarity D is then given by summing the absolute differences of the proportions of each group living in each subset.

$$D = \frac{1}{2} \sum_i \left| \frac{a_i}{N_A} - \frac{b_i}{N_B} \right| \tag{1}$$

Math. Mag. **94** (2021) 163–172. doi:10.1080/0025570X.2021.1908044
MSC: 91D20

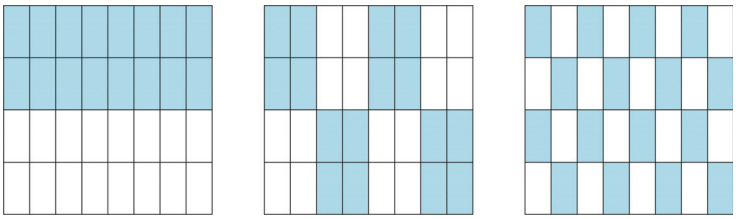

Figure 1 Three different segregation patterns with the same index of dissimilarity.

If the two groups are evenly distributed, then we would expect to see similar proportions of each in every subset, resulting in a value of D near zero. On the other hand, if the region is completely segregated, each subset would contain zero of one group, so the above summation would simply tally up the proportions of each, resulting in $D = 1$.

The index of dissimilarity has two glaring weaknesses. First, it is highly sensitive to how the subsets are defined. A different allocation of census tracts could result in a different value of D. Second, it suffers from the so-called checkerboard problem [**12**]. To illustrate this second issue, consider the three different segregation patterns in Figure 1. Suppose that $N_A = N_B$ and that each of the 32 rectangular subsets contains the same number of residents. For a fixed proportion p, suppose that p of each shaded subset is from group A and $1 - p$ is from group B, while p of each non-shaded region is from group B and $1 - p$ from group A. It is easy to check that $D = |2p - 1|$ in all three cases, even though the first pattern seems objectively more segregated than the third.

To address these two weaknesses, O'Sullivan and Wong [**13**] propose a generalization of D using surfaces. Let $a(x, y)$ and $b(x, y)$ be two-dimensional probability density functions describing the distribution of groups A and B, respectively, in our region R. The segregation index S is then defined as

$$S = 1 - \frac{V_\cap}{V_\cup}, \tag{2}$$

where $V_\cap$ and $V_\cup$ are the volumes of the intersection and union of the solid regions above the xy-plane and below the surfaces $z = a(x, y)$ and $z = b(x, y)$. In other words, these volumes are given by

$$V_\cap = \iint_R \min(a, b)\, dA \quad \text{and} \quad V_\cup = \iint_R \max(a, b)\, dA. \tag{3}$$

If groups A and B are identically distributed, then $V_\cap$ will equal $V_\cup$, resulting in $S = 0$. However, more segregation will tend to reduce the volume $V_\cap$ under both surfaces relative to the total volume $V_\cup$, yielding values of S closer to 1.

For example, consider the segregation patterns in Figure 1, letting the region R be the square $[0, 1] \times [0, 1]$, and suppose that $0.5 < p \leq 1$. Suppose that $a(x, y)$ is a piecewise constant density function, taking the value $2p$ in the shaded regions and $2(1 - p)$ in the non-shaded regions. (The top row of graphs in Figure 2 shows the density functions $a(x, y)$ corresponding to the three segregation patterns.) Similarly, let $b(x, y)$ take the value $2(1 - p)$ in the shaded regions and $2p$ in the non-shaded regions. Using Equations (2) and (3), we obtain

$$V_\cap = 2(1 - p) \qquad \text{and} \qquad V_\cup = 2p,$$

giving $S = (2p - 1)/p$ for all three patterns. So it appears that this measurement also has the checkerboard problem.

However, it is somewhat unreasonable to assume that the true density functions that describe our population would be piecewise constant. Instead, O'Sullivan and Wong

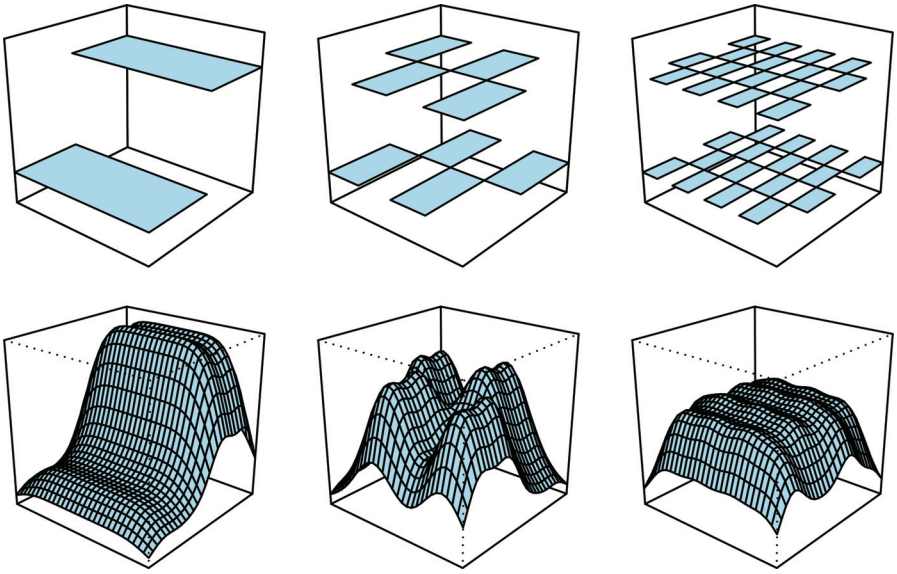

Figure 2 The top row shows the three piecewise constant density functions corresponding to the patterns in Figure 1. The bottom row shows smoothed versions obtained using kernel density estimation.

approximate a and b by smooth surfaces $\hat{a}$ and $\hat{b}$ using *kernel density estimation*. A kernel density estimate is a smooth function that approximates a probability density based on a set of data points [**18**]. In our case, this estimate is a weighted sum of 32 bivariate normal distributions, each centered on one of 32 rectangles that make up our region. There are lots of different ways to construct kernel density estimates; see and Deng and Wickham [**4**] Wand and Jones [**18**] for details.

Figure 2 shows the graphs of density functions for the three patterns in Figure 1, using $p = 0.8$. The top row shows the corresponding three piecewise-constant density functions a, while the bottom row shows the smoothed versions $\hat{a}$. (The functions b and $\hat{b}$ are similar.) The smoothing has the effect of eliminating the checkerboard problem. While Equations (2) and (3) yield $S = 0.75$ using all three piecewise-constant versions of a and b, their smooth counterparts $\hat{a}$ and $\hat{b}$ give S-values of 0.68, 0.37, and 0.05, respectively.

It is important to note that these results are not uniquely determined. The surfaces, and the values of S they produce, depend on the choice of kernel estimator and on adjustable smoothing parameters. More on this later.

There are many other measures of segregation. Good summaries of the literature include Harris and Johnson [**6**], Reardon and O'Sullivan [**15**], and Yao, Wong, Bailey, and Minton [**19**]. All of these measures summarize the segregation patterns in a given region by a number—usually an index between zero and one. In the next section, we will consider how to go beyond these numerical summaries and create visualizations of segregation patterns using the geometric properties of the surfaces that define some of the commonly used segregation indexes.

Drawing segregation boundaries

Given geographic data on where the members of two groups A and B live, is it possible to discern boundaries between neighborhoods where the residents are mostly from group A and neighborhoods where the majority are from group B? In terms of

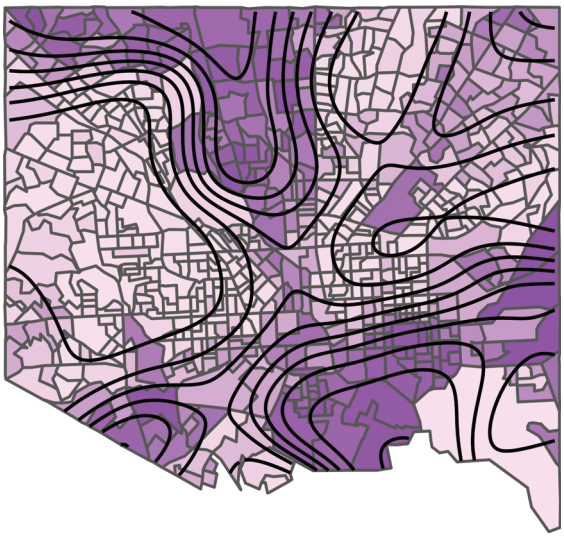

Figure 3 Choropleth map of Baltimore, Maryland, with superimposed contours. Census block groups are shaded according to the proportion of white residents. The contour lines show levels of the estimated conditional probability $\hat{f}(x, y)$ that a resident is white, given that the resident lives at point (x, y).

probability, we would like to determine the set of points (x, y) where, if you were to encounter a resident, the probability that the resident is from group A is 0.5. In other words, we need to calculate a conditional probability.

As above, let $a(x, y)$ and $b(x, y)$ be the probability density functions that describe the distribution of groups A and B in our region. In addition, let $u(x, y)$ be the probability density function that describes the distribution of the entire population U, the disjoint union of A and B. Using Bayes' theorem, the conditional probability $f(x, y)$ that a resident belongs to group A, given that the resident lives at point (x, y), is given by

$$f(x, y) = \frac{|A| \cdot a(x, y)}{|U| \cdot u(x, y)}. \tag{4}$$

The 50% contour of $f(x, y)$ will then be the border between a majority A-neighborhood and a majority B-neighborhood.*

In practice, the functions a, b, and u can be estimated from data using kernel density estimation. Suppose that we have population counts for the n subsets in a partition of our region (e.g., census block groups). Let (x_i, y_i) be the centroids of each of these subsets, and assign weights w_i to each subset based on the population counts, such that $\sum w_i = n$. We then can estimate u as

$$\hat{u}(x, y) = \frac{1}{n} \sum_{i=1}^{n} w_i K\left(\frac{x - x_i}{h_x}, \frac{y - y_i}{h_y}\right),$$

where $K(x, y)$ is a bivariate normal kernel function, and h_x, h_y are smoothing parameters, or *bandwidths*. Estimates $\hat{a}$ and $\hat{b}$ for a and b are defined similarly, and then Equation (4) gives an estimate $\hat{f}$.

*A function similar to f appears in Reardon and O'Sullivan [**15**], though it is motivated and defined differently, and allows for a distinction between geometric proximity and sociological proximity. Their function $\tilde{\pi}_{pm}$ represents "the population composition that a person living at point p would experience in his or her local environment."

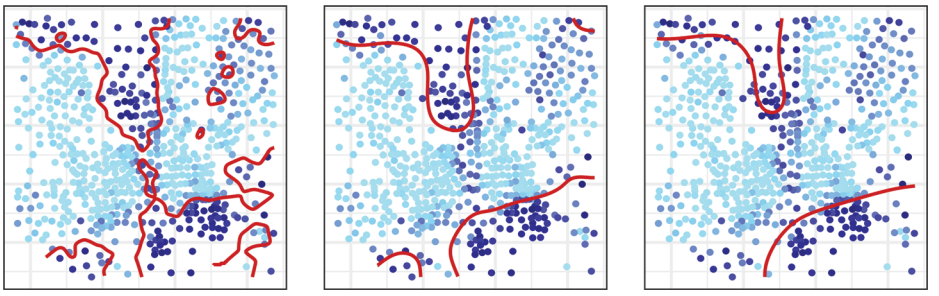

Figure 4 Fifty-percent contours of $\hat{f}$ for three choices of smoothing parameters. The left plot shows undersmoothing, while the right plot shows oversmoothing.

Figure 3 illustrates the result of this construction using census block group-level data on the proportion of white residents in Baltimore, Maryland. Each census block is shaded according to the proportion of white residents, forming a *choropleth* map. The contour lines show levels of $\hat{f}(x, y)$, which estimates the probability that a resident is white, given that the resident lives at point (x, y). Since this probability is constant along these contours, we expect each curve to pass through regions with similar shading.

The choice of smoothing parameters h_x, h_y greatly affects the geometry of the surface $z = \hat{f}(x, y)$ and its contours. Small values produce very bumpy surfaces that closely fit the data points, while large values give smooth surfaces that loosely approximate the data points. Figure 4 shows the 50% contours of $\hat{f}$ for three different choices of smoothing parameters, using the same data as in Figure 3, but with each shaded region replaced by its centroid. The plot on the left appears to be *undersmoothed*, because the very wiggly contours give neighborhood boundaries that are overly sensitive to particular data points. On the other hand, the plot on the right is *oversmoothed*, because the contours fail to capture the granularity in the data.

The segregation gradient

In addition to locating segregation boundaries, the surface $z = \hat{f}(x, y)$ can identify the rate at which population proportions change with respect to distance. In particular, the *segregation gradient* $\nabla \hat{f}(x, y)$ gives the magnitude and direction of this change.

Plotting segregation gradients on a map of a region can highlight geographic features that affect how segregated neighborhoods form. For example, Figure 5 shows racial segregation patterns in the near-west suburbs of Chicago, where A is the set of white residents, and B is the set of nonwhite residents, according to data from the 2017 American Community Survey (ACS). Areas with large segregation gradients correspond to neighborhoods where the racial composition changes markedly over a short distance. For example, the vertical green strip about a third of the way from the left is a forest preserve. The eastward pointing segregation gradients suggest that the neighborhoods to the east of this forest are predominately white, in contrast to some of the neighborhoods to the west.

The magnitude of the segregation gradient can quantify the severity of segregation in a given location. In particular, along the 50% contours that divide majority A neighborhoods from majority B neighborhoods, the segregation gradient indicates how fast these neighborhoods change from A to B. For example, Figure 6 shows two maps of income segregation in San Francisco, CA, using ACS data from 2013 and 2017.

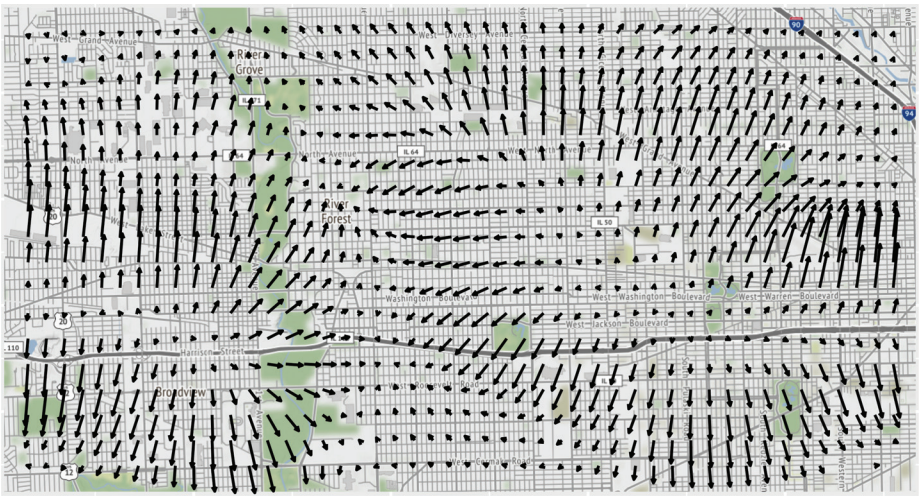

Figure 5 White/non-white segregation gradients in the near-west suburbs of Chicago. The arrows indicate the directions in which the proportion of white residents increases. The longer the arrow, the more sudden the change.

In these data sets, group A consists of residents whose income is above the county median, while group B contains residents with below-median income. The thickness of the 50% contour lines corresponds to the magnitude of the segregation gradient. Thin contour lines indicate a gradual change in the income of the residents, while thick contour lines indicate stark divisions. In both maps, the thickest contour is in the southeast corner, separating the India Basin neighborhood from the more popular Central Waterfront neighborhood to the north.

Figure 6 also shows how income segregation has changed in San Francisco from 2013 to 2017. In the 2013 plot on the left, the small closed curves enclose lower-income (group B) neighborhoods. In the 2017 data, these areas of below-median income have vanished, and the large region in the middle populated by higher-income residents has expanded. These trends in the data are consistent with anecdotal observations of gentrification in San Francisco [**14**].

Measuring segregation with gradients

In relatively integrated regions, we would expect the magnitude of the segregation gradient to be small, on average, along the 50% contours. In regions where groups A and B tend to cluster together (such as in Figure 5), the magnitude $\|\nabla \hat{f}\|$ will exhibit more variability. So we can define a new segregation index G_C by averaging the value of $\|\nabla \hat{f}\|$ along the 50% contour C of a region. Since segregation indexes are traditionally numbers between zero and one, we use the arctangent function to convert this average from a slope to an angle.

$$G_C = \frac{2}{\pi} \arctan\left(\frac{1}{\text{length}(C)} \int_C \|\nabla \hat{f}\| \, ds \right) \tag{5}$$

Applying this formula to the three segregation patterns in Figure 1, we obtain the values $G_C = 0.79$, $G_C = 0.65$, and $G_C = 0.13$, respectively.

Of course, Equation (5) only makes sense if our function $\hat{f}$ takes the value 0.5 somewhere in its domain. For example, in Figure 6, we ensure that this will happen by

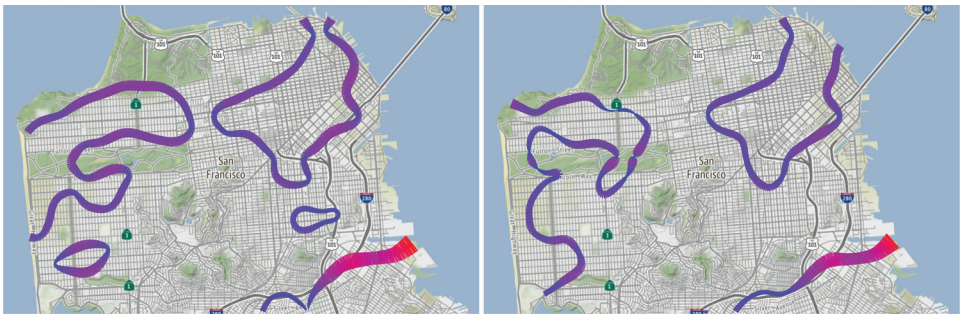

Figure 6 Gentrification in San Francisco. Income segregation patterns have changed from 2013 (left) to 2017 (right). The contours enclose neighborhoods whose residents tend to have incomes below the county median. Some of these neighborhoods have been shrinking. Thicker contours represent starker divisions.

taking groups A and B to be the same size. In a region where, say, group A is much larger than group B, and the members of group B are fairly well dispersed, there may fail to be any points on the 50% contour C. In this situation, G_C would be undefined. When applying Equation (5) to data, the lack of a contour C is usually an indication that there is not much diversity in terms of the groups A and B.

The problem of a nonexistent 50% contour can be avoided by averaging the magnitude of the gradient across the entire region, without regard to neighborhood boundaries. Doing so gives us G_R, a second measure of segregation.

$$G_R = \frac{2}{\pi} \arctan\left(\frac{1}{\text{area}(R)} \iint_R \|\nabla \hat{f}\| \, dA \right) \tag{6}$$

When applied to the patterns in Figure 1, Equation (6) yields $G_R = 0.26$, $G_R = 0.56$, and $G_R = 0.16$, respectively. In this case, the first segregation pattern gives us a lower value of G_R because the gradient is close to zero in the large homogeneous areas. On these artificial examples, it appears that G_R underestimates segregation in highly-divided regions with relatively few clusters of each group.

How do G_C and G_R compare when applied to real data? On a sample of 74 large, racially diverse counties in the United States, G_C and G_R show a fairly strong correlation ($r \approx 0.8$), when computed using 2017 ACS data on race (white/nonwhite). A scatterplot of these 74 observations appears in Figure 7. Regions with large values of both G_C and G_R tend to be large, established urban centers, while smaller values generally correspond to areas having a more suburban character. The unusual observations in this scatterplot illustrate the difference between G_C and G_R. For example, Denver, Colorado has several small nonwhite clusters of population, but lacks large areas with starkly defined borders. As a result, Denver has a fairly typical value of G_R, but a low G_C value. On the other side of the trend line, Riverside, California has one or two nonwhite clusters among a large swath of majority white neighborhoods, resembling a version of the first pattern in Figure 1, where G_R seems to underestimate the amount of segregation.

Caution should always be exercised when trying to quantify segregation, as there are many different types of patterns of division. Massey and Denton [**11**] propose five "dimensions" of segregation: evenness, exposure, clustering, centralization, and concentration. Discussion and revisions of this framework can be found in Brown and Chung [**2**] and Johnston, Poulsen, and Forrest [**10**]. From another perspective, Reardon and O'Sullivan [**15**] argue in favor of two orthogonal continua, clustering—evenness and isolation—exposure. A notable lack of consensus still persists in the social science

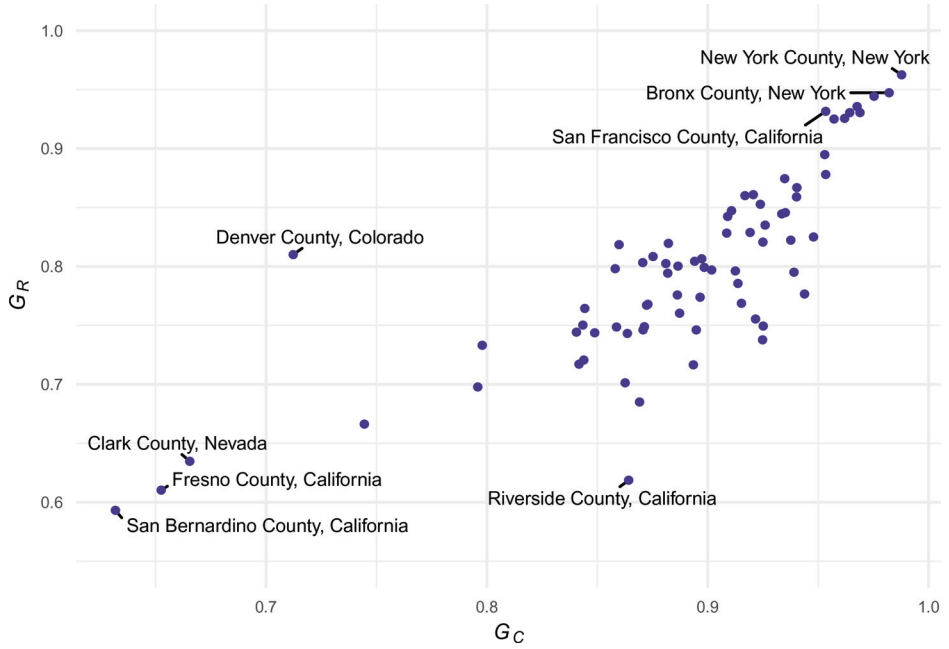

Figure 7 A scatterplot showing the correlation between G_C and G_R, when computed on 74 large, diverse US counties.

literature, and the multifaceted nature of the phenomenon has motivated a bewildering variety of measurements for it [**6**].

We can test some of these measurements on our sample of 74 counties. Table 1 shows the pairwise correlations of the gradient measures G_C and G_R, along with five other indexes: O'Sullivan and Wong's S of Equation 2, the spatial dissimilarity index $\tilde{D}$, the spatial information theory index $\tilde{H}$, and the exposure/isolation index $\tilde{P}^*$, and the Geary ratio C. Three of these, $\tilde{D}$, $\tilde{H}$, $\tilde{P}^*$, are defined in Reardon and O'Sullivan [**15**] and implemented in Hong, O'Sullivan, and Sadahiro [**7**]. Geary's C measures *spatial autocorrelation* [**3**], and is implemented in Bivand [**1**]. Since small values of C indicate that neighboring block groups tend to be similar, C is negatively correlated with the smooth dissimilarity index S, as well as to other measures of segregation.

TABLE 1: Correlation matrix for several different segregation measures, when computed on a sample of 74 large U.S. counties.

	G_C	G_R	S	$\tilde{D}$	$\tilde{H}$	$\tilde{P}^*$	C
G_C	1.0	0.8	0.6	0.0	0.1	0.2	-0.7
G_R		1.0	0.5	−0.1	0.3	0.4	-0.6
S			1.0	0.6	0.0	0.2	−0.9
$\tilde{D}$				1.0	0.1	−0.1	−0.5
$\tilde{H}$					1.0	0.5	−0.1
$\tilde{P}^*$						1.0	−0.2

Resources and questions for future investigation

All of the figures and calculations given in this note can be reproduced using the data and R code in the GitHub repository at https://github.com/djhunter/segregation. An enormous trove of ACS census data is readily available online [**16**], and convenient interfaces such as tidycensus [**17**] allow for its integration with geographic data.

Because of its interdisciplinary nature, the study of segregation naturally lends itself to student projects. Ideas for future undergraduate research problems include the following:

- All of the examples discussed above considered two groups, A and B. Invent a way of visualizing segregation patterns involving more than two groups. How could you extend the definitions of G_C and G_R to this case?
- When studying population dynamics, we generally regard data as two-dimensional. However, our definition of $\hat{f}$ could easily be modified for domains that are subsets of $\mathbb{R}$ or $\mathbb{R}^3$. Can you think of an application of segregation gradients using one- or three-dimensional data?
- In baseball, when the batter does not swing at a pitch, the home plate umpire decides whether the pitch is a ball or a strike. Ideally, umpires should call these pitches consistently. A consistent arrangement of called balls and strikes should look like a highly segregated city, with a well-defined border between strikes (group A) and balls (group B). Can segregation indexes be used to assess umpire performance? Compare these measurements with those given in Hunter [**9**].
- When computing G_C and G_R, our function $\hat{f}$ was estimated from data. Compute these indexes for families of surfaces $z = f(x, y)$ for which you have analytic formulas. Are G_C and G_R related to other quantifiable properties of these surfaces (e.g., total curvature)?
- Ultrasound images consist of two-dimensional plots of the locations of reflected sound pulses, along with their intensities. Can the methods above for finding borders between neighborhoods be used to discern outlines of objects in these images, and quantify their sharpness? Investigate using raw data.
- Huff [**8**] uses equiprobability contours of a certain surface to estimate the likelihood that residents from location (x, y) will patronize a business at a given location. Given data on where clients of a given business reside, can we apply Bayes' Theorem (as in the construction of $\hat{f}(x, y)$) to obtain a similar estimating surface? Compare this approach to Huff's model.

REFERENCES

[1] Bivand, R. (2019). spdep: Spatial dependence: weighting schemes, Statistics. R package version 1.1-3. Online at: https://cran.r-project.org/web/packages/spdep/

[2] Brown, L. A., Chung, S.-Y. (2006). Spatial segregation, segregation indices and the geographical perspective. *Popul. Space Place.* 12(2): 125–143. doi:10.1002/psp.403

[3] Cliff, A. D., Ord, J. K. (1982). *Spatial Processes: Models and Applications*. London: Pion.

[4] Deng, H., Wickham, H. (2011). Density estimation in R. https://vita.had.co.nz/papers/density-estimation.pdf

[5] Duncan, D., Duncan, B. (1955). A methodological analysis of segregation indexes. *Amer. Sociol. Rev.* 20(2): 210–217. doi:10.2307/2088328

[6] Harris, R., Johnson, R. (2018). Measuring and modelling segregation—new concepts, new methods and new data. *Environ. Plan. B: Urban Analyt. City Sci.* 45(6): 999–1002. doi:10.1177/2399808318808889

[7] Hong, S., O'Sullivan, D., Sadahiro, Y. (2014). Implementing spatial segregation measures in R. *PLoS One*. 9(11): e113767. doi: 10.1371/journal.pone.0113767

[8] Huff, D. L. (1963). A probabilistic analysis of shopping center trade areas. *Land Econ.* 39(1): 81–90. doi: 10.2307/3144521

[9] Hunter, D. (2018). New metrics for evaluating home plate umpire consistency and accuracy. *J. Quantit. Anal. Sports.* 14(4): 159–172. doi:10.1515/jqas-2018-0061

[10] Johnston, R., Poulsen, M., Forrest, J. (2007). Ethnic and racial segregation in U.S. metropolitan areas, 1980–2000. *Urban Aff. Rev.* 42(4): 479–504. doi:10.1177/1078087406292701

[11] Massey, D., Denton, N. (1988). The dimensions of residential segregation. *Social Forces.* 67(2): 281–315. doi:10.1093/sf/67.2.281

[12] Morrill, R. (1991). On the measure of spatial segregation. *Geogr. Res. Forum.* 11: 25–36.

[13] O'Sullivan, D., Wong, D. (2007). A surface-based approach to measuring spatial segregation. *Geogr. Anal.*, 39(2): 14–168. doi:10.1111/j.1538-4632.2007.00699.x

[14] Pogash, C. (2015). Gentrification spreads an upheaval in San Francisco's mission district. *The New York Times*. May 22, 2015, Section A, p. 10.

[15] Reardon, S., O'Sullivan, D. (2004). Measures of spatial segregation. *Sociol. Methodol.* 34: 121–162. doi:10.1111/j.0081-1750.2004.00150.x

[16] U. S. Census Bureau. (2019). *American Community Survey 5-year estimates.* https://www.census.gov/programs-surveys/acs

[17] Walker, K., Eberwein, K., Herman, K. (2019). tidycensus: load US Census Boundary and Attribute Data as `tidyverse` and `sf`-Ready Data Frames. R package version 0.9.2. https://cran.r-project.org/web/packages/tidycensus/

[18] Wand, M. P., Jones, M. C. (2011). *Kernel smoothing*, London: Chapman & Hall.

[19] Yao, J., Wong, D. W. S., Bailey, N., Minton, J. (2018). Spatial segregation measures: a methodological review. *Tijdschrift Voor Economische En Sociale Geografie.* 110(3): 235–250. doi:10.1111/tesg.12305

Summary. Social scientists have developed dozens of different ways to quantify urban segregation with numerical statistics. Behind the scenes, some of these measurements are defined using multivariable functions that model the distribution of various groups in a geographical region. Using Bayes' theorem and kernel density estimation, we describe how to summarize population data in terms of smooth, two-dimensional surfaces. These surfaces give us ways of identifying neighborhood boundaries and visualizing segregation patterns. We also propose two new segregation measures using some familiar tools from third-semester calculus. Applications to United States census data are included.

DAVID J. HUNTER (MR Author ID: 633493) received his Ph.D. from the University of Virginia, Charlottesville in 1997 and now teaches mathematics and computer science at Westmont College, Santa Barbara, CA. As a transplanted Chicagoan living in Santa Barbara, he loves to walk around cities and hike in the mountains.

CHISONDI WARIOBA is a senior at Westmont College, Santa Barbara, CA, triple majoring in Physics, Chemistry, and Biology. He will be pursuing a Ph.D., in Medical Physics at the University of Chicago after graduation. He enjoys playing soccer, listening to music, and rewatching the original *Star Wars* movies.

An Analysis of TENZI Using Combinatorics and Markov Chains

MICHAEL H. VEATCH
Gordon College
Wenham, MA 01984
mike.veatch@gordon.edu

The game of TENZI sounds deceptively simple. Each player gets 10 dice. Then everyone rolls as fast as they can, setting aside the dice they want to keep. The first person to get all their dice on the same number wins. It is advertised as "the world's fastest game." How fast is it? That is, on average how many rolls does it take to get 10 matches? To answer that requires knowing the optimal strategy. For most configurations of dice, the following strategy is compelling: keep a largest group (LG) of dice showing the same number, pick up all the other dice and roll them together (we count that as one roll). Call this the LG strategy. However, if there are five pairs showing (so that the LG strategy keeps one pair), it is conceivable that more than one pair should be kept. We will show that even in this configuration the LG strategy minimizes the average number of rolls.

Other strategies may be of interest because of the human factor of how quickly one can pick up and roll the remaining dice. For example, early in the game players are deciding which number(s) to keep and which to pick up. Making this decision may reduce the number of rolls, but it takes time. Another consideration is visual processing speed: Separating the sixes might be faster than separating fours. We analyze alternative strategies that may be faster to play to see how their average number of rolls compare. These "faster to play" strategies are also much simpler to analyze and lay some groundwork that is needed to analyze the LG strategy.

The expected number of rolls for several strategies is shown in Table 1. Rolling one die at a time is obviously slow. The "fixed goal" strategy picks a goal in advance, e.g., keep the sixes until all dice are sixes. It is fairly close to optimal. The probabilistic analysis is introduced as an extension of a deterministic approximation and a connection made with order statistics. Next, a refinement that picks the goal after the first roll is analyzed using the maximum of a multinomial distribution. A longer but straightforward derivation from basic combinatorics is also provided. It is nearly optimal. Finally, the LG strategy is analyzed using similar methods. We verify that the LG strategy is optimal by showing that the optimization reduces to a smaller dynamic program that we solve numerically.

Strategy	Expected number of rolls
One die at a time	55
Fixed goal	16.56
Approximation of fixed goal	17.56
Goal fixed after first roll	15.35
LG	15.33

TABLE 1: Results for various strategies.

The number of rolls in TENZI with the fixed goal strategy is a first passage time problem in the study of Markov chains; see [**11**]. This strategy is analyzed in an under-

Math. Mag. **94** (2021) 173–185. doi:10.1080/0025570X.2021.1916295
MSC: 60-01

graduate thesis by Barhite [1] using a Markov chain approach. TENZI is also mentioned with this strategy in [6]. We offer two simpler analyses of this strategy. Optimizing over all strategies is an example of a Markov decision process [8]. Analysis of games involving repeated dice rolls can also be found in [4] and [7]. TENZI can be thought of as a probability model of how a group of people reach consensus about, say, what movie to watch, where people randomly change their preferences each time they are asked. Such an interpretation connects probability with social choice theory, which is reviewed in [10].

The fixed goal strategy: deterministic approximation

In this section we consider the simple strategy of picking a number, say six, before rolling. Only dice that show a six are kept; the rest are rolled again. Call six the goal. Let N_k be the number of rolls from when there are k dice remaining until all dice match the goal. A player's number of rolls is N_{10}. We will find its mean, or expectation

$$E[N_{10}] = \sum_{n=1}^{\infty} n P(N_{10} = n). \tag{1}$$

Note that all remaining dice are rolled together.

As a momentary digression, consider the strategy of rolling one die at a time and matching the first die rolled. Call the number of rolls under this strategy N^S. Since one die is rolled, only N_1 is needed. Each roll has probability $1/6$ of matching, $P(N_1 = n) = \frac{1}{6}(\frac{5}{6})^{n-1}$, $n = 1, 2, 3, \ldots$ (known as the geometric distribution), and $E[N_1] = 6$. Summing the number of rolls of each of the dice, $E[N^S] = 1 + 9E[N_1] = 55$, where the 1 is for the first die. The distribution of $N^S - 1$ (which we avoided) is called negative binomial with probability of success $p = 1/6$ and number of successes $r = 9$. Its mean is $r/p = 54$, agreeing with the calculation above.

Before finding $E[N_{10}]$, we will quickly approximate it using a continuous deterministic model. Let M_k be the number of matches when k dice are rolled. Its mean is $k/6$. Our approximation replaces M_k by its mean and allows the number of dice to be continuous, not just integers. Let $n(k)$ be the number of rolls when there are k dice remaining in the continuous approximation. It obeys the recursion

$$n(k) = 1 + n\left(\frac{5}{6}k\right). \tag{2}$$

The continuous approximation becomes less accurate as k gets smaller. We will use equation (2) until fewer than two dice remain, then interpolate linearly between $E[N_1] = 6$ (found above) and $E[N_2] = 96/11$, which is also easy to find. We want the smallest integer t for which $10(5/6)^t \le 2$, or $t \ge \ln 5/\ln(6/5) = 8.83$, so $t = 9$. Applying equation (2) nine times,

$$\begin{aligned} n(10) &= 9 + n(10(5/6)^9) = 9 + n(1.94) \\ &\approx 9 + 0.94E[N_2] + 0.06E[N_1] = 17.56. \end{aligned}$$

The fixed goal strategy: exact analysis

To find $E[N_{10}]$ we need the probability distribution of M_k, not just its mean. Its distribution is binomial with k trials and probability of success $p = 1/6$. Denote this

Dice	1	2	3	4	5
Expected rolls	6	8.73	10.55	11.93	13.02
Dice	6	7	8	9	10
Expected rolls	13.94	14.72	15.41	16.02	16.56

TABLE 2: Fixed goal strategy.

probability mass function

$$b(m; k, p) = P(M_k = m) = C_m^k p^m (1-p)^{k-m}, m = 0, \ldots, k \tag{3}$$

where C_m^k is the combinations of k things taken m at a time and write n_k for $E[N_k]$. The probabilistic analogue to equation (2) is

$$n_k = 1 + \sum_{m=0}^{k-1} P(M_k = m) n_{k-m}. \tag{4}$$

For example, $n_1 = 1 + \frac{5}{6}n_1$, so $n_1 = 6$, and $n_2 = 1 + \frac{10}{36}n_1 + \frac{25}{36}n_2$, with solution $n_2 = 96/11$. Although n_k appears on both sides of equation (4), rearranging and using equation (3) gives the explicit

$$n_k = \frac{6^k + \sum_{m=1}^{k-1} C_m^k 5^{k-m} n_{k-m}}{6^k - 5^k}. \tag{5}$$

Values of n_k are shown in Table 2. The deterministic approximation is within 6% of the exact answer, providing a simple approximation for a fairly good strategy.

One justification for replacing M_k by its mean in the previous section is the Strong Law of Large Numbers [**9**]: writing M_k as the sum of indicator random variables, one for each die, $\lim_{k\to\infty} M_k/k = 1/6$ with probability one. However, with convergence at rate $1/\sqrt{k}$, one would think a large k is needed for accuracy. The reason (2) is accurate when used for small k is that $E[N_k|M_k]$ is nearly linear in M_k. Indeed, for a linear function $L(X)$, $E[L(X)] = L(E[X])$, i.e., one can replace the random variable by its mean.

Another view of the fixed goal strategy

The previous section analyzed the fixed goal strategy using recurrence over the number of dice remaining. Another approach is to consider each die separately. Let T_d be the number of rolls of die d to get the goal (e.g., to roll a six). They are independently identically distributed with the same geometric distribution as N_1. Starting with k dice, they all match the goal after

$$N_k = \max\{T_1, \ldots, T_k\}$$

rolls. The distribution of the maximum, known as the first order statistic (see [**9**]), is

$$P(N_k \le t) = [P(T \le t)]^k = [1 - (5/6)^t]^k. \tag{6}$$

Computing the mean using equation (1) is difficult, so we use the alternative formula for an integer-valued, non-negative random variable: $E[N] = \sum_{t=0}^{\infty} P(N > t)$ (see [**9**] Section 5.2). Starting with equation (6),

$$n_k = \sum_{t=0}^{\infty} \left(1 - [1 - (5/6)^t]^k\right).$$

Now expand the expression in brackets with the binomial theorem

$$n_k = \sum_{t=0}^{\infty} \left(1 - \sum_{j=0}^{k} C_j^k [(-5/6)^t]^j \right).$$

Cancel the $j = 0$ term and interchange the order of summation:

$$n_k = \sum_{j=1}^{k} (-1)^{j-1} C_j^k \sum_{t=0}^{\infty} [(5/6)^j]^t.$$

The inner summation is a geometric series. Evaluating it

$$n_k = \sum_{j=1}^{k} (-1)^{j-1} C_j^k \frac{1}{1 - (5/6)^j}.$$

Although this looks different than equation (5), it gives the same results. There are also nice approximations for the maximum of geometric random variables, such as [3].

The first roll

Under the LG strategy, all we need to know about the dice after any roll is the size of the LG. Let X_i^k be the number of i's among k dice that are rolled. After the first roll, the number of dice to be rolled again is

$$D = 10 - \max_{i=1,\ldots,6} X_i^{10} \tag{7}$$

To find the distribution of D, extend the definition above to $X_i^{k,t}$ for t-sided dice. Then $X_i^{k,t}$ has a binomial distribution (3) with k trials and probability of success $1/t$. Taken together, $\{X_i^{k,t}\}$ have a symmetric multinomial distribution. It results from any experiment where k objects are randomly placed into t bins. We need the distribution of its maximum, addressed in [2]. Let $F(m; k, t) = P(\max_{i=1,\ldots,t} X_i^{k,t} \le m)$ be its distribution function. The recursive formula

$$F(m; k, t) = \sum_{j=0}^{m} C_j^k (1/t)^j (1 - 1/t)^{k-j} F(m; k - j, t - 1) \tag{8}$$

is given in [5]. The initial values are $f(1; 1, t) = 1$ and $f(k; k, 1) = 1$, where f is the probability mass function, found by subtracting. Apply equations (7) and (8) with $k = 10$, $t = 6$; the probability mass function is tabulated in Table 3. A method of computing these results using only counting arguments is given in Appendix A.

Dice	0	1	2	3	4
Probability	1E-7	5E-6	0.0001	0.0015	0.0130
Dice	5	6	7	8	
Probability	0.0781	0.3105	0.5293	0.0675	

TABLE 3: Distribution of the number of unmatched dice after the first roll.

Changing goals

This section combines the LG strategy for the first roll with two strategies for successive rolls: keep the goal from the first roll, or continue to use the LG strategy. Because they only keep rolls that all match, the progress of the game can be described by the number of dice to be rolled again. Figure 1 shows the possible transitions from one roll to the next. Associated with each arrow is the probability of that transition occurring when rolling the given number of dice and using a given strategy.

First, suppose that after the first roll the goal is never changed. After the first roll, the fixed goal mean number of rolls n_k from equation (5) applies, so

$$E[N_{10}] = 1 + \sum_{k=1}^{8} P(D = k) n_k.$$

Using Tables 2 and 3, the mean number of rolls is $E[N_{10}] = 15.35$.

Now consider the LG strategy. Assume that if there is a tie for the LG, the goal does not change. The solid arrows in Figure 1 represent transitions that occur without changing the goal; dashed arrows represent transitions where the goal could change. Let p_{kl} be the probability that the next state, or number of dice, is l given that the current state is k. Using the same reasoning as equation (4),

$$n_k = 1 + \sum_{l=1}^{k} p_{kl} n_l = \left(1 + \sum_{l=1}^{k-1} p_{kl} n_l\right) / (1 - p_{kk}), \tag{9}$$

where n_k now represents the mean number of rolls with k dice *under the LG strategy*. Under the fixed goal strategy,

$$p_{kl} = P(M_k = k - l) \tag{10}$$

($k - l$ matches leaves l dice). For $k \leq 5$, the goal cannot change, so equation (10) applies to the LG strategy.

It remains to find p_{kl} for $k = 6, 7, 8$. Recall that X_i^k has probability mass function $b(\cdot; k, 1/6)$ from equation (3) and that $\max_{i=1,\ldots,6} X_i^k$ has distribution function $F(\cdot; k, 6)$ and probability mass function $f(\cdot; k, 6)$. Suppose the goal is six, so that $M_k = X_6^k$. The conditional distribution of $\max_{i=1,\ldots,5} X_i^k$ given $X_6^k = l$ can be thought of as rolling $k - l$ five-sided dice. Let Y_i^{k-l}, $i = 1, \ldots, 5$ be these five-sided dice counts, i.e., a symmetric multinomial distribution with parameters $k - l$ and 5. Then $\max_{i=1,\ldots,5} Y_i^{k-l}$ has distribution function $F(\cdot; k - l, 5)$. The computation begins by partitioning on whether the goal changes and on the number of matches with the current goal. For $k = 6$, 7, or 8

$$p_{kl} = P(X_6^k = k - l \text{ and don't change}) + P(\max_{i=1,\ldots,5} X_i^k = 10 - l \text{ and change})$$

$$= P(X_6^k = k - l \cap X_i^k \leq 10 - l, i \leq 5) + \sum_{j=0}^{k-l-1} P(X_6^k = j \cap \max_{i \leq 5} X_i^k = 10 - l).$$

Now use the multiplicative rule and the random variables Y for the conditional distribution:

$$p_{kl} = P(X_6^k = k - l) P(Y_i^l \leq 10 - l, i \leq 5) + \sum_{j=0}^{k-l-1} P(X_6^k = j) P(\max_i Y_i^{k-j} = 10 - l)$$

$$= b(k - l; k, 1/6) F(10 - l; l, 5) + \sum_{j=0}^{k-l-1} b(j; k, 1/6) f(10 - l; k - j, 5). \tag{11}$$

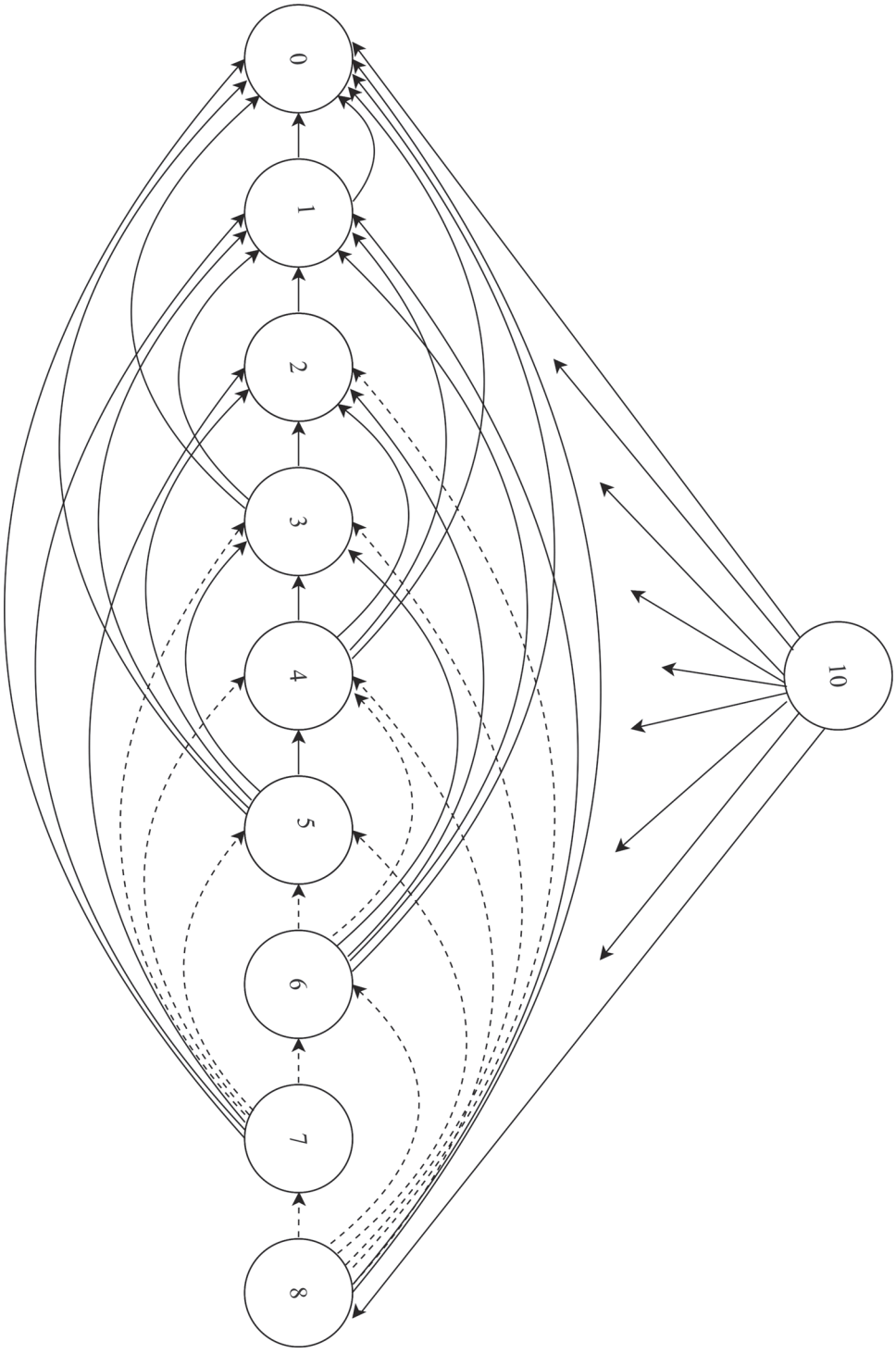

Figure 1 Transitions of the number of dice rolled; for dotted lines the goal may change.

Note that equation (11) expresses the transition probabilities in terms of binomial and multinomial probabilities. Some of these probabilities are 0 or 1. For $k = 8$,

$$p_{87} = b(1; 8, 1/6)F(3; 7, 5) + b(0; 8, 1/6)f(3; 8, 5)$$

$$p_{86} = b(2; 8, 1/6)F(4; 6, 5) + b(1; 8, 1/6)f(4; 7, 5) + b(0; 8, 1/6)f(4; 8, 5)$$

have every term, but

$$p_{85} = b(3; 8, 1/6) + b(2; 8, 1/6)f(5; 6, 5) + b(1; 8, 1/6)f(5; 7, 5) + b(0; 8, 1/6)f(5; 8, 5).$$

$$p_{84} = b(4; 8, 1/6) + b(2; 8, 1/6)f(6; 6, 5) + b(1; 8, 1/6)f(6; 7, 5) + b(0; 8, 1/6)f(6; 8, 5)$$

$$p_{83} = b(5; 8, 1/6) + b(1; 8, 1/6)f(7; 7, 5) + b(0; 8, 1/6)f(7; 8, 5)$$

$$p_{82} = b(6; 8, 1/6) + b(0; 8, 1/6)f(8; 8, 5)$$

and p_{81} and p_{80} are given by equation (10) because, for these transitions, the goal cannot change. Also, $p_{88} = 1 - \sum_{l=0}^{7} p_{8l.}$

To summarize, the LG strategy is evaluated using equation (9) with $p_{10,l}$ from Table 3 and p_{kl} from equation (11) for $k = 6, 7, 8$ and from equation (10) for $k \leq 5$. We noticed that using equation (11) just for $k = 8$, which is a strategy that allows for changing goals when there are 8 dice remaining, only reduced the mean number of rolls from 15.35 to 15.33. The goal is much more likely to change when $k = 8$ than $k = 6$ or 7, so changing goals when 6 or 7 dice remain will have a negligible effect and we did not do these computations. Also, $n_8 = 15.14$ and $n_9 = 15.33$ for the LG strategy, while $n_1, \ldots, n_7$ are the same as Table 2.

As in Appendix A, one can derive equation (11) without using the multinomial result (8). For example, $P(\max_i Y_i^7 = 4) = 5P(Y_1^7 = 4) = 5b(4; 7, 1/5)$ because the events $Y_i^7 = 4$ are mutually exclusive. The random process $\{D(t)\}$, where $D(t)$ is the number of dice remaining after t rolls, is called a discrete-time Markov chain. It is defined by its transition probabilities p_{kl} and initial state $D(0) = 10$. Equation (9) is an example of finding mean first passage times from each state of a Markov chain into a specific state; see [**11**, Section 5.5].

The LG strategy is optimal

To verify that the LG strategy is optimal, we formulate TENZI as a Markov decision process (MDP). In an MDP, a decision is made at each stage (time) to minimize the expected total cost. Because the process is memoryless, only Markovian strategies need be considered, where the decision depends only on the current state; see [**8**]. Although we are not aware of a simple proof that LG is optimal, we will show that many actions–and therefore states–are not optimal, greatly reducing the state space. This smaller MDP is then solved numerically. First, note that any configuration of dice can be represented as a canonical state vector, listing the sizes of the groups in decreasing order. For example, 4442222261 is represented as (5, 3, 1, 1) and we append 0's when needed. Let C be the set of canonical states of 10 or fewer dice and $l(x)$ denote the number of nonzero components of x.

A stage of the game begins in a state x of the dice that are kept, so that $d(x) = 10 - \sum_i x_i$ dice are rolled. The outcome of the roll is $y = (y_1, \ldots, y_6)$ where y_i is the number of dice that match the ith LG. After the roll, the configuration is $x + y$; call its canonical form $z = \Phi(x + y)$. The decision of which dice to keep becomes the next state. The set of allowable actions in configuration z is $C(z) = \{x : x \le z$ and $x_1 \ge x_2 \cdots \ge x_6\}$, i.e., keep some of the dice and represent them in canonical order. However, we can restrict attention to strategies that have finite $E[N_{10}]$, even though the (random) number of stages is unbounded. This is called an infinite-horizon, finite total cost MDP.

One algorithm for solving such an MDP is value iteration, which iterates over a time horizon of $t = 1, 2, \ldots$ rolls or stages. The optimal actions and expected number of rolls, $v_t(x)$, are computed for each state x for a game that stops after t rolls. By the principle of dynamic programming,

$$v_{t+1}(x) = 1 + E[\min_{x' \in C(\Phi(x+Y))} v_t(x')], \quad x \in C, x \ne 10. \tag{12}$$

Here the expectation is over the roll Y of $d(x)$ dice. In words, the expected number of rolls is 1 (for the next roll) plus the expected number of rolls in the next state x'. When $x' = 10$ is reached the game ends, so $v_t(10) = 0$. The minimum chooses the best dice to keep for each configuration $\Phi(x + Y)$ of dice showing. Unlike the standard MDP formulation, the minimum is inside the expectation, because we are using a "post-transition state," or configuration, $\Phi(x + Y)$ to choose an action x'.

Starting with $v_0(x) = 0$, equation (12) will converge to the optimal infinite-horizon values $v(x) = \lim_{t\to\infty} v_t(x)$ and actions. The optimal strategy is the same at each stage, so it is described as a mapping from configurations to actions: when showing z take action $a(z) \in C(z)$, i.e., keep this configuration of dice. In particular, $E[N_{10}] = v(0)$ where $x = 0$ represents the beginning of the game where no dice are showing. However, the complexity of the state space C makes equation (12) difficult to implement. Next we show that some states and actions are not optimal and can be eliminated. The remainder considers only the infinite-horizon problem. The first lemma asserts that it is better to hold dice that are more concentrated in larger groups: moving a die from a smaller group to a larger group decreases the expected rolls remaining. Let e_i denote the vector with a 1 in the ith component and 0's elsewhere.

Lemma 1. *For $i < j$, $v(x + e_i - e_j) \le v(x)$.*

The proof is in Appendix B.

Lemma 2. *There is an optimal strategy that does not keep singleton groups.*

Proof. We will show that $v(x) \le v(x')$ for all x, where $x' = x + e_{l(x)+1}$ adds a singleton group to x. In state x, one more die is rolled than in x'. Getting a roll of y^0 for this die can be thought of as transitioning to a hold state $x + y^0$. Taking the expectation over y^0,

$$v(x) = \frac{6 - l(x)}{6} v(x') + \frac{1}{6} \sum_{i=1}^{l(x)} v(x + e_i). \tag{13}$$

By Lemma 1, $v(x + e_i) \le v(x')$ for all i. Substituting into equation (13), $v(x) \le v(x')$. ■

Lemma 3. *There is an optimal strategy that keeps at least one LG.*

Proof. Suppose holding x when z is showing does not hold an LG. Consider two cases. First, if $x_2 = 0$ (x contains one group) then $x' = z_1 = x + me_1$ holds the LG for some $m > 0$. Applying equation (13) to this x,

$$v(x) = \frac{1}{6}v(x + e_1) + \frac{5}{6}v(x + e_2) \geq v(x + e_1),$$

where the inequality holds by Lemma 1. Iterating, $v(x') \leq v(x)$ and holding the LG is at least as good.

Second, if $x_2 > 0$ (x contains more than one group) then $x' = x + e_1 - e_j$ is a feasible action from z for some $j > 1$. By Lemma 1, again $v(x') \leq v(x)$. ■

Lemma 4. *There is an optimal strategy that does not keep partial groups.*

The proof of Lemma 4 is similar to that of Lemma 2 and is omitted.

With these lemmas, we know that the only states with $x_1 \leq 4$ visited by an optimal strategy are those listed in Table 4. Call this set of states $\mathcal{T}$. Furthermore, the optimal action in each state must keep entire groups, including the LG. Thus, the number of actions to be considered in a state is small. For example, in state 3 the actions are to hold 1, 2, or 3 groups and in state 10 the actions are (3), (3,3), (3,2), and (3,3,2). When a configuration with $z_1 \geq 5$ is reached, it is optimal to keep the same goal for the rest of the game, so the LG strategy must be optimal in this configuration (and in all future configurations, since z_1 can only increase) and the next state is $x = z_1$. Let $\mathcal{A}$ be the set of such states, namely, those with $x_1 \geq 5$ and $l(x) = 1$. Although we could solve the reduced MDP using equation (12) for $x \in \mathcal{T} \cup \mathcal{A}$, we already know the action and cost (the expected number of rolls) in states $x \in \mathcal{A}$. Thus, it is easier to solve equation (12) on just the transient class of states $\mathcal{T}$ with this modification: when a transition into $x \in \mathcal{A}$ occurs, apply a terminal cost $v_t(x) = E[N_{10-x}]$ from Table 2, then remain in that state and incur no more cost. In Markov chains, a state that is never left is called *absorbing* while *transient* states are those where the probability of ever returning to the state is less than one; the probability of being in a transient state approaches 0 as time increases.

We solved equation (12) using just the transient states $\mathcal{T}$ and these actions. After $t = 7$ stages, the optimal policy is the LG strategy; it remained optimal until we stopped at 43 stages, at which point the optimal value $v_t(x)$ is changing by less than 10^{-12}. This level of precision strongly suggests that the infinite-horizon optimal policy is indeed LG. Interestingly, when a larger initial cost is used, such as $v_0(x) = 100$, the optimal policy is LG starting at stage 1 because there is an incentive to finish the game before the time horizon is reached and the cost $v_0(x)$ is incurred; cost also converges slightly faster, requiring 42 stages to terminate. The expected number of rolls found by the MDP is $v_t(0) = 15.375$, nearly agreeing with the analysis of the LG strategy above. The slight discrepancy could be due to roundoff error in our method of computing the transition probabilities in the MDP, where we computed the probability of each roll Y from the multinomial distribution, then summed over all Y that yield the same canonical state $\Phi(x + Y)$.

Appendix A. Distribution of the first roll

The distribution of D found in equation (8) can be constructed using inclusion-exclusion and the binomial and multinomial distributions. First, to have $D = k \leq 4$ dice remaining, there must be $X_i = 10 - k \geq 6$ matching dice for some i. These are

#	State	#	State	#	State
1	2	7	3,2,2	13	4,2
2	2,2	8	3,2,2,2	14	4,2,2
3	2,2,2	9	3,3	15	4,3
4	2,2,2,2	10	3,3,2	16	4,3,2
5	3	11	3,3,3	17	4,4
6	3,2	12	4		

TABLE 4: Transient states of the MDP.

mutually exclusive events (only one of the X_i can be this large) so the probability of their union is the sum of their probabilities:

$$\begin{aligned} P(D = k) &= P(X_1 = 10 - k \cup \ldots \cup X_6 = 10 - k) \\ &= 6P(X_1 = 10 - k) = 6b(10 - k; 10, 1/6), \quad k \le 4. \end{aligned}$$

For larger k, one must take into account that more than one of the events could occur, e.g., $X_1 = 5$ and $X_2 = 5$. In the case of two events, $P(A \cup B) = P(A) + P(B) - P(A \cap B)$. The generalization to any number of events is called the inclusion-exclusion principle; see [9]. Under complete symmetry, i.e., $P(A_{i_1} \cap \ldots \cap A_{i_k})$ constant for all $i_1, \ldots, i_k$ for each $k = 1, \ldots, n$, it can be stated

$$P(A_1 \cup \ldots \cup A_n) = \sum_{k=1}^{n} (-1)^{k+1} C_k^n P(A_1 \cap \ldots \cap A_k). \tag{14}$$

For shorthand, use the notation V_i for the event $X_i = 5$. Since at most two of these events can occur, only $k = 1$ and 2 are used in equation (14)

$$\begin{aligned} P(D = 5) &= P(V_1 \cup \ldots \cup V_6) \\ &= P(V_1) + \ldots + P(V_6) - [P(V_1 \cap V_2) + \ldots + P(V_5 \cap V_6)] \\ &= 6P(V_1) - C_2^6 P(V_1 \cap V_2) \\ &= 6b(5; 10, 1/6) - C_2^6 C_5^{10}/6^{10}. \end{aligned}$$

The quantity in square brackets is the probability of rolling five each of two numbers. First, C_2^6 counts the choices for the two numbers, which is the number of pairs in the second line. Then C_5^{10} counts the ways of choosing which of the 10 dice show the first number.

The calculation is similar for $D = 6$, but since this occurs when $\max\{X_1, \ldots, X_6\} = 4$, we must exclude rolls such as $X_1 = 4$ and $X_2 = 6$, even though there were 4 ones. Let F_i denote the event $X_i = 4$ and $C_{k_1,k_2,k_3}^n = n!/(k_1!k_2!k_3!)$ be the number of partitions of n objects into groups of size k_1, k_2, k_3. Then

$$\begin{aligned} P(D = 6) &= P(F_1 \cup \cdots \cup F_6) - P(F_i \cap X_j > 4 \text{ for some } i \ne j) \\ &= 6P(F_1) - C_2^6 P(F_1 \cap F_2) - 6(5)[P(F_1 \cap X_2 = 5) + P(F_1 \cap X_2 = 6)] \\ &= 6b(4; 10, 1/6) - C_2^6 C_{4,4,2}^{10} 4^2/6^{10} - 6(5)[C_{4,5,1}^{10} 4/6^{10} + C_4^{10}/6^{10}]. \end{aligned}$$

To evaluate the last term in the first line, there are 6×5 ways of choosing $i \ne j$. For $F_1 \cap X_2 = 5$, there are 4 ones, 5 twos, and 1 other, which has 4 choices. The partition $C_{4,5,1}^{10}$ counts how many ways the ones, two, and other can be arranged. For

$F_1 \cap X_2 = 6$, there are 4 ones and 6 twos; C_4^{10} counts how many ways they can be arranged.

We skip $D = 7$ because it is easier to find $P(D = 8)$. It can be computed from the symmetric multinomial distribution with 10 trials and 6 outcomes, which has probability mass function

$$f(x_1, \ldots, x_6) = \frac{10!}{x_1! \cdots x_6!} \left(\tfrac{1}{6}\right)^{10}.$$

The event $D = 8$ requires five groups of 2 or four groups of 2 and two singletons. Thus,

$$\begin{aligned} P(D = 8) &= C_1^6 f(2, 2, 2, 2, 2, 0) + C_2^6 f(2, 2, 2, 2, 1, 1) \\ &= 6\left(\frac{10!}{2^5 \cdot 6^{10}}\right) + \frac{6 \cdot 5}{2}\left(\frac{10!}{2^4 \cdot 6^{10}}\right) \\ &= \frac{10!}{2^5 \cdot 6^8}. \end{aligned}$$

Then $P(D = 7) = 1 - \sum_{k=0}^{6} P(D = k) - P(D = 8)$.

We conclude with an alternative, direct approach to compute $P(D = 7)$. This event occurs when $\max\{X_1, \ldots, X_6\} = 3$. Let R_i denote the event $X_i = 3$, up to three of which can occur, and recall that F_i is the event $X_i = 4$. Using $k = 1, 2, 3$ in equation (14),

$$\begin{aligned} P(D = 7) &= P(R_1 \cup \ldots \cup R_6) - P(R_i \cap X_j > 3 \text{ for some } i \neq j) \\ &= 6P(R_1) - C_2^6 P(R_1 \cap R_2) + C_3^6 P(R_1 \cap R_2 \cap R_3) \\ &\quad - P(R_i \cap F_j \text{ for some } i \neq j) \\ &\quad - 6(5)[P(R_1 \cap X_2 = 5) + P(R_1 \cap X_2 = 6) + P(R_1 \cap X_2 = 7)] \\ &= 6b(3; 10, 1/6) - C_2^6 C_{3,3,4}^{10} 4^4/6^{10} + C_3^6 C_{3,3,3,1}^{10} 3/6^{10} \\ &\quad - P(R_i \cap F_j \text{ for some } i \neq j) \\ &\quad - 6(5)[P(R_1 \cap X_2 = 5) + P(R_1 \cap X_2 = 6) + P(R_1 \cap X_2 = 7)]. \end{aligned}$$

To compute $P(R_1 \cap R_2 \cap R_3)$, $C_{3,3,3,1}^{10}$ counts how many ways 3 ones, 3 twos, 3 threes, and one other can be arranged. The other die has 3 possible values. The terms with $X_2 = 5$, 6, and 7 are very similar to those for $P(D = 6)$. The term with F_j is complicated by the fact that the events $R_i \cap F_j$ are not mutually exclusive: if $X_1 = X_2 = 3$ and $X_3 = 4$, then $R_1 \cap F_3$ and $R_2 \cap F_3$ both occur. To account for the overlap, first we condition on F_j. The remaining possibilities are the same as rolling 6 five-sided die. Using $k = 1, 2$ in equation (14),

$$\begin{aligned} P(R_i \cap F_j \text{ for some } i \neq j) &= P(R_i \text{ for some } i \neq 1 | F_1) P(F_1 \cup \ldots \cup F_6) \\ &= [5P(R_2|F_1) - C_2^5 P(R_2 \cap R_3|F_1)] P(F_1 \cup \ldots \cup F_6) \\ &= [5C_3^6 4^3/5^6 - C_2^5 C_3^6/5^6][6b(4; 10, 1/6) - C_2^6 C_{4,4,2}^{10} 4^2/6^{10}]. \end{aligned}$$

In the event $R_2|F_1$, the six dice must have 3 twos and 3 others, each of which has 4 choices. For $R_2 \cap R_3|F_1$, the six dice must have 3 twos and 3 threes. The formula for $P(F_1 \cup \ldots \cup F_6)$ is from $P(D = 6)$.

Appendix B. Proof of Lemma 1

Recall that for $x \in C$ and $i < j$, $x_i \geq x_j$. Let $x' = x + e_i - e_j$. Consider two Markov chains: system 1 starts in state x' and system 2 in state x. Let $R = (R_1, \ldots, R_6)$ be the roll in system 2, where R_i is the number of i's rolled. Note that both roll the same number of dice, $d(x) = d(x + e_i - e_j)$. Let the roll for system 1 be $R' = \Gamma(R)$ for some one-to-one function Γ on $\{1, \ldots, 6\}^{d(x)}$. Because R has the uniform distribution $P(R = r) = 1/6^{d(x)}$, R' has the same distribution. Thus, we can play two games that start in states x and x' by rolling dice for just one game.

Define the concentration measure $\delta(w) = |w_i - w_j|$ on state w. Note that $\delta(x') - \delta(x) = 2$, meaning that system 1 (state x') is more concentrated. We will construct a Γ for which system 1 is either more concentrated by 2 or tied after the roll. More precisely, if $y(r)$ is the vector of counts for roll r, $z = \Phi(x + y(r))$ and $z' = \Phi(x + y(\Gamma(r)))$ are the configurations after the roll. We will show that either $z' = z$ or $z' = z + e_k - e_l$ for some $k < l$. In the latter case, the concentration measure is now $\delta_{kl}(w) = |w_k - w_l|$ and $\delta_{kl}(z') - \delta_{kl}(z) = 2$. System 2 uses the optimal strategy, holding $a(z)$ in configuration z, and system 1 uses the actions $\hat{a}(z) = a(z')$ if feasible, i.e., if $a(z') \leq z$, and $\hat{a}(z) = a(z') - e_k + e_l$ otherwise. In the first case the systems merge, having the same next state. In the second case, their next states still differ in concentration by 2. Do the same at each stage: map the roll by Γ (suitable for that state) and use these actions. System 1 will remain more concentrated until they merge. Note that system 2 cannot reach the final state without merging because when only one group is held ($x_2 = 0$) the systems merge. Hence, system 1 always reaches the final state before, or at the same roll, as system 2 and the expected number of rolls satisfies $v(x') \leq v(x)$.

It remains to construct such a Γ. This is possible because the concentration measure of system 2 is stochastically dominated by that of system 1 after a roll. A random variable V is stochastically dominated by W if their distribution functions satisfy the ordering $F_V(x) \geq F_W(x)$. Since all r are equiprobable, a larger set of r's giving a value of δ is equivalent to a larger probability. Partition $\{1, \ldots, 6\}^{d(x)}$ into subsets where a certain set of n dice, $0 \leq n \leq d(x)$, show i or j and the other dice are fixed at values other than i or j. In this subset, there are $C^n_{y_i}$ outcomes that contain y_i i's, for $y_i = 0, \ldots, n$. For example, if $\delta(x) = 0$, so that $\delta(x') = 2$, and $n = 4$ then the distribution of y_i over these outcomes and the resulting concentration measures are shown in Table 5. Notice that there are more outcomes that lead to lower concentration in system 2: for $\delta = 0$, 6 vs. 4, for $\delta = 0$ or 2, 14 vs. 11, for $\delta = 0$, 2, or 4, 16 vs. 15. Thus, Γ can map these 16 rolls for system 2 into rolls for system 1 so that $\delta(x' + y(\Gamma(r))) - \delta(x + y(r)) = 0$ or 2. Simply arrange the rolls in increasing order of $\delta(x + y(r))$ and assign Γ so that $\delta(x' + y(\Gamma(r)))$ is also in increasing order.

Number of outcomes	1	4	6	4	1
y_i	0	1	2	3	4
System 1 $\delta(x + y)$	2	0	2	4	6
System 2 $\delta(x' + y)$	4	2	0	2	4

TABLE 5: Concentration measures after rolling 4 i's and j's starting with $\delta(x) = 0$.

The same argument can be made for any n and $\delta(x) \geq 0$. Observe that $\delta(x + y) = |2y_i + \delta(x) - n| = 0$ for $y_i = (n - \delta(x))/2 \leq n/2$. This is the center of the interval of values of y_i for which $\delta(x + y) \leq m$ for any $m \geq 0$. Recall that the number of outcomes containing y_i i's is the binomial coefficient $C^n_{y_i}$ and notice that the center of the interval is on the left half, $y_i \leq n/2$. Compare this with system 1, where $\delta(x' +$

$y) = |2y_i + \delta(x) - n + 2| = 0$ for $y_i = (n - \delta(x) - 2)/2$ and we see that the interval for which $\delta(x' + y) \le m$ is shifted left by one. Because the binomial coefficients are symmetric about the midrange $n/2$ and decrease moving away from the midrange, their sum is larger on the first interval (system 2).

Since we have constructed the required Γ on an arbitrary subset of the partition, we can construct it on the entire set of rolls. ■

Acknowledgment I would like to thank my wife Cindy for introducing me to TENZI and my student Isaac Bleecker for writing the computer program to check the form of the optimal policy.

REFERENCES

[1] Barhite, J. (2016). An analysis of the game Tenzi. Undergraduate thesis. Carthage College, Kenosha, WI.
[2] Corrado, C. J. (2011). The exact distribution of the maximum, minimum and the range of multinomial/Dirichlet and multivariate hypergeometric frequencies. *Statistics and Computing.* 21(3): 349–359.
[3] Eisenberg, B. (2008). On the expectation of the maximum of IID geometric random variables. *Statistics & Probab. Lett.* 78(2): 135–143.
[4] Goering, D., Canada, D. (2007). The river crossing game. *Mathematics Magazine.* 80(1): 3–15.
[5] Good, I. J. (1957). Saddle-point methods for the multinomial distribution. *Ann. Math. Stat.* 28(4): 861–881.
[6] Hess, R. I. (2016). *The Population Explosion and Other Mathematical Puzzles.* Singapore: World Scientific.
[7] Kaigh, W. D. (1979). An attrition problem of gambler's ruin. *Mathematics Magazine.* 52(1): 22–25.
[8] Puterman, M. L. (2014). *Markov Decision Processes: Discrete Stochastic Dynamic Programming.* Hoboken, NJ: John Wiley & Sons.
[9] Ross, S. M. (2014). *A First Course in Probability.* London: Pearson.
[10] Sen, A. (1986). Social choice theory. In: Arrow, K.J., Intriligator, M., eds. *Handbook of Mathematical Economics*, Vol. 3. Amsterdam: North Holland, pp. 1073–1181.
[11] Winston, W. L. (2004) *Introduction to Probability Models: Operations Research*, Volume 2. Boston, MA: Brooks/Cole-Thomson Learning.

Summary. TENZI, "the world's fastest game," sounds too simple: roll 10 dice until they all match, setting aside the dice you want to keep. How fast is it? That is, on average how many rolls does it take to get 10 matches? An intuitive strategy that keeps the largest group (LG) of matching dice after each roll turns out to be optimal. The average number of rolls, for both the optimal and a naive policy, are found recursively from basic combinatorics, with some ideas from order statistics and Markov chains. The LG strategy is shown to be optimal by formulating TENZI as a dynamic program, showing that it can be reduced to a much smaller problem, and numerically solving this problem to obtain the optimal policy.

MICHAEL H. VEATCH holds a B.A. in mathematics from Whitman College, a M.S. in Operations Research and Statistics from Rensselaer Polytechnic Institute, and a Ph.D. in Operations Research from Massachusetts Institute of Technology. He is a professor of mathematics at Gordon College in Wenham, MA. Prior to his academic appointment he spent six years at The Analytic Sciences Corp. studying Air Force supply systems. His research interests include stochastic network control problems and humanitarian logistics.

Quasi-Exponential Growth and Decay

DAVID BURTON
Franciscan University
Steubenville, Ohio 43952
dburton@franciscan.edu

JOHN COLEMAN
Franciscan University
Steubenville, Ohio 43952
jcoleman@franciscan.edu

Every decreasing exponential function has an invariant half-life. Since nonexponential decay curves typically do not have invariant half-lives, it is natural to conjecture that exponential curves are characterized by this property. In this paper we show that this natural conjecture is false. As a very easy example, take the function $f(t) = 2^{-\lfloor t \rfloor}$, where $\lfloor t \rfloor$ denotes the floor function. It has an invariant half-life, but it is not an exponential function. While this function is not continuous, it is not difficult to find examples that are continuous and even smooth. We provide several such examples. These examples might have applications to the modeling of certain natural phenomena. We investigate some of the issues that these examples raise and explore what additional assumptions are needed to guarantee exponential growth or decay. From these explorations, we conclude with an open problem that we hope others will find interesting enough for further investigation.

Definitions and preliminary results

To avoid the tedium of constantly using the phrase "growth or decay," we will concentrate on the case of decay in this and the following section, leaving to the reader the easy generalization to the dual case of growth. We begin by generalizing the notion of an exponential decay curve.

Definition. A *decay curve* is a continuous function $f : \mathbb{R} \to \mathbb{R}^+$ that is strictly decreasing, has $\lim_{t\to-\infty} f(t) = \infty$, and $\lim_{t\to\infty} f(t) = 0$.

Definition. Suppose that f is a decay curve.

1. The *half-life* of f is the number t_H that satisfies $f(t_H) = \frac{1}{2} f(0)$.
2. The half-life, t_H, is *invariant* if it satisfies $f(t + t_H) = \frac{1}{2} f(t)$ (for all $t \in \mathbb{R}$)).
3. The function f is *semi-exponential* if its half-life is invariant.

All decay curves clearly possess a unique half-life, and the half-life of exponential decay curves is invariant in the requisite way. The invariance of half-life for exponential decay curves is often thought of as independence from initial amount. The perspective is that $y = Ae^{\lambda t}$ is a family of curves parameterized by the initial amount A and that the half-life is independent of A. We can adopt this perspective for arbitrary semi-exponential curves as well. If f is semi-exponential, then it is one-to-one and onto from $(-\infty, \infty)$ to $(0, \infty)$. Hence for any $A > 0$, there exists a unique t_A with $f(t_A) = A$. If we define $f_A(t) = f(t_A + t)$ then

$$f_A(0) = f(t_A + 0) = f(t_A) = A.$$

Math. Mag. **94** (2021) 186–193. doi:10.1080/0025570X.2021.1908073
MSC: 26A09

We thus obtain a 1-parameter family of curves parameterized by the initial amount. Furthermore,

$$f_A(t_H) = f(t_A + t_H) = \frac{1}{2} f(t_A) = \frac{1}{2} f(t_A + 0) = \frac{1}{2} f_A(0).$$

Thus the t-invariance of half-life implies that it is also independent of initial amount.

Preliminary examples

The following lemma is useful for constructing semi-exponential decay curves.

Lemma 1. *Suppose that $h : [0, 1] \to [\frac{1}{2}, 1]$ is a continuous decreasing function with $h(0) = 1$ and $h(1) = \frac{1}{2}$. Then for any $A, k > 0$, the function*

$$f(t) = A \cdot 2^{-\lfloor t/k \rfloor} \cdot h(\{t/k\})$$

(where $\lfloor x \rfloor$ is the floor function and $\{x\}$ is the sawtooth function defined by $\{x\} = x - \lfloor x \rfloor$) is a decay curve with initial value A and invariant half-life k.

Proof. Note that for all x, $\lfloor x + 1 \rfloor = \lfloor x \rfloor + 1$ and $\{x + 1\} = \{x\}$. Thus for any t we have

$$\begin{aligned} f(t + k) &= A \cdot 2^{-\lfloor (t+k)/k \rfloor} \cdot h(\{(t + k)/k\}) \\ &= A \cdot 2^{-\lfloor t/k + 1 \rfloor} \cdot h(\{t/k + 1\}) \\ &= A \cdot 2^{-(\lfloor t/k \rfloor + 1)} \cdot h(\{t/k\}) \\ &= 2^{-1} \cdot A \cdot 2^{-\lfloor t/k \rfloor} \cdot h(\{t/k\}) = \frac{1}{2} f(t). \end{aligned}$$

Thus f has k for an invariant half-life. To see that f is continuous and decreasing, first note that this is clearly true on all intervals of the form $(nk, (n + 1)k)$ since the graph of f on those intervals is obtained by stretching and translating the graph of h. Hence, it is enough to check for continuity at integer multiples of k. But this follows since

$$\begin{aligned} \lim_{t \to nk^-} f(t) &= \lim_{t \to nk^-} A \cdot 2^{-\lfloor t/k \rfloor} \cdot h(\{t/k\}) \\ &= A \cdot 2^{-(n-1)} \cdot h(1) = A \cdot 2^{-(n-1)} \cdot \frac{1}{2} = A \cdot 2^{-n} \end{aligned}$$

and

$$\begin{aligned} \lim_{t \to nk^+} f(t) &= \lim_{t \to nk^+} A \cdot 2^{-\lfloor t/k \rfloor} \cdot h(\{t/k\}) \\ &= A \cdot 2^{-n} \cdot h(0) = A \cdot 2^{-n} \cdot 1 = A \cdot 2^{-n}. \end{aligned}$$

Thus, the 2-sided limit exists and is equal to $f(nk) = A \cdot 2^{-n}$. ∎

It is clear that all semi-exponential f arise in this way since h can be defined via $h(t) = \frac{1}{f(0)} f(kt)$ for $t \in [0, 1]$. Note that h is a normalized version of the first half-life of f. Figure 1 shows what f looks like for h linear and $A = 1$ and $k = 2$. Note that f is the piecewise linear function which interpolates $\ldots, (-4, 4), (-2, 2), (0, 1), (2, \frac{1}{2}), (4, \frac{1}{4}), \ldots$. It fails to be differentiable at the junction points.

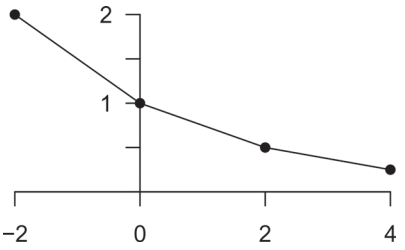

Figure 1 A piecewise linear semi-exponential function.

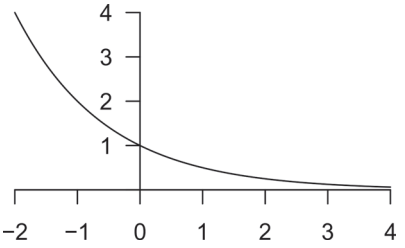

Figure 2 A piecewise cubic semi-exponential function.

We can extend this interpolating idea by using a piecewise cubic interpolation. This leads to the following cubic:

$$h(t) = \frac{-1}{26}t^3 + \frac{3}{13}t^2 - \frac{9}{13}t + 1.$$

The resulting $f(t)$ can be shown to be twice-differentiable. Figure 2 shows what f looks like for $A = k = 1$. The graph appears to be virtually indistinguishable from that of $y = 2^{-t}$. It fails to be thrice-differentiable.

In the next section, we will prove a fairly general result that will make it easy to find examples which are infinitely differentiable.

Quasi-exponential curves

In this section, we generalize the notion of semi-exponential decay curves.

Definition. A continuous function $f : \mathbb{R} \to (0, \infty)$ is *quasi-exponential* f there exist constants $r, k > 0$ such that $f(t + k) = r \cdot f(t)$ for all t.

Note that semi-exponential decay curves are quasi-exponential with $r = \frac{1}{2}$. A quasi-exponential f is a decay curve if it is decreasing and is a growth curve if increasing. A quasi-exponential function might be neither a decay nor a growth curve. In the case that f is either a growth or a decay curve, it is one-to-one. In this case k is uniquely determined given r. In this case we call k the *r-life* of f.

There is a nice characterization of quasi-exponential functions in the case that they are continuously differentiable.

Theorem 1. *Suppose that f is a strictly positive function defined on $\mathbb{R}$ with $f'(t)$ continuous. Then f is quasi-exponential if and only if the ratio $f'(t)/f(t)$ is periodic.*

Proof. Suppose that f is quasi-exponential with constants r and k such that $f(t+k) = rf(t)$. Taking logarithms yields that $\ln(f(t+k)) = \ln(f(t)) + \ln(r)$. Hence

$$\frac{d}{dt}\ln(f(t+k)) = \frac{d}{dt}\ln(f(t)) + 0 = \frac{d}{dt}\ln(f(t)).$$

Thus the derivative of the logarithm of f, which is $f'(t)/f(t)$, is periodic.

Conversely, suppose that $p(t) = f'(t)/f(t)$ is periodic of period k. The assumptions on f guarantee that p is continuous. Note that $p(t)$ can be written as $\lambda + q(t)$ where $q(t)$ is periodic of period k with $\int_0^k q(t)\,dt = 0$ and λ constant: simply take $\lambda = \frac{1}{k}\int_0^k p(t)\,dt$ and let $q(t) = p(t) - \lambda$. Note that $f(t)$ satisfies the separable differential equation

$$\frac{y'}{y} = p(t) = \lambda + q(t).$$

Solving this we see that

$$f(t) = e^{\lambda t + Q(t) + C} = Ae^{\lambda t + Q(t)}$$

where $A = f(0)$ and

$$Q(t) = \int_0^t q(s)\,ds.$$

Note that

$$Q(t+k) = \int_0^{t+k} q(s)\,ds = \int_0^t q(s)\,ds + \int_t^{t+k} q(s)\,ds = \int_0^t q(s)\,ds + 0 = Q(t).$$

Thus $Q(t)$ is periodic of period k. Let $r = e^{\lambda k}$. Then:

$$f(t+k) = Ae^{\lambda(t+k)+Q(t+k)} = Ae^{\lambda t + \lambda k + Q(t)} = e^{\lambda k}Ae^{\lambda t + Q(t)} = rf(t).$$

Thus f is quasi-exponential. ∎

Note that the $Q(t)$ in the previous proof can be written as $d(t) + M$ where $d(t)$ has average value 0 (over its period) and M is constant. Multiplying A by e^M and relabeling we get that quasi-exponential functions can always be written in the form

$$f(t) = Ae^{\lambda t + d(t)}.$$

Note that the A is no longer guaranteed to be $f(0)$. $d(t)$ represents a periodic deviation about the mean λt. In this sense, quasi-exponential functions can be thought of as curves which fluctuate periodically about exponential curves.

It is interesting to note that curves that fluctuate about exponential curves have been observed in measurements of radioactive decay. The fluctuations have been associated with several periodic phenomena such as earth–sun distance, solar rotation, and earth rotation. There is ongoing debate about whether the observed fluctuations are due to true changes in decay rate or to environmental influences on the detectors. See, for example, [**1**] and [**2**].

The following observations are easily verified.

1. If $\lambda > 0$, then $\lim_{t\to\infty} f(t) = \infty$.
2. If $\lambda < 0$, then $\lim_{t\to\infty} f(t) = 0$.
3. If $\lambda = 0$, then f is periodic.

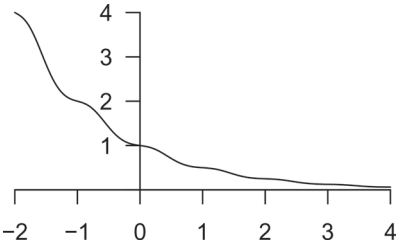

Figure 3 An analytic semi-exponential function.

4. The function f is a decay curve if $\lambda + d'(t) < 0$ for all t.
5. The function f is a growth curve if $\lambda + d'(t) > 0$ for all t.
6. If $\lambda < 0$, but $\lambda + d'(t) > 0$ for some t, then $f(t)$ sometimes grows and sometimes shrinks but has an overall downwards trend.

It is now easy to create analytic semi-exponential decay curves. For example,

$$f(t) = e^{\frac{1}{4\pi}\sin(2\pi t) - t\ln 2}.$$

This is shown in Figure 3.

A probabilistic approach

Exponential decay is closely related to exponential random variables. These are continuous random variables on $[0, \infty)$ with distribution functions of the form $F(t) = 1 - e^{-\lambda t}$. The relation is that if a large number of elements (e.g., atoms of a radioactive isotope) have lifetimes which are independent, exponentially distributed random variables with parameter λ, then the expected percentage of elements which remain at time t decays exponentially with decay curve $e^{-\lambda t}$. Motivated by this, we call a nonnegative continuous random variable *semi-exponential* if its distribution function is of the form $G(t) = 1 - f(t)$ (for $t \geq 0$) where f is a semi-exponential function with $f(0) = 1$.

Whether or not semi-exponential random variables are useful in their own right, they shed an interesting light on the well-known memoryless property of exponential random variables. This is the property that if T is eponentially distributed then for any $s > 0$, we have

$$P(T - s > t \mid T > s) = P(T > t).$$

From this it follows that both its median (which is simply the half-life) and its expected value (often called *mean lifetime* in the context of exponential decay) are time-invariant in the sense that $Median(T - s \mid T > s) = Median(T)$ and $E(T - s \mid T > s) = E(T)$.

If T is a semi-exponential random variable it follows that its median is time-invariant. It is natural to ask if this extends to mean lifetime. The answer is "no" – unless T itself is exponential (at least in the case when the corresponding function f is differentiable).

Theorem 2. *Suppose that f is a differentiable semi-exponential decay curve with half-life k and $f(0) = 1$, and suppose that T is the corresponding semi-exponential random variable. Then T satisfies*

$$E(T - s \mid T > s) = E(T)$$

for all $s \geq 0$ if and only if T is exponentially distributed.

Proof. By linearity of expectation, $E(T - s \mid T > s) = E(T|T > s) - s$. We will concentrate on the second expression, denote it by $M(s)$, and refer to it as the *mean remaining lifetime*. If $G(t) = 1 - f(t)$ (for $t \geq 0$) is the distribution function, then the corresponding density function is $g(t) = G'(t) = -f'(t)$. Expectation is thus

$$E(T) = \int_0^\infty (-tf'(t))\,dt = -tf(t)\Big|_0^\infty + \int_0^\infty f(t)\,dt = \int_0^\infty f(t)\,dt. \tag{1}$$

The first term vanishes since continuity guarantees that f is bounded on $[0, k]$, hence the identity $f(t + k) = \frac{1}{2}f(t)$ implies that $tf(t)$ tends to 0 as t tends to ∞. Note that

$$\begin{aligned}
\int_0^\infty f(t)\,dt &= \int_0^k f(t)\,dt + \int_k^{2k} f(t)\,dt + \int_{2k}^{3k} f(t)\,dt + \cdots \\
&= \int_0^k f(t)\,dt + \int_0^k f(t+k)\,dt + \int_0^k f(t+2k)\,dt + \cdots \\
&= \int_0^k f(t)\,dt + \frac{1}{2}\int_0^k f(t)\,dt + \frac{1}{4}\int_0^k f(t)\,dt + \cdots \\
&= (1 + \frac{1}{2} + \frac{1}{4} + \frac{1}{8} + \cdots)\int_0^k f(t)\,dt \\
&= 2\int_0^k f(t)\,dt.
\end{aligned}$$

Thus, the mean lifetime, $E(T)$, is finite and is twice the integral of f over its first half-life.

The conditional mean lifetime given $T > s$, $E(T \mid T > s)$, is computed using the conditional density of T given $T > s$. This is

$$g(t|T > s) = \frac{g(t)}{1 - G(s)} = \frac{g(t)}{f(s)} = \frac{-f'(t)}{f(s)} \text{ (for } t > s,\ 0 \text{ otherwise).}$$

The mean *remaining* lifetime is $M(s) = E(T|T > s) - s$ If $f(t) = e^{-\lambda t}$ then a simple calculation shows that this equals $E(T) = 1/\lambda$ for all $s \geq 0$.

Conversely, suppose that $M(s) = E(T)$ for all $s \geq 0$. Note that this implies that $M(s)$ is constant. We can use integration by parts to evaluate this.

$$\begin{aligned}
M(s) &= E(T \mid T > s) - s \\
&= \int_s^\infty t g(t \mid T > s)\,dt - s \\
&= \int_s^\infty \frac{-tf'(t)}{f(s)}\,dt - s \\
&= \frac{1}{f(s)}\left[-tf(t)|_s^\infty + \int_s^\infty f(t)\,dt\right] - s
\end{aligned}$$

$$= \frac{1}{f(s)}\left[sf(s) + \int_s^\infty f(t)\,dt\right] - s$$
$$= \frac{\int_s^\infty f(t)\,dt}{f(s)}.$$

Let $y(s)$ denote the numerator in this last expression. Note that by Equation 1, $y(0) = E(T)$. By the fundamental theorem of calculus, $y'(s) = -f(s)$. Hence $f(s) = -y'(s)$. Thus the assumption that $M(s) = E(T)$ is equivalent to the differential equation $y/(-y') = E(T)$. Or, equivalently, $y'/y = -1/E(T)$. But this implies that

$$y(s) = y_0 e^{-s/E(T)} = E(T)e^{-s/E(T)},$$

which in turn implies that

$$f(s) = -y'(s) = e^{-s/E(T)}.$$

■

When is a quasi-exponential function exponential?

The equation $f(t + k) = rf(t)$ is a special case of Schröder's functional equation: $f(\alpha(t)) = sf(t)$ [3]. This has been much-studied in the theory of functional equations, but mostly in the context of functions α which possess a fixed point. Quasi-exponential functions $\alpha(t) = t + k$, have no fixed point. Thus much of the resulting theory from functional equations is not directly relevant.

We can, however, use the theory of functional equations to prove that if f is a quasi-exponential decay curve which has enough invariant p-lives then f is in fact exponential.

Theorem 3. *Suppose that f is a decay curve which has invariant p-life for all p in $(0, 1)$. Then f is an exponential decay curve.*

Proof. We can without loss of generality assume that $f(0) = 1$ since we can replace $f(t)$ by $f(t)/f(0)$ if need be. For each $p \in (0, 1)$ let τ_p be the p-life. Thus $f(t + \tau_p) = pf(t)$ for all $t \in \mathbb{R}$, $p \in (0, 1)$. In particular,

$$f(\tau_p) = f(0 + \tau_p) = pf(0) = p \cdot 1 = p.$$

This implies that $\tau_p = f^{-1}(p)$. Since f is a strictly decreasing function which continuously maps $[0, \infty)$ onto $(0, 1]$ it follows that

1. τ_p is a strictly decreasing continuous function of p.
2. $\lim_{p\to 0^+} \tau_p = \infty$.
3. $\lim_{p\to 1^-} \tau_p = 0$.

Suppose that $s, t \geq 0$. If $t = 0$ then obviously

$$f(s + t) = f(s + 0) = f(s) = f(s) \cdot 1 = f(s)f(0) = f(s)f(t).$$

If $t > 0$, then by the above observations there exists a $p \in (0, 1)$ with $t = \tau_p$. But then $f(t) = f(\tau_p) = p$, hence

$$f(s + t) = f(s + \tau_p) = pf(s) = f(s) \cdot p = f(s)f(t).$$

Hence f satisfies the exponential Cauchy equation ($f(x+y) = f(x)f(x)$ [3]) hence it must be of the form $f(t) = e^{\lambda t}$, at least for $t \geq 0$. But since f is determined by its restriction to $[0, k]$ we can conclude that $f(t) = e^{\lambda t}$ for all t. ■

Conclusion

We have seen several examples of functions that have invariant half-lives, but which are not exponential. Such examples can help us understand more precisely what characterizes exponential functions. While it is somewhat speculative, quasi-exponential functions might have applications to real-world phenomena such as radioactive decay. We have also seen some conditions that can be added that only true exponential functions satisfy. We suppose that other ways to create quasi-exponential functions could be explored.

We end with an open problem. How much invariance is sufficient to guarantee that a decay function is an exponential decay function? More precisely: call a subset $S \subseteq (0, 1)$ *sufficient* if having an invariant p-life for all $p \in S$ implies that a decay curve is exponential. By Theorem 3, $(0, 1)$ itself is sufficient. Is there a nice characterization of sufficient sets? Are there any finite ones? Is it enough for a set to contain two elements which are not rational multiples of each other?

REFERENCES

[1] Jenkins, J. H., Mundy, D. W., Fischbach, E. (2010). Analysis of environmental influences in nuclear half-life measurements exhibiting time-dependent decay rates. *Nuclear Instrum. Meth. Phys. Res. A*. 620(2/3): 332–342. doi.org: 10.1016/j.nima.2010.03.129

[2] Parkhomov, A. (2011). Deviations from beta radioactivity exponential drop. *J. Modern Phys.* 2(11): 1310–1317. doi.org: 10.4236/jmp.2011.211162.

[3] Small, C. G. (2007). *Functional Equations and How to Solve Them*. New York: Springer.

Summary. In this paper, we study functions which share with exponential functions the property of having invariant half-lives. We show various examples of what we call quasi-exponential functions. These are non-exponential functions with invariant half-lives or doubling times (or more generally an invariant r-life for a fixed value of r). Characterizations and properties of such functions are explored along with some possible applications.

DAVID BURTON (MR Author ID: 898096) graduated from the U.S. Naval Academy in 1981. After serving in the submarine fleet for several years, he returned to school and earned a Ph.D. in mathematics from Vanderbilt in 1997, specializing in functional analysis. He teaches in the Mathematics and Computer Science Department at Franciscan University of Steubenville.

JOHN COLEMAN (MR Author ID: 600815) received his Ph.D. from the University of Colorado at Boulder in 1992, specializing in universal algebra. His main research interest is in the interplay between algebra and topology in topological algebras. He teaches math and computer science at Franciscan University of Steubenville and also serves as department chair.

A Calculus Approach to Complex Variables

STEVEN G. KRANTZ
Washington University in St. Louis
St. Louis, MO 63130
sk@math.wustl.edu

Many complex analysis texts, especially undergraduate texts, define a holomorphic function f on a domain $\Omega \subseteq \mathbb{C}$ to be one which has a complex derivative

$$f'(z) = \lim_{\mathbb{C} \ni h \to 0} \frac{f(z+h) - f(z)}{h}$$

at each point $z \in \Omega$. Such a definition has historical antecedents in the calculus of Newton and Leibniz, but is not useful in developing the ideas of complex function theory—especially the Cauchy theory and its consequences. It is actually quite difficult to prove that a function holomorphic according to the definition above is infinitely differentiable, indeed has a local power series expansion.

The purpose of this article is to present another approach to holomorphicity. We cannot claim that this perspective is due to the present author. But it deserves to be better known. The main point here is that we show that complex analysis is just a way to interpret the key ideas of multivariable calculus. It is not really anything new; it is just a new notation. The book by Greene and Krantz [2] is a good reference for the basic ideas of complex function theory.

The basic idea

Our approach here is based on Green's theorem. Green's theorem is a common topic in third-semester calculus (see Blank and Krantz [1], but for our purposes we must render the theorem in notation compatible with complex analysis.

We write a complex number as $z = x + iy$. The conjugate is $\overline{z} = x - iy$.

Definition 1. *We define the differential operators*

$$\frac{\partial}{\partial z} = \frac{1}{2}\left(\frac{\partial}{\partial x} - i\frac{\partial}{\partial y}\right),$$
$$\frac{\partial}{\partial \overline{z}} = \frac{1}{2}\left(\frac{\partial}{\partial x} + i\frac{\partial}{\partial y}\right).$$

It is straightforward to calculate that

$$\frac{\partial}{\partial z} z = 1, \qquad \frac{\partial}{\partial z}\overline{z} = 0, \qquad \frac{\partial}{\partial \overline{z}}\overline{z} = 1, \qquad \text{and} \qquad \frac{\partial}{\partial \overline{z}} z = 0.$$

The dual objects to these complex partial derivatives are

$$dz = dx + i\,dy \qquad \text{and} \qquad d\overline{z} = dx - i\,dy.$$

It is useful to write the element of area in the complex plane as

$$dA = dx\,dy = \frac{i}{2} dz\,d\overline{z},$$

Math. Mag. **94** (2021) 194–200. doi:10.1080/0025570X.2021.1908074
MSC: Primary 30-01, Secondary 30E20

because $i/2$ is the Jacobian of the change of variable

$$x = \frac{1}{2}(z + \overline{z}), \qquad y = \frac{1}{2i}(z - \overline{z}).$$

One of the nice features of this notation is that we have an elegant way to define holomorphic functions.

Definition 2. *Let f be a complex-valued, continuously differentiable function on a domain $\Omega \subseteq \mathbb{C}$. Then f is holomorphic on Ω if and only if*

$$\frac{\partial}{\partial \overline{z}} f(z) \equiv 0 \tag{1}$$

on Ω.

Where does this definition come from? Let us write $f = u + iv$ and write out what equation (1) means. Then we have

$$\begin{aligned} 0 \equiv \frac{\partial}{\partial \overline{z}} f &= \frac{1}{2}\left(\frac{\partial}{\partial x} + i\frac{\partial}{\partial y}\right)(u + iv) \\ &= \frac{1}{2}\left(\left[\frac{\partial u}{\partial x} - \frac{\partial v}{\partial y}\right] + i\left[\frac{\partial u}{\partial y} + \frac{\partial v}{\partial x}\right]\right). \end{aligned}$$

The only way that the expression on the right can be identically zero is if the real part is zero and the imaginary part is zero. So

$$\frac{\partial u}{\partial x} = \frac{\partial v}{\partial y} \qquad \text{and} \qquad \frac{\partial v}{\partial x} = -\frac{\partial u}{\partial y}.$$

These are nothing other than the Cauchy-Riemann equations. So our complex notation has given us a new and elegant way to specify holomorphicity.

When we do calculus in the context of the complex number system, it is most convenient to use this new notation. Now let us recall the statement of Green's theorem as can be found in most any calculus book. In what follows, a *domain* is a connected, open set.

Theorem 1. *Let $\Omega \subseteq \mathbb{R}^2$ be a bounded domain whose boundary is a continuously differentiable curve. Let*

$$\mathbf{F}(x, y) = M(x, y)\mathbf{i} + N(x, y)\mathbf{j}$$

be a continuously differentiable vector field on $\overline{\Omega}$. Let $\mathbf{r}(t) = (r_1(t), r_2(t))$ be a positively oriented parameterization of $\partial\Omega$. Then

$$\oint_{\mathbf{r}} \mathbf{F} \cdot d\mathbf{r} \equiv \int \mathbf{F}(\mathbf{r}(t)) \cdot \mathbf{r}'(t)\, dt = \iint_{\Omega} \left(\frac{\partial N}{\partial x} - \frac{\partial M}{\partial y}\right) dA. \tag{2}$$

Our job now is to translate this theorem to complex notation.

For simplicity, we work on the unit disc with boundary the unit circle. We begin by replacing the vector field $\mathbf{F}$ with a complex-valued function

$$f(x + iy) = u(x, y) + iv(x, y).$$

We think of the curve $\mathbf{r}$ as the complex valued function

$$r(t) = \cos t + i \sin t.$$

Then we rewrite the left-hand side of equation (2) as

$$\begin{aligned}\int_0^{2\pi} f(r(t)) \cdot r'(t)\, dt &= \int_0^{2\pi} \big(u(r(t)) + i v(r(t))\big) \cdot (-\sin t + i \cos t)\, dt \\ &= \int_0^{2\pi} (-u \sin t - v \cos t) + i(-v \sin t + u \cos t)\, dt \\ &= \int_0^{2\pi} (u, v) \cdot (-\sin t, -\cos t)\, dt \\ &\qquad + i \int_0^{2\pi} (u, -v) \cdot (\cos t, \sin t)\, dt \\ &= \int_0^{2\pi} (u, -v) \cdot (-\sin t, \cos t)\, dt \\ &\qquad + i \int_0^{2\pi} (v, u) \cdot (-\sin t, \cos t)\, dt.\end{aligned}$$

Now we apply Green's theorem as stated in Theorem 1. We obtain that the last line equals

$$\begin{aligned}&= \iint_\Omega \left(-\frac{\partial v}{\partial x} - \frac{\partial u}{\partial y}\right) dA + i \iint_\Omega \left(\frac{\partial u}{\partial x} - \frac{\partial v}{\partial y}\right) \\ &= 2i \left[\iint_\Omega \frac{i}{2}\left(\frac{\partial v}{\partial x} + \frac{\partial u}{\partial y}\right) dA + \frac{1}{2}\left(\frac{\partial u}{\partial x} - \frac{\partial v}{\partial y}\right)\right] dA. \qquad (3)\end{aligned}$$

Also

$$\frac{\partial f}{\partial \overline{z}} = \frac{1}{2}\left(\frac{\partial}{\partial x} + i\frac{\partial}{\partial y}\right)(u + iv) = \frac{1}{2}\left[\left(\frac{\partial u}{\partial x} - \frac{\partial v}{\partial y}\right) + i\left(\frac{\partial u}{\partial y} + \frac{\partial v}{\partial x}\right)\right].$$

So equation (3) is nothing other than

$$2i \iint_\Omega \frac{\partial f}{\partial \overline{z}}\, dA.$$

We have proved the following complex version of Green's theorem:

Theorem 2. *Let $D \subseteq \mathbb{C}$ be the unit disc. Let f be a continuously differentiable function on $\overline{D}$. Let*

$$\mathbf{r}(t) = \cos t + i \sin t$$

be a parametrization of ∂D. Then

$$\oint_{\mathbf{r}} f(z)\, dz = 2i \cdot \iint_\Omega \frac{\partial f}{\partial \overline{z}}\, dA.$$

If we were to write the conclusion of this last theorem entirely in complex notation it would read

$$\oint_{\mathbf{r}} f(z)\, dz = \iint_\Omega \frac{\partial f}{\partial \overline{z}}\, (-2i) dA = \iint_\Omega \frac{\partial f}{\partial \overline{z}}\, d\overline{z}\, dz.$$

Even though we stated and proved the complex Green's theorem only for the disc, we shall take it to be true for any bounded domain with continuously differentiable boundary. The proof of the more general result is just the same.

Applications to the Cauchy theory

Let us begin by proving a version of the Cauchy integral theorem.

Theorem 3. *Let $\Omega \subseteq \mathbb{C}$ be a bounded domain with continuously differentiable boundary. Let f be a function that is continuously differentiable on $\overline{\Omega}$ and holomorphic on Ω. Let $\mathbf{r}$ be a C^1 curve that is a positively oriented parameterization of $\partial\Omega$. Then*

$$\oint_{\mathbf{r}} f(z)\, dz = 0. \tag{4}$$

Proof. We apply the complex Green's theorem to the left-hand side of equation (4). Thus

$$\oint_{\mathbf{r}} f(z)\, dz = -2i \iint_{\Omega} \frac{\partial f}{\partial \overline{z}}\, dA = 0\,.$$

We have used the fact that a holomorphic function is annihilated by the $\partial/\partial\overline{z}$ operator. ∎

Our next job is to prove the Cauchy integral formula, but we will actually prove something considerably more general.

Theorem 4. *Let $\Omega \subseteq \mathbb{C}$ be a bounded domain with continuously differentiable boundary. Let f be a function that is continuously differentiable on $\overline{\Omega}$. Let $\mathbf{r}$ be a C^1 curve that is a positively-oriented parameterization of $\partial\Omega$. Let $z \in \Omega$. Then*

$$f(z) = \frac{1}{2\pi i} \oint_{\mathbf{r}} \frac{f(\zeta)}{\zeta - z}\, d\zeta - \frac{1}{2\pi i} \iint_{\Omega} \frac{\partial f/\partial\overline{\zeta}}{\zeta - z} d\overline{\zeta}\, d\zeta. \tag{5}$$

Proof. Let $\epsilon > 0$ be smaller than the distance of z to $\partial\Omega$. Define $\Omega_\epsilon \equiv \Omega \setminus \overline{D}(z, \epsilon)$. Refer to Figure 1 to understand what Ω_ϵ is.

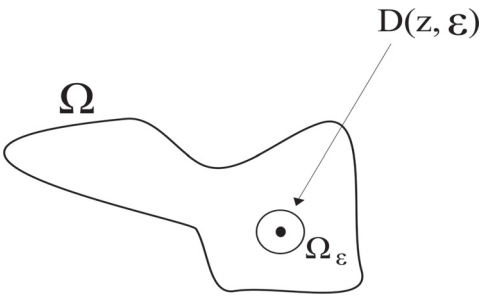

Figure 1 The domain Ω_ϵ.

We apply the complex Green's theorem to the function

$$\zeta \mapsto \frac{f(\zeta)}{\zeta - z}$$

(which has a singularity at the point $z = \zeta$) on the domain Ω_ϵ. Thus,

$$\frac{1}{2\pi i}\oint_{\partial\Omega_\epsilon}\frac{f(\zeta)}{\zeta - z}d\zeta = \frac{1}{2\pi i}\int_{\Omega_\epsilon}\frac{\partial}{\partial\overline{\zeta}}\left(\frac{f(\zeta)}{\zeta - z}\right)d\overline{\zeta}\,d\zeta. \tag{6}$$

Now, first notice that

$$\frac{\partial}{\partial\overline{\zeta}}\left(\frac{f(\zeta)}{\zeta - z}\right) = \frac{(\zeta - z)\cdot(\partial f/\partial\overline{\zeta}) - f\cdot 0}{(\zeta - z)^2} = \frac{\partial f/\partial\overline{\zeta}}{\zeta - z}.$$

So equation (6) becomes

$$\frac{1}{2\pi i}\oint_{\partial\Omega_\epsilon}\frac{f(\zeta)}{\zeta - z}d\zeta = \frac{1}{2\pi i}\int_{\Omega_\epsilon}\frac{\partial f/\partial\overline{\zeta}}{\zeta - z}\,d\zeta.$$

Because the integrand on the right is integrable, it is easy to see that the limit as $\epsilon \to 0^+$ of the right-hand side is

$$\frac{1}{2\pi i}\int_{\Omega}\frac{\partial f/\partial\overline{\zeta}}{\zeta - z}\,d\zeta.$$

Our job now is to calculate the term on the left-hand side of equation (6). We write it as

$$\frac{1}{2\pi i}\oint_{\partial\Omega}\frac{f(\zeta)}{\zeta - z}d\zeta - \frac{1}{2\pi i}\oint_{\partial D(z,\epsilon)}\frac{f(\zeta)}{\zeta - z}d\zeta. \tag{7}$$

Now, the first term in equation (7) is part of equation (5) and is something that we want. For the second term in equation (7), we write

$$\begin{aligned}\frac{1}{2\pi i}\oint_{\partial D(z,\epsilon)}\frac{f(\zeta)}{\zeta - z}d\zeta &= \frac{1}{2\pi i}\int_0^{2\pi}\frac{f(z+\epsilon e^{it})}{\epsilon e^{it}}\cdot i\epsilon e^{it}\,dt\\ &= \frac{1}{2\pi}\int_0^{2\pi} f(z+\epsilon e^{it})\,dt\\ &= \frac{1}{2\pi}\int_0^{2\pi} f(z)\,dt + \frac{1}{2\pi}\int_0^{2\pi} f(z+\epsilon e^{it}) - f(z)\,dt\\ &= f(z) + \mathcal{E}(z).\end{aligned} \tag{8}$$

The first term on the right of equation (8) equals $f(z)$ and the second term on the right of equation (8) vanishes as $\epsilon \to 0^+$.

In summary, as $\epsilon \to 0^+$, we see that equation (6) now becomes

$$\frac{1}{2\pi i}\int_{\partial\Omega}\frac{f(\zeta)}{\zeta - z}\,d\zeta - f(z) = \frac{1}{2\pi i}\iint_{\Omega}\frac{\partial f/\partial\overline{\zeta}}{\zeta - z}\,d\overline{\zeta}\,d\zeta\,.$$

This is just the same as equation (5). ■

Corollary 1. *Let $\Omega \subseteq \mathbb{C}$ be a bounded domain with continuously differentiable boundary. Let f be a function that is continuously differentiable on $\overline{\Omega}$ and holomorphic on Ω. Let $\mathbf{r}$ be a C^1 curve that is a positively oriented parameterization of $\partial\Omega$.*

Let $z \in \Omega$. Then

$$f(z) = \frac{1}{2\pi i} \oint_{\mathbf{r}} \frac{f(\zeta)}{\zeta - z}\, d\zeta.$$

Proof. Because f is holomorphic, the second term on the right-hand side of equation (5) is 0. ∎

The inhomogeneous Cauchy–Riemann equations

We are interested in solving the differential equation $(\partial/\partial\overline{z})u = f$ for a given function f. This is a powerful technique in the function theory of several complex variables, somewhat less familiar in the context of one complex variable. Our result is this

Theorem 5. *Let f be a continuously differentiable function with compact support in $\mathbb{C}$. Then the function defined by*

$$u(z) = -\frac{1}{2\pi i} \iint \frac{f(\zeta)}{\zeta - z}\, d\overline{\zeta}\, d\zeta = -\frac{1}{\pi} \iint \frac{f(\zeta)}{\zeta - z}\, dA(\zeta)$$

satisfies $(\partial/\partial\overline{z})u = f$.

Proof. Let $D(0, R)$ be a large disc that contains the support of f. Then

$$\begin{aligned}
\frac{\partial u}{\partial \overline{z}}(z) &= -\frac{1}{2\pi i} \frac{\partial}{\partial \overline{z}} \int_{\mathbb{C}} \frac{f(\zeta)}{\zeta - z} d\overline{\zeta}\, d\zeta \\
&= -\frac{1}{2\pi i} \frac{\partial}{\partial \overline{z}} \int_{\mathbb{C}} \frac{f(\zeta + z)}{\zeta} d\overline{\zeta}\, d\zeta \\
&= -\frac{1}{2\pi i} \int_{\mathbb{C}} \frac{\partial f(\zeta + z)/\partial \overline{\zeta}}{\zeta} d\overline{\zeta}\, d\zeta \\
&= -\frac{1}{2\pi i} \int_{D(0,R)} \frac{\partial f(\zeta)/\partial \overline{\zeta}}{\zeta - z} d\overline{\zeta}\, d\zeta.
\end{aligned}$$

By Theorem 4, this last equals

$$f(z) - \frac{1}{2\pi i} \int_{\partial D(0,R)} \frac{f(\zeta)}{\zeta - z} d\zeta = f(z)\,.$$

Here, we have used the support condition on f to see that the integral vanishes. This is the result that we wish to prove. ∎

An inspection of the proof shows that we may weaken the hypothesis on f to f is continuous with compact support.

An application of Theorem 5

A version of Weierstrass's classical theorem is this:

Theorem 6. *Let Ω be a bounded domain in $\mathbb{C}$. Let $\{p_j\}$ be a sequence of points in Ω with no interior accumulation point. Let k_j be positive integers. Then there is a meromorphic function f on Ω with a pole of order k_j at each p_j.*

Proof. Let φ_j be a continuous function with compact support of diameter

$$\frac{\operatorname{dist}(p_j, \partial\Omega)}{10},$$

with $\varphi_j(z) = 1$ in a small neighborhood of p_j. Shrinking the supports of the φ_j as needed, we may assume that the φ_j have pairwise disjoint supports.

Choose positive numbers a_j that tend to 0 as $j \to +\infty$ so rapidly that

$$\sum_{j=1}^{\infty} a_j \left(\frac{\partial}{\partial \overline{z}} \varphi_j \right) \cdot (z - p_j)^{-k_j} \equiv v$$

converges to an integrable function v. Use Theorem 5 to solve the equation $(\partial/\partial\overline{z})u = v$. Then the function

$$w(z) = \sum_{j=1}^{\infty} a_j \varphi_j \cdot (z - p_j)^{-k_j} - u$$

is the function that we seek. ■

By a small modification of this proof, we can prove Weierstrass's original theorem:

Theorem 7. *Let Ω be a bounded domain in $\mathbb{C}$. Let $\{p_j\}$ be a sequence of points in Ω with no interior accumulation point. Let k_j be positive integers. Then there is a holomorphic function g on Ω with a zero of order k_j at each p_j.*

Finally, one can multiply together the results of the last two theorems to obtain a full version of the original Mittag–Leffler theorem (see Greene and Krantz [2]):

Theorem 8. *Let Ω be a bounded domain in $\mathbb{C}$. Let $\{p_j\}$ be a sequence of points in Ω with no interior accumulation point. Let $\{q_j\}$ be another sequence of points in Ω, distinct from the $\{p_j\}$, with no interior accumulation point. Let k_j, ℓ_j be positive integers. Then there is a meromorphic function f on Ω with a pole of order k_j at each p_j and a zero of order ℓ_j at each q_j.*

Concluding remarks

Complex analysis as a subject is at least 400 years old, and it continues to grow and prosper. Its applications are many and diverse. This paper is a small contribution to our understanding of the subject. It is a pleasure to thank John P. D'Angelo and Harold Boas for helpful remarks concerning the subject matter of this paper. Let me also thank the referees for many useful comments and insights.

REFERENCES

[1] Blank, B. E., Krantz, S. G. (2006). *Calculus: Multivariable*. Emeryville, CA: Key College Publishing.

[2] Greene, R. E. Krantz, S. G. (2006). *Function Theory of One Complex Variable*, 3rd ed. Providence, RI: American Mathematical Society.

Summary. We present a definition of *holomorphic function* and an approach to the Cauchy theory that presents complex function theory as a natural outgrowth of multivariable calculus.

STEVEN G. KRANTZ was born in San Francisco, CA in 1951. He received the B.A. degree from the University of California in 1971 and the Ph.D. from Princeton University, NJ in 1974. Krantz has taught at the University of California, Los Angeles, Princeton University, Pennsylvania State, and Washington University in St. Louis. He was Chair of the latter department for five years. Krantz has had nine Master's students and 20 Ph.D. students. He has written more than 135 book and more than 270 scholarly papers. He edits five journals, and is Managing Editor of three. He is the creator, founder, and editor of the new journal *Complex Analysis and its Synergies*. Krantz has won the Chauvenet Prize, the Beckenbach Book Award, and the Kemper Prize. He was recently named to the Sequoia High School Hall of Fame. He is an AMS Fellow.

When to Hold 'Em

KAITY PARSONS
Loyola University, Chicago
Chicago, IL 60660
kaityscarlett22@gmail.com

PETER TINGLEY
Loyola University, Chicago
Chicago, IL 60660
ptingley@luc.edu

EMMA ZAJDELA
Northwestern University
Evanston, IL 60208
emma.zajdela@gmail.com

So you want to win at poker? Certainly you need to know how good any hand is, but that isn't the whole story: You still need to know what to do. That is, in the words of Don Schlitz [**16**] (made famous by Kenny Rogers [**15**]), you gotta know when to hold 'em, know when to fold 'em, know when to walk away, know when to run. Well, you're on your own for when to walk away and when to run. That leaves when to hold 'em, when to fold 'em, and a crucial question that was left out: when to bet.

We should pay attention to the real world, and the real world tells us the answers are probably interesting. Good poker players do some strange-looking things:

- Bet with very bad hands.
- Fail to bet with very good hands.
- Fold with good hands.

They even have names for these. The first is called bluffing and the second is called slow-playing. The third I guess is just called folding. One thing to think about is, are these actually good strategies? In some sense they must be, since the best players use them, but why? One possibility is that it is psychological: the players are messing with each other, trying to get each other to make mistakes. Let's eliminate that explanation. What if you are playing against a computer, and the computer is programmed to play perfectly. Then does it make sense to bluff? Or to slow-play?

We will answer these questions, but starting with real poker is too complicated. Instead we think about some simplified games to gain insight into the real thing. Simplified poker has been studied before, including by Borel [**2**] and von-Neumann and Morgenstern [**14**], and more recently by Chen and Ankenman [**4**] and Ferguson, Ferguson, and Gawargy [**8**]. This last we draw on quite heavily.

Dice poker

Here are the rules to the first game we will consider:

- There are only two players, P1 and P2.
- Each player begins by putting $1 in the pot (the "ante").

Math. Mag. **94** (2021) 201–212. doi:10.1080/0025570X.2021.1908785
MSC: 91-01

- Each player's hand is determined by rolling a die, so the possible hands are 1,2,3,4,5,6, and all are equally likely. The roll is hidden from the other player.
- After seeing their hand, P1 can either bet another \$1 or pass.
- If P1 bet, P2 can either *call* by also placing an extra \$1 in the pot, or *fold*, in which case P1 gets the money in the pot.
- If P1 passed or P1 bet and P2 called they compare hands and the higher number gets all the money in the pot. If there is a tie, they split the pot.

What we call passing is often called checking in poker. We use the term pass because call and check both start with C, which messes up notation.

We want to understand how P1 should play, where, as in the introduction, P2 is a computer that plays perfectly. But first we need to understand what we mean when we say that P2 plays perfectly. This is confusing because how P2 should play certainly depends on how P1 is playing . . . it gets circular!

Here is how we get around this: Instead of just letting them play, we make the players each write a computer program to play for them (like in pokerbots [**3**]). Furthermore, we make P1 write their program first, and *they let P2 see it*. We assume P2 is an expert poker player/programmer and writes the perfect program to do as well as possible, using their knowledge of P1's program. The question is, under these conditions, what is P1's best strategy?

Letting P2 see P1's strategy seems unfair, but it is also sort of realistic: Players can usually observe each other and learn about each other's strategies. So another way of wording this is that P2 has been observing P1 for a long time, and knows how P1 plays. Note that P2 does not get to see P1's hand.

We are looking for P1's best strategy, but what exactly is a strategy? Well, it is the program P1 writes, which has to take P1's hand and decide whether to bet or pass. So a strategy should be the information of what to do with each possible hand.

Let's try a reasonable looking strategy and see what happens: say P1 passes if they have 1, 2, or 3 and bets if they have 4, 5, or 6. P2 gets to take this information and figure out what to do. They should only think about what to do if P1 bets, since if P1 passes then hands are revealed without P2 ever having to make a decision. If P1 bets then P2 *knows they have 4, 5, or 6*. If P2 has 1, 2, or 3, they will definitely lose, and therefore should fold. If P2 has 6, they definitely don't lose, and therefore should call. The only question is what to do with 4 or 5. To figure that out, P2 can use Table 1. The rows show what happens after P1 bets if P2 has 4 or 5 and either calls or folds. In each case, the expected payout to P2 is the average the three entries in that row. If P2 has 4, then folding is better ($-1 > -\frac{4}{3}$), and if P2 has 5, then calling is better. We have just figured out that P2's *best response* to P1's strategy is to fold if they have 1234, and call if they have 5 or 6.

TABLE 1: Deciding on a response to P1 betting on 4, 5 and 6.

	4	5	6	Average
4C	0	−2	−2	−1.33
4F	−1	−1	−1	−1
5C	2	0	−2	0
5F	−1	−1	−1	−1

So, is this a good strategy for P1? To decide, we need to find the expected payout, which we do by making a table of possibilities, showing payouts to P2. See Table 2. All pairs of hands are equally likely, so the expected payout to P2 is the average of the 36 possibilities, which is $\frac{1}{36}$.

TABLE 2: Possible outcomes to P2 if P1 bets with 456 and P2 calls with 56.

Hand	1P	2P	3P	4B	5B	6B	Total of row
1F	0	−1	−1	−1	−1	−1	−5
2F	1	0	−1	−1	−1	−1	−3
3F	1	1	0	−1	−1	−1	−1
4F	1	1	1	−1	−1	−1	0
5C	1	1	1	2	0	−2	3
6C	1	1	1	2	2	0	7

P1 is losing money! Is this reasonable? Maybe, since P2 did get to look at P1's strategy . . . but actually P1 has an obvious strategy to break even: never bet! Then both players are equally likely to have the better hand and win $1.

Can P1 do better than break even? We could try some other straightforward strategies. Similar calculations show that betting on 56 or betting on only 6 both lead to breaking even. Betting on more highish hands, such as on 3456, loses even more money. There is no way for P1 to make money with this type of strategy.

Right, but we forgot one of our main questions: should P1 bluff? We need to try a strategy involving bluffing! That is, P1 should try betting on some bad hands. They should probably bet on more good hands than bad hands, so let's try betting on 156. To figure out P2's best response, we fill out the whole table of possibilities, see Table 3. This shows that P1 should fold with 1 and call with 23456. The expected outcome to P2 is the average of the resulting 36 possibilities, which is now $-\frac{2}{36}$. This time P1 is making money. And to do so their strategy *must* involve bluffing!

You should pause and think about this: We just showed that, even though P2 knows P1's strategy, and plays perfectly, P1 can still make money, but only if their strategy includes bluffing. So bluffing is a necessary part of a good strategy for P1. It is not just psychological. This is a simplified game, but we hope you agree it is realistic enough to suggest that bluffing is a good idea more generally (which it is).

Notice, though, that P2 is playing pretty strangely. For instance, does it really make sense to call with 2? This should suggest that we don't have the full answer yet.

If both players know each other's strategies: Nash equilibrium

One part of this setup tends to make people uncomfortable: letting P2 see P1's strategy. We argued that this was reasonable because over time P2 could observe what P1 does and figure out their strategy. But by that logic P1 can just as easily observe P2's strategy. So, if good players play each other many times, it seems they should end up each playing a best response to the other. This is essentially the idea of a Nash equilibrium.

This idea is usually attributed to John Nash [**10**, **11**] for his work from the early 1950s, but the concept existed earlier, at least in special cases. See, for instance,

TABLE 3: P2's possible responses if P1 bets on 156, showing payouts to P2. P2's best response is to choose the behaviors (call or fold) that has the highest expected outcome with each possible hand. So they should fold with 1 and call with 23456.

Hand	1B	2P	3P	4P	5B	6B	Row Total
1F	−1	−1	−1	−1	−1	−1	**−6**
1C	0	−1	−1	−1	−2	−2	−7
2F	−1	0	−1	−1	−1	−1	−5
2C	2	0	−1	−1	−2	-2	**−4**
3F	−1	1	0	−1	−1	−1	−3
3C	2	1	0	−1	−2	−2	**−2**
4F	−1	1	1	0	−1	−1	−1
4C	2	1	1	0	−2	−2	**0**
5F	−1	1	1	1	−1	−1	0
5C	2	1	1	1	0	−2	**3**
6F	−1	1	1	1	−1	−1	0
6C	2	1	1	1	2	0	**7**

Cournot's work from 1838 [**5**]. Our games are zero-sum (gain to one player equals loss to the other), and Nash equilibria in that setting were studied by von Neumann and Morgenstern in the 1940s [**14**], where they are called saddle points in strategies. Anyway, this is so crucial we will actually define it!

Definition 1. A *Nash equilibrium* for a two-player game is a pair of strategies, one for each player, such that each is a best response to the other.

This means that, if one player changes their strategy and the other does not, the player who changes does no better (on average) than they would have done by following their original strategy. Essentially, each is doing as well as possible assuming their opponent is playing well, so in that sense the strategies are optimal.

Let's think about dice poker some more. We found that P1 betting on 156 is a pretty good strategy, and that P2's best response is to call with 23456. But, if P1 knows that P2 will call with 23456, do they still want to bet on 156? The answer is no: As shown in Table 4, P1 would now like to bet with 56 and pass with 123, and it doesn't matter with 4. So P1 betting on 156 is not their best response, and hence these strategies (P1 bet on 156, P2 call on 23456) are not a Nash equilibrium.

Is there a Nash equilibrium? Well, if you let two good players play repeatedly, they should settle on strategies somehow, and it seems that these should be an equilibrium. Or they could just keep changing strategies, so maybe not.

In fact, with the type of strategy we've been using, there is no Nash equilibrium. One way to see this is to check that, for any P1 strategy, if you (i) find P2's best response, and then (ii) find P1's best response to that, you don't get back the same P1 strategy. So, that strategy cannot be part of an equilibrium pair. Doing this in every case is annoying, but you can probably convince yourself it is true by checking a few plausible P1 strategies (maybe bet on 1456 or on 1256).

TABLE 4: P1's options if P2 will call with 23456. Payouts are to P1. For each hand P1 should choose the behavior (bet or pass) with the highest expected payout, so they should bet with 56 and pass with 123, and either choice is equally good with 4.

Hand	**1P**	1B	**2P**	2B	**3P**	3B	4P	**4B**	5P	**5B**	6P	**6B**
1F	0	1	1	1	1	1	1	1	1	1	1	1
2C	−1	−2	0	0	1	2	1	2	1	2	1	2
3C	−1	−2	−1	−2	0	0	1	2	1	2	1	2
4C	−1	−2	−1	−2	−1	−2	0	0	1	2	1	2
5C	−1	−2	−1	−2	−1	−2	−1	−2	0	0	1	2
6C	−	−2	−1	−2	−1	−2	−1	−2	−1	−2	0	0
Column total	**−5**	−9	**−3**	−7	**−1**	−3	1	**1**	4	**5**	5	**9**

It might seem that we are stuck, but we missed another important thing you can learn from the real world: poker players like to be unpredictable, and don't always do the same thing in the same situation. We need more randomness!

Mixed strategies

A *mixed strategy* is a strategy where a player doesn't always do the same thing in the same situation. For instance, P1 can decide that, if they have 4, they will bet half the time and pass half the time. Then, whenever they are dealt 4, they randomize, maybe by flipping a coin, to decide which to do.

The famous (but kind of difficult) von-Neumann mini-max theorem [**13**] (see also, for example, Barron [**1**, Chapter 1.2]) implies that, if mixed strategies are allowed, Nash equilibria always exist (provided the number of unmixed strategies is finite, or some other more technical conditions hold). In any case, such an equilibrium does exist for our game. It is: P1 bets with 56, and bets $\frac{2}{3}$ of the time with 1. P2 calls with 456, and also calls $\frac{2}{3}$ of the time with 3. The table of payouts is given in Table 5, and works out to an expected payout to P2 of $\frac{-3.33}{36}$. So P1 is making significantly more money than with the strategy "bet with 156" we studied before (which is actually the best possible unmixed strategy).

To check that this is a Nash equilibrium just check that, in every situation, each player's expected value does not go up if they change strategies. For instance, if P1 decided to pass with 5, their expected payout would be 3, which is worse than the 3.66 they are currently getting. If P2 has a 4 and decides to fold, they get exactly the same as if they call (−0.33), which is still alright.

Something interesting: If P1 has 1, sometimes they bet and sometimes they pass. If this is a Nash equilibrium, in either case they should not want to change. That means the two possible strategies must lead to the same expected payout: if one was worse, P1 would never want to play it! This observation is called the *principle of indifference*. By the same argument P2 should get the same payout for passing and calling with 3.

If we somehow knew P1 and P2 should randomize with 1 and 3 respectively, this gives a way to find the Nash equilibrium: Let x be the probability $P1$ bets with 1. If

TABLE 5: Table of payouts to P2 for the Nash equilibrium in dice poker. Some outcomes now have probabilities associated with them. For instance, if P1 has 1 and P2 has 3, there is a probability of $\frac{1}{3}\frac{2}{3}$ that the outcome is -1 to P2, because P1 bets with probability $\frac{2}{3}$, and then P2 folds with probability $\frac{1}{3}$.

	Hand	1: $\frac{2}{3}$B	$+\frac{1}{3}P$	2P	3P	4P	5B	6B	Total of row
1	F	$\frac{2}{3}(-1)$	$+\frac{1}{3}0$	-1	-1	-1	-1	-1	-5.66
2	F	$\frac{2}{3}(-1)$	$+\frac{1}{3}1$	0	-1	-1	-1	-1	-4.33
3	$\frac{1}{3}F$	$\frac{1}{3}\frac{2}{3}(-1)$	$+\frac{1}{3}\frac{1}{3}1$	$\frac{1}{3}1$	$\frac{1}{3}0$	$\frac{1}{3}$(-1)	$\frac{1}{3}(-1)$	$\frac{1}{3}(-1)$	-2.33
	$+\frac{2}{3}C$	$\frac{2}{3}\frac{2}{3}(2)$	$+\frac{2}{3}\frac{1}{3}1$	$\frac{2}{3}1$	$\frac{2}{3}0$	$\frac{2}{3}$(-1)	$\frac{2}{3}$(-2)	$\frac{2}{3}$(-2)	
4	C	$\frac{2}{3}(2)$	$+\frac{1}{3}1$	1	1	0	-2	-2	-0.33
5	C	$\frac{2}{3}(2)$	$+\frac{1}{3}1$	1	1	1	0	-2	2.66
6	C	$\frac{2}{3}(2)$	$+\frac{1}{3}1$	1	1	1	2	0	6.66

P2 gets a 3, then their expected payouts are:

$$\text{Fold:}\quad \frac{x(-1)+(1-x)1+1+0-1-1-1}{6}=\frac{-1-2x}{6}.$$

$$\text{Call:}\quad \frac{x(2)+(1-x)1+1+0-1-2-2}{6}=\frac{-3+x}{6}.$$

These must be equal. Solving gives $x=\frac{2}{3}$. A similar calculation using P1's indifference with 1 gives that P2 should fold with probability $\frac{1}{3}$ with a 3.

We had to guess which hands to randomize with. If we had guessed wrong, we would have figured that out. For instance, if we guessed that P2 should fold with 3 and randomize with 4, then P1's indifference with 1 would imply that P2 should call with probability $\frac{5}{3}$ with 4, which is impossible. We could keep trying until we got it right, but that is annoying. We now move to a more continuous situation, which eliminates some of the guessing.

Allowing infinitely many possible hands

Now let's think about the same game but with one change: each player's hand is now a random number in the interval [0,1]. This is actually closer to real poker, where there are lots of possible hands and each has a different probability of winning, which can be expressed as a number in [0, 1]. This has been studied many times before, dating to von-Neumann and Morgenstern [**14**, Sections 19.14–19.16] (see also, for example, Chen and Ankenman [**4**, Ex. 11.3], Ferguson and Ferguson [**6**,**7**]; Ferguson, Ferguson, and Gawargy [**8**], and Mazalov [**12**, Chapter 5],). A variant where P1 must fold if they don't bet was studied even earlier by Borel [**2**, Chapter 5] (see also Karlin [**9**, §9.2]).

We want to find optimal strategies, which we now know means we are looking for a Nash equilibrium. We start by guessing that things are qualitatively similar to the dice game, and P1 should use a bluffing strategy: For some $x_1 < x_2$ P1 should bet with hands $h < x_1$ and $h > x_2$, and pass for $x_1 \le h \le x_2$. P2 should call with hands better than some cutoff value y_1. It also seems reasonable to guess that $x_1 \le y_1 \le x_2$. The strategies and payouts to P2 are then described by a "table," as in Figure 1.

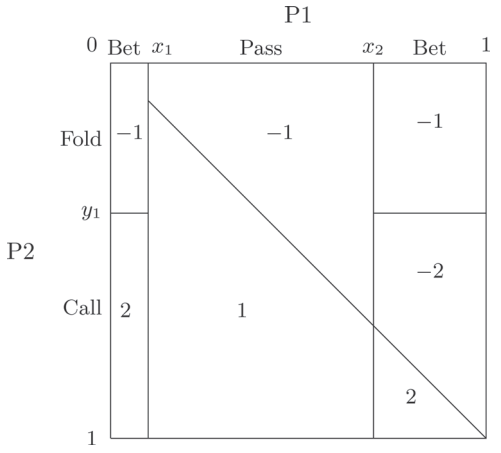

Figure 1 Strategies and payouts for the continuous game. This is interpreted as follows: If P1 gets hand x and P2 gets hand y, plot x and y on the top and left respectively, and then read off what they do. The number in the region containing (x, y) is the resulting payout to P2.

We want to find the cutoffs. The key idea is that, if e.g. P1 has hand exactly x_1, it shouldn't matter if they bet or pass. This is because with a slightly better hand passing is better, and with a slightly worse hand betting is better. But if the behavior (bet or pass) is kept fixed and the hand varies the payout changes continuously. So the payout for a bet and a pass with exactly x_1 must be identical. This is really an indifference principle as above: P1 can play a mixed strategy with x_1 if they like, although getting exactly x_1 has probability zero, so never happens.

To find the payout if P1 has x_1 and bets, we average over possible P_2 hands:

- If P2 has hand $h < y_1$ they fold and P1 wins \$1. This has probability y_1
- If P2 has hand $h > y_1$ they call and P1 loses \$2. This has probability $1 - y_1$.

If P1 has hand x_1 and passes,

- If P2 has hand $h < x_1$ then P1 wins \$1. This has probability x_1
- If P2 has hand $h > x_1$ then P1 loses \$1. This has probability $1 - x_1$.

So we get the *indifference equation*:

$$y_1 - 2(1 - y_1) = x_1 - (1 - x_1).$$

We also get equations from P1's indifference with x_2 and P2's indifference with y_1:

$$\begin{aligned} &\text{P1 with } x_2: \quad -x_2 + (1 - x_2) = -y_1 - 2(x_2 - y_1) + 2(1 - x_2), \\ &\text{P2 with } y_1: \quad -x_1 - (1 - x_2) = 2x_1 - 2(1 - x_2). \end{aligned} \tag{1}$$

This is just a system of three equations in three unknowns! Solving,

$$x_1 = \frac{1}{10}, \quad x_2 = \frac{7}{10}, \quad y_1 = \frac{4}{10}.$$

We made a guess: that the solution has the rough form shown in Figure 1. So we need to check that our answer really is a Nash equilibrium. There are three cases:

1. If P2 has hand $h = \frac{4}{10}$, they get the same payout for calling and folding. After a bet, the payout for folding is constant (-1), and the payout for calling is weakly increasing with h. Thus, folding is best if $h < \frac{4}{10}$ and calling is best if $h > \frac{4}{10}$.
2. P1 gets the same payout for passing as bluffing with hand $h = \frac{1}{10}$. The payout for bluffing is independent of h for $h \leq \frac{4}{10}$ and the payout for passing is increasing, so this implies that bluffing is better than passing for $h < \frac{1}{10}$, and that passing is better than bluffing for $\frac{1}{10} < h < \frac{4}{10}$.
3. If P1 has a hand $h > \frac{4}{10}$, their expected payout if they bet is

$$\frac{4}{10} + 2(h - \frac{4}{10}) - 2(1 - h),$$

and their expected payout if they pass is $2h - 1$. Subtracting, they expect to win $2h - \frac{7}{5}$ more by betting, which is positive for $h > \frac{7}{10}$ and negative for $h < \frac{7}{10}$, so passing is better if $\frac{4}{10} < h < \frac{7}{10}$ and betting is better if $h > \frac{7}{10}$.

Neither player wants to change in any situation, so this is in fact a Nash equilibrium.

Things often work this way: you make some guesses, then solve indifference equations to get an answer, then you have to check that it really is an equilibrium, which proves your guesses were correct . . . or they weren't, and you try again.

Anyway, we have an answer! P1 bluffs with the worst 10% of hands, *value bets* on the best 30% of hands, and otherwise passes. P2 calls a bet with any hand better than 0.4. To find the expected payout, just add up the payout in each region times its area (the probability of landing in that region). It works out to P2 losing \$0.1 a hand.

This game makes sense for any bet size a. The "table" is the same, except all 2s become $1 + a$. The cutoffs are the solutions x_1, x_2, y_1 to the indifference equations

$$2(y_1 - x_1) = a(1 - y_1), \quad 1 - x_2 = x_2 - y_1, \quad (2 + a)x_1 = a(1 - x_2). \tag{2}$$

Different bet sizes lead to different payouts, and it turns out that $a = 2$ is best for P1, giving a payout of $\frac{1}{9}$ (see Ferguson, Ferguson, and Gawarkey [**8**, §1.1]). However, if P1 can bet different amounts with different hands, then they can do even better, up to a payout of $\frac{1}{7}$ (see Mazalov [**12**, §5.2]).

More betting

We now allow P2 to bet, but only if P1 passes. That is, we consider the game as above, with P1's bet size being a, and the following new options:

- If P1 passes then P2 can choose to bet a fixed amount b.
- If P2 bets then P1 can call or fold.

We do not assume P1 and P2 use the same bet size, but we do assume each uses a single fixed bet size whenever they bet. This can be described by the tree in Figure 2. This game has been studied before, for instance in Ferguson, Ferguson, and Gawarkey[**8**], where all the results presented here can be found. See also [**4**, Example 17.1].

As usual we have to guess the rough layout, and this time we make two separate guesses. See Figure 3. For any value of a, b we solve indifference equations to find the cutoffs. The diagram also implies an assumed ordering on the cutoffs. For example, in (L), $x_1 \leq y_1 \leq x_2$, $y_2 \leq x_3 \leq y_3 \leq x_4$. These constraints must hold in addition to the indifference equations. We will see that (L) works when $a \leq b$ and (R) works when $a \geq b$. If $a = b$ this means there are two natural Nash equilibria!

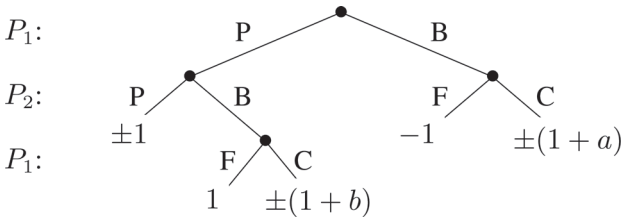

Figure 2 Betting tree if P2 can bet after a P1 pass. Here payouts are to P2 and ± means + if P2 has the higher hand and − if P1 has the higher hand.

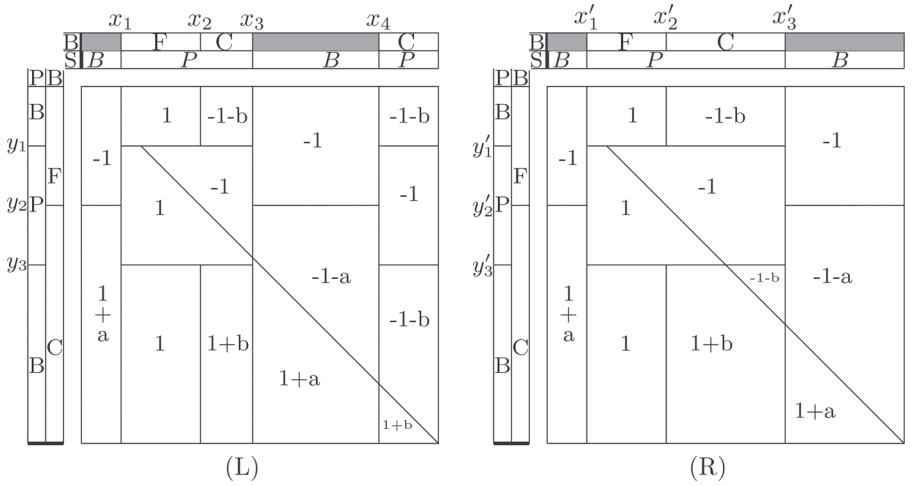

Figure 3 Two candidate Nash equilibria. Here P1's hand is increasing left to right and P2's hand is increasing top to bottom. The strategies are given on the top and left respectively, where B stands for bet, P for pass, C for call, and F for fold. There are two rows for P1's strategy, since there are two situations where they may have to make a choice: at the start of the game (S) and after a P2 bet (B). Similarly there are two columns for P2's strategy, showing what P2 does if P1 passed (P) or bet (B). The quantities in the interior show payouts to P2.

Each cutoff determines one indifference equation: If a player has exactly that hand, then the strategies on the two sides of the cutoff must give the same expected payout. For instance, for (L), there are 7 equations:

$$-y_2 + (1+a)(1-y_2) = 1 \tag{3}$$

$$y_1 + (1-y_3) = -(1+b)y_1 + (1+b)(1-y_3) \tag{4}$$

$$\begin{aligned} -(1+b)y_1 - (x_3 - y_1) + (y_3 - x_3) + (1+b)(1-y_3) = \\ -y_2 - (1+a)(x_3 - y_2) + (1+a)(1-x_3) \end{aligned} \tag{5}$$

$$\begin{aligned} -y_2 - (1+a)(x_4 - y_2) + (1+a)(1-x_4) = \\ -(1+b)y_1 - (y_3 - y_1) - (1+b)(x_4 - y_3) + (1+b)(1-x_4) \end{aligned} \tag{6}$$

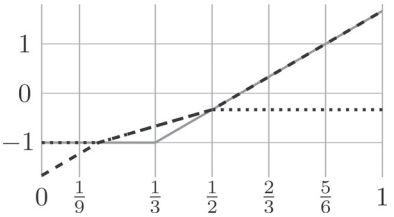

Figure 4 P1's expected payout as a function of hand for their three possible behaviors if P2 plays with cutoffs from equation (10). Here the dotted line is for PF, the dashed line for PC, and the gray line for B.

$$(x_2 - y_1) - (1+b)(x_3 - x_2) - (1+b)(1 - x_4) = -(x_3 - y_1) - (1 - x_4) \tag{7}$$

$$-x_1 - (x_4 - x_3) = (1+a)x_1 - (1+a)(x_4 - x_3) \tag{8}$$

$$(x_3 - x_2) - (1 - x_4) = (1+b)(x_3 - x_2) - (1+b)(1 - x_4). \tag{9}$$

We solve using Mathematica*. For $a = b = 1$ we get

$$\begin{aligned} (L): &\quad x_1 = \frac{1}{9},\ x_2 = \frac{1}{3},\ x_3 = \frac{1}{2},\ x_4 = \frac{5}{6},\ y_1 = \frac{1}{6},\ y_2 = \frac{1}{3},\ y_3 = \frac{1}{2}. \\ (R): &\quad x_1' = \frac{1}{9},\ x_2' = \frac{1}{3}\ x_3' = \frac{2}{3},\ y_1' = \frac{1}{6},\ y_2' = \frac{1}{3},\ y_3' = \frac{1}{2}. \end{aligned} \tag{10}$$

Note that for these values $P2$ uses the same strategy in both (L) and (R).

We made some guesses, so we need to check if these really are Nash equilibria. For now we restrict to $a = b = 1$ when we show that both are. They then give the same payout (as they must, see, e.g., [**1**, §1.1]) which is $\frac{1}{18}$ to P2.

We start by showing that P1 is responding optimally to P2's strategy. Consider P1's expected payout as a function of their hand h if P2 uses the cutoffs $y_1 = \frac{1}{6},\ y_2 = \frac{1}{3},\ y_3 = \frac{1}{2}$ from (10) and P1 plays

PF: pass then fold if P2 bets, PC: pass then call if P2 bets, B: bet.

A little work shows these functions are

$$\mathrm{PF}(h) = \begin{cases} -1 & h \le \frac{1}{6} \\ -\frac{4}{3} + 2h & \frac{1}{6} \le h \le \frac{1}{2} \\ -\frac{1}{3} & h \ge \frac{1}{2} \end{cases} \qquad \mathrm{PC}(h) = \begin{cases} -\frac{5}{3} + 4h & h \le \frac{1}{6} \\ -\frac{4}{3} + 2h & \frac{1}{6} \le h \le \frac{1}{2} \\ -\frac{7}{3} + 4h & h \ge \frac{1}{2} \end{cases} \tag{11}$$

$$\mathrm{B}(h) = \begin{cases} -1 & h \le \frac{1}{3} \\ -\frac{7}{3} + 4h & h \ge \frac{1}{3}. \end{cases}$$

These are shown in Figure 4. Both of P1's strategies in equation (10) always choose an optimal response. For instance for $h > \frac{5}{6}$, (L) plays PC and (R) plays B, but both are optimal because the dashed and gray lines coincide and are at the top in that range.

*Our code is available at http://webpages.math.luc.edu/~ptingley/

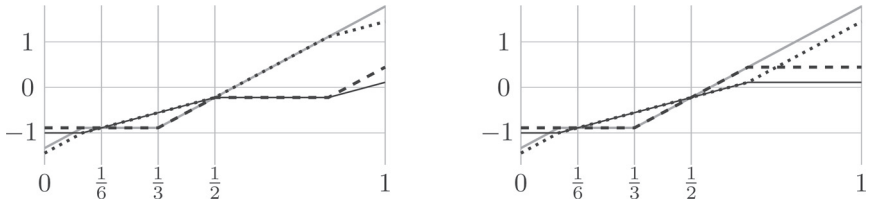

Figure 5 P2's payout as a function of hand if P1 plays as in (L), shown on the left, and (R), on the right. The lines are for P2 playing: (i) Solid: FP, fold after a bet and pass after a pass. (ii) Dashed: FB, fold after a bet and bet after a pass. (iii) Dotted: CP, call after a bet and pass after a pass. (iv) Gray: CB, call after a bet and bet after a pass.

We also need to show that P2 is responding optimally in every situation. This time we need two graphs to show what happens against P1's two different strategies in (10). See Figure 5. In both cases the dashed line is maximal for $h < \frac{1}{6}$, the solid line is maximal for $\frac{1}{6} < h < \frac{1}{3}$, the dotted line is maximal for $\frac{1}{3} < h < \frac{1}{2}$, and the gray line is maximal for $h > \frac{1}{2}$. So this P2 strategy is a best response to both P1 strategies.

We have now shown that, at $a = b = 1$, both (L) and (R) really are Nash equilibria! In (L) P1 is slow-playing their very best hands, by passing and hoping P2 bets. So slow-playing is a reasonable strategy. Although, as discussed in Ferguson, Ferguson, and Gawarkey [**8**], (R) may be better for P1 in practice since it penalizes more common P2 errors.

This argument works to show that (L) is an equilibrium in most cases with $a \leq b$, (R) is an equilibrium in most cases with $a \geq b$, and both are equilibria whenever $a = b$. If a and b are far apart some other cases appear, basically because the bluff cutoffs x_1 and y_1 reverse, changing the indifference equations. These are handled in our previously mentioned Mathematica code.

If $b > a$ then (R) is never an equilibrium, even though solving the equations often gives cutoffs in the correct order (this happens at e.g. $a = 1, b = 2$). This is because, if $b > a$, then $\mathrm{PC}(h)$ is increasing faster than $\mathrm{B}(h)$ for $h > x_3'$. But $\mathrm{B}(x_3') = \mathrm{PC}(x_3')$ so, for $h > x_3'$, $\mathrm{PC}(h) > \mathrm{B}(h)$. Since (R) plays B for $h > x_3'$ this violates the Nash condition. Similarly (L) is never a Nash equilibrium if $a > b$.

Remark. A situation like this one shows up in real poker: if there are only two players, and one of them has so few chips that only one bet can be made. But even then there are additional complications, for instance due to a flop or draw. Some of our conclusions, such as that optimal play involves bluffing, certainly still hold. But we will not analyze even the simplest situation in a real game here.

Acknowledgments P.T. thanks Yan X Zhang for his awesome talk "Myths of Poker Mathematics" which partly inspired this work, E. Barron for convincing him to teach game theory, and his game theory students for all they taught him. We also thank the many students who commented on early versions of this work, and especially Emily Danning He for a very careful proofreading. K.P. and E.Z. received REU funds from NSF grant DMS 1265555. K.P. was also supported by a Loyola Provost's fellowship.

REFERENCES

[1] Barron, E. N. (2013). *Game Theory: An Introduction*. Sec. Ed. Hoboken: John Wiley & Sons.
[2] Borel, É. (1938). *Traité du Calcul des Probabilités et ses Applications Volume IV, Fascicule 2, Applications aux jeux des hazard*. Paris: Gautier-Villars.
[3] Pokerbots: http://pokerbots.org/
[4] Chen, B., Ankenman, J. (2006). *The Mathematics of Poker*. Pittsburgh, PA: ConJelCo.
[5] Cournot, A. (1838). *Researches on the Mathematical Principles of the Theory of Wealth*. London: The Macmillan Co.

[6] Ferguson, C., Ferguson, T. (2003). On the Borel and von Neumann poker models. In *Game Theory and Applications*, Vol. 9. Hauppauge: Nova Science, pp. 17–32.
[7] Ferguson, C., Ferguson, T. The endgame in poker. https://www.math.ucla.edu/ tom/papers/poker3.pdf
[8] Ferguson, C., Ferguson, T., Gawargy, C. (2004). Uniform (0, 1) two-person poker models. In *Game Theory and Applications*, Vol. 12. Hauppauge: Nova Science, pp. 17–37.
[9] Karlin, S. (1959). *Mathematical Methods and Theory in Games, Programming and Economics. Vol. I: Matrix Games, Programming, and Mathematical Economics. Vol. II: The Theory of Infinite Games*. Reading, MA and London: Addison-Wesley Publishing.
[10] Nash, J. (1950). Equilibrium points in n-person games. *Proc. Nat. Acad. Sci. USA*. 36(1): 48–49. doi.org/10.1073/pnas.36.1.48
[11] Nash, J. (1951). Non-cooperative games. *Ann. Math.* Second Series. 54(2): 286–295. doi.org/10.2307/1969529
[12] V. Mazalov. (2014). *Mathematical Game Theory and Applications.* Chichetser: John Wiley & Sons, Ltd.
[13] von Neumann, J. (1928). Zur Theorie der Gesellschaftsspiele *Math. Annalen.* 100(1): 295–320. doi.org/10.1007/BF01448847.
[14] von Neumann, J., Morgenstern, O. (1944). *Theory of Games and Economic Behavior*. Princeton, NJ: Princeton University Press.
[15] Rogers, K. (1978). "The Gambler". From *The Gambler*, United Artists Group.
[16] Schlitz, D. (1976). "The Gambler" (song).

Summary. We consider the age-old question: how do I win my fortune at poker? First a disclaimer: this is a poor career choice. But thinking about it involves some great math! Of course, you need to know how good your hand is, which leads to some super-fun counting and probability, but you are still left with questions: Should I hold 'em? Should I fold 'em? Should I bet all my money? It can be pretty hard to decide! Here we get some insight into these questions by thinking about simplified games. Along the way we introduce some ideas from game theory, including the idea of Nash equilibrium.

KAITY PARSONS (MR Author ID: 1345241) received a B.S. in Mathematics from Loyola University Chicago in 2017. Since graduating, Kaity has been working as a center director at the Town and Country Mathnasium in St. Louis Missouri. She and her partner are currently planning a one-way cross-country road trip with their dog, Angel and their cat, Salem, to seek what they will find.

PETER TINGLEY (MR Author ID: 679482) received a Ph.D. in Mathematics from the University of California, Berkeley in 2008. He spent short periods at the University of Melbourne (Australia) and MIT, and since 2012 has been at Loyola University Chicago. He also helps run the Chicago Math Teachers' circle, which he co-founded in 2015, and is the current blue division racquetball champion at the Evanston YMCA.

EMMA ZAJDELA (MR Author ID: 1345242) received a B.S. in math and physics from Loyola University Chicago in 2016 and an M.S. in math from the University of Illinois, Chicago in 2018. She is currently an NSF fellow and Ph.D. student in Applied Mathematics at Northwestern University. Since 2016 she has served as Assistant to the President of the Malta Conferences Foundation, a nonprofit that uses science as a bridge to peace in the Middle East. She also recently received her yellow belt in judo.

Report on the 61st Annual International Mathematical Olympiad

BÉLA BAJNOK
Gettysburg College
Gettysburg, PA 17325
bbajnok@gettysburg.edu

EVAN CHEN
Massachusetts Institute of Technology
Cambridge, MA 02139
evan@evanchen.cc

The International Mathematical Olympiad (IMO) is the world's leading mathematics competition for high school students, and is organized annually by different host countries. The competition consists of three problems each on two consecutive days, with an allowed time of four-and-a-half hours both days. In recent years, more than one hundred countries have sent teams of up to six students to compete.

The 61st IMO was to take place in July of 2020 in St. Petersburg, Russia. Due to the COVID-19 pandemic, the competition was postponed and held remotely. The competition was ultimately given on September 21 and 22, 2020, at universally coordinated times (which meant that students in the Americas had to start their work in the middle of the night).

The members of the US team are chosen during the Math Olympiad Program (MOP) each year, a year-long endeavor organized by the Mathematical Association of America's American Mathematics Competitions (AMC) program. Students gain admittance to MOP based on their performance on a series of examinations, culminating in the USA Mathematical Olympiad (USAMO). A report on the 2020 USAMO can be found in the April 2021 issue of this *Magazine*; more information on the American Mathematics Competitions program can be found on the site https://www.maa.org/math-competitions.

The members of the 2020 US team were Quanlin Chen (11th grade, Princeton International School of Mathematics and Science, Princeton, NJ); Gopal Krishna Goel (11th grade, Krishna Homeschool, Portland, OR); Tianze Jiang (11th grade, Princeton International School of Mathematics and Science, Princeton, NJ); Jeffrey Kwan (12th grade, Harker Upper School, San Jose, CA); Luke Robitaille (10th grade, Robitaille Homeschool, Euless, Texas); and William Wang (West Windsor-Plainsboro High School North, Plainsboro Township, NJ). Chen, Robitaille, and Wang each earned Gold Medals, and Goel, Jiang, and Kwan each earned Silver Medals. In the unofficial ranking of countries, the United States finished third after China (first) and Russia (second).

Below we present the problems and solutions of the 61st IMO. The solutions we feature here are those of the indicated students, as edited by the two authors of this report.*

Problem 1 *Proposed by Dominik Burek, Poland.* Consider the convex quadrilateral

Math. Mag. **94** (2021) 215–224. doi:10.1080/0025570X.2021.1909378

*The online version of this article has color diagrams. We have not edited out the few references to color aspects of the diagrams for this print version.

ABCD. The point P is in the interior of *ABCD*. The following ratio equalities hold:

$$\angle PAD : \angle PBA : \angle DPA = 1 : 2 : 3 = \angle CBP : \angle BAP : \angle BPC.$$

Prove that the following three lines meet in a point: the internal bisectors of angles $\angle ADP$ and $\angle PCB$ and the perpendicular bisector of segment *AB*.

Solution by Isabella Quan, 10th grade, Westlake High School, Austin, TX. Let O be the circumcenter of $\triangle PAB$ (see Figure 1). We will prove that each of the three lines specified in the problem go through O. Since $AO = BO$, this clearly holds for the perpendicular bisector of *AB*. Below we prove that O lies on the internal bisector of $\angle PCB$; the claim about the internal bisector of $\angle ADP$ can be verified similarly.

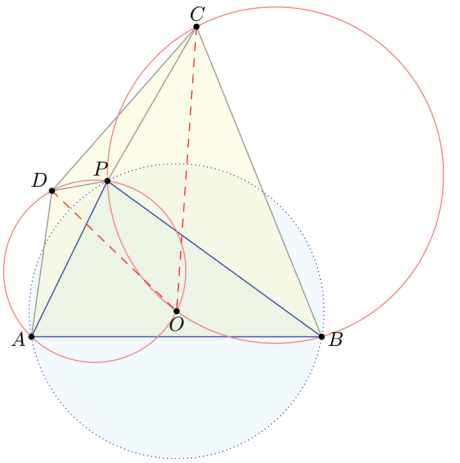

Figure 1 The diagram for Problem 1.

Note that

$$\angle PCB = \pi - (\angle CBP + \angle BPC)$$

and, by the given condition,

$$\angle CBP + \angle BPC = 2\angle BAP.$$

But by the inscribed angle theorem, $\angle BOP = 2\angle BAP$ as well, and thus $\angle PCB$ and $\angle BOP$ are supplementary, which implies that quadrilateral *BOPC* is cyclic. Because $OP = OB$, the inscribed angles $\angle PCO$ and $\angle OCB$ in the circumcircle of quadrilateral *BOPC* are equal, and hence O lies on the angle bisector of $\angle PCB$, as claimed.

Problem 2 *Proposed by Stijn Cambie, Netherlands.* The real numbers a, b, c, d are such that $a \geq b \geq c \geq d > 0$ and $a + b + c + d = 1$. Prove that

$$(a + 2b + 3c + 4d)a^a b^b c^c d^d < 1.$$

Solution by Luke Robitaille, 10th grade, Robitaille Homeschool, Euless, TX. We will prove that, for real numbers a, b, c, and d satisfying the conditions of the problem, we have:

$$a^a b^b c^c d^d \leq a^2 + b^2 + c^2 + d^2 \tag{1}$$

and

$$(a+2b+3c+4d)(a^2+b^2+c^2+d^2) < 1. \tag{2}$$

These two inequalities together clearly imply the claim of the problem.

Our first inequality follows from the weighted AM-GM inequality, as we now explain. Let us recall that for a positive integer n and nonnegative real numbers $x_1, \ldots, x_n, w_1, \ldots, w_n$ with

$$w = w_1 + \cdots + w_n > 0,$$

the *weighted arithmetic mean* of $x_1, \ldots, x_n$ with corresponding weights $w_1, \ldots, w_n$ is defined as

$$\frac{w_1x_1 + \cdots + w_nx_n}{w},$$

and their *weighted geometric mean* is defined as

$$\sqrt[w]{{x_1}^{w_1} \cdot \cdots \cdot {x_n}^{w_n}}.$$

The *weighted AM-GM inequality* then states that the weighted arithmetic mean is always at least as much as the weighted geometric mean; that is:

$$\sqrt[w]{{x_1}^{w_1} \ldots {x_n}^{w_n}} \leq \frac{w_1x_1 + \cdots + w_nx_n}{w}.$$

(The case when all weights equal 1 yields the regular AM-GM inequality.) Applying the weighted AM-GM inequality for

$$n = 4, \quad x_1 = w_1 = a, \quad x_2 = w_2 = b, \quad x_3 = w_3 = c, \quad x_4 = w_4 = d,$$

and noting that $a + b + c + d = 1$, readily gives equation (1).

To establish equation (2), we prove more generally that for real numbers a, b, c, and d with $a \geq b \geq c \geq d > 0$, we have

$$(a+2b+3c+4d)(a^2+b^2+c^2+d^2) < (a+b+c+d)^3. \tag{3}$$

In order to do so, we transform to new variables r, s, t, u, defined as $r = a - b$, $s = b - c$, $t = c - d$, and $u = d$; our assumptions imply that $r, s, t \geq 0$ and $u > 0$. Since

$$a = r + s + t + u, \quad b = s + t + u, \quad c = t + u, \quad d = u,$$

we have

$$a + 2b + 3c + 4d = r + 3s + 6t + 10u$$

and

$$\begin{aligned} a^2 + b^2 + c^2 + d^2 &= (r+s+t+u)^2 + (s+t+u)^2 + (t+u)^2 + u^2 \\ &= r^2 + 2s^2 + 3t^2 + 4u^2 + 2rs + 2rt + 2ru + 4st + 4su + 6tu, \end{aligned}$$

and thus we get

$$\begin{aligned} (a+2b+3c+4d)(a^2+b^2+c^2+d^2) = {} & r^3 + 6s^3 + 18t^3 + 40u^3 + \\ & 5r^2s + 8r^2t + 12r^2u + 8rs^2 + 24s^2t + 32s^2u + \end{aligned}$$

$$15rt^2 + 33st^2 + 66t^2u + 24ru^2 + 52su^2 + 84tu^2 + 22rst + 30rsu + 38rtu + 82stu.$$

Furthermore,

$$\begin{aligned}(a+b+c+d)^3 &= (r+2s+3t+4u)^3 \\ &= r^3 + 8s^3 + 27t^3 + 64u^3 + \\ &\quad 6r^2s + 9r^2t + 12r^2u + 12rs^2 + 36s^2t + 48s^2u + \\ &\quad 27rt^2 + 54st^2 + 108t^2u + 48ru^2 + 96su^2 + 144tu^2 + \\ &\quad 36rst + 48rsu + 72rtu + 144stu.\end{aligned}$$

Making term-wise comparisons, we can verify that

$$(a+2b+3c+4d)(a^2+b^2+c^2+d^2) \le (a+b+c+d)^3,$$

and since $u > 0$ implies that $40u^3 < 64u^3$, we see that, in fact, strict inequality holds, which proves equation (3). This completes our proof.

Problem 3 *proposed by Milan Haiman (Hungary) and Carl Schildkraut (USA).* There are $4n$ pebbles of weights $1, 2, 3, \ldots, 4n$. Each pebble is colored in one of n colors, and there are four pebbles of each color. Show that we can arrange the pebbles into two piles, so that the total weights of both piles are the same and each pile contains two pebbles of each color.

Solution by Alex Zhao, 8th grade, Kamiakin Middle School, Kirkland, WA. We begin by pairing off the pebbles so that each pair sums to the same value; namely, pairing 1 and $4n$, 2 and $4n-1$, 3 and $4n-2$, …, so that each pair adds up to $4n+1$. Then, it is sufficient to split these $2n$ *pairs* into two groups of n pairs each, such that each pile contains two pebbles of each color.

We separate the pebbles by color and put pebbles of the same color into a box of their own. We then draw a line between the two pebbles of each pair. (Some of the lines could start and end in the same box.) The problem can then be rephrased as follows: we wish to color each of the lines either blue or green, such that each box has two pebbles which are endpoints of blue lines, and two pebbles which are endpoints of green lines. (These new colors are not related to the colors in the original problem. They correspond to whether we put the pair in one pile or the other.) An example with $n = 5$ is illustrated in Figure 2.

We can capture this information in a single multigraph G. (A multigraph is like a graph, but edges may be repeated. We also allow an edge to join a vertex to itself.) Each box is a vertex of G, and each line is an edge of the multigraph. Hence, this graph will have n vertices and degree 4 at every vertex. Figure 3 is the multigraph G corresponding to our previous example. (The circle that passes through A denotes the edge from A to itself.)

Consider any connected component of this multigraph. Since the degree of every vertex is even, the component has an *Eulerian cycle*—a cycle passing through every edge. (In the above figure, one example of an Eulerian cycle is *AABCDEBECDA*.)

So, consider any connected component and one of its Eulerian cycles. Since the degree of each vertex is 4, the sum of all degrees is a multiple of 4, and so the number of edges (half the sum of the degrees) is even. Therefore we can alternately color the edges in the Eulerian cycle blue and green. Figure 4 shows an alternating coloring of *AABCDEBECDA* in this way.

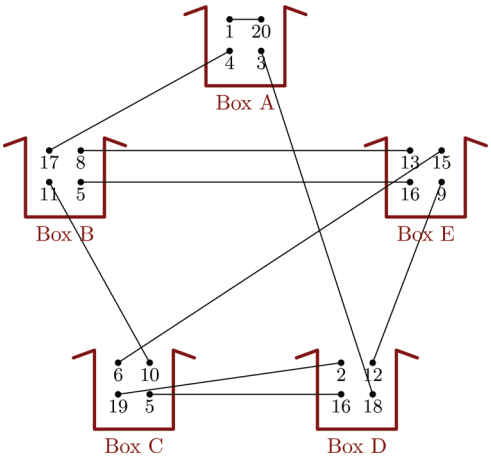

Figure 2 An example for $n = 5$ in Problem 3.

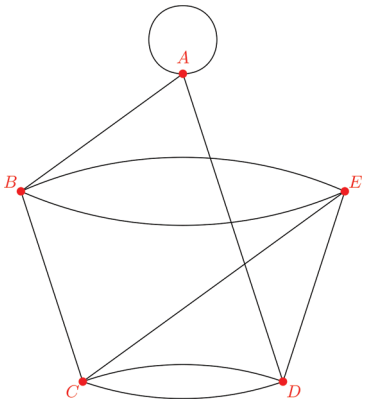

Figure 3 The multigraph corresponding to the example in Figure 2.

We can now easily see that this coloring works:

- If the vertex has one self-loop, the two outgoing edges must be colored the same, and differently from the self-loop.
- If the vertex has no self-loops, the cycle visits the vertex twice, and the two edges going in and out of each visit are colored differently from each other.
- If the vertex has two self-loops (which can only happen if the connected component has only a single vertex) then those two self-loops are colored differently.

Having found the desired coloring, the problem is solved. Figure 5 shows the translation of our coloring example into a valid partition of the pairs.

Problem 4 *Proposed by Tejaswi Navrinarekallu, India*. Let $n > 1$ be an integer. There are n^2 stations on a slope of a mountain, all at different altitudes. Each of two cable car companies, A and B, operates k cable cars; each cable car provides a transfer from one of the stations to a higher one (with no intermediate stops). The k cable cars of A have k different starting points and k different finishing points, and a cable car that starts higher also finishes higher. The same conditions hold for B. We say that two stations are linked by a company if one can start from the lower station and reach the higher

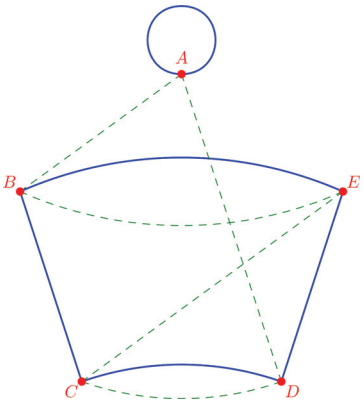

Figure 4 A coloring of an Eulerian cycle.

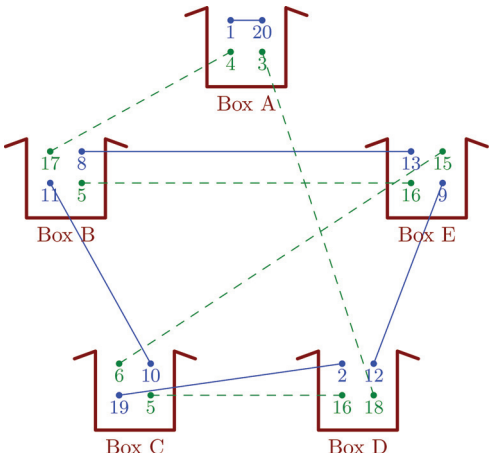

Figure 5 Translating the coloring into a valid partition of pairs.

one by using one or more cars of that company (no other movements between stations are allowed). Determine the smallest positive integer k for which one can guarantee that there are two stations that are linked by both companies.

Solution by Ryan Li, 10th grade, Solon High School, Solon, OH. We claim that the answer is $k = n^2 - n + 1$.

We label the stations by $0, 1, 2, \ldots, n^2 - 1$ in ascending order of altitude. Let G_A be a simple graph with n^2 vertices defined as follows:

- The vertices are the n^2 stations.
- Two vertices are joined by an edge if and only if they are joined by a cable car from company A.

The graph G_B is defined in an analogous way, with the connections from company B instead of company A.

Lemma. *Two stations are linked by A (as defined in the problem statement) if and only if they are connected in the graph G_A.*

Proof. Obviously, being linked implies being connected. It remains to be verified that the converse is true.

Suppose we have a path from station i to station j in G_A, where $i < j$, given by labels

$$i = a_0 \to a_1 \to \cdots \to a_{m-1} \to a_m = j.$$

We claim that $i < a_1 < a_2 < \cdots < a_{m-1} < j$.

Indeed, note that for $r = 1, 2, \ldots, m-1$, each a_r is connected to a_{r-1} and a_{r+1} by cable cars . Since the starting points and ending points of each cable car are unique, a_{r-1} and a_{r+1} cannot be both higher or lower than a_r, so either

$$a_{r-1} < a_r < a_{r+1} \qquad \text{or} \qquad a_{r-1} > a_r > a_{r+1}$$

for each r.

Since $i < j$, this implies $i = a_0 < a_1, a_1 < a_2, \ldots, a_{m-1} < a_m = j$, as claimed. ■

Now we prove that $k = n^2 - n + 1$. First, we show that there exists a construction for $k = n^2 - n$ such that no two stations are linked by both company A and company B. Consider the situation in which for every integer $0 \le i \le n-1$, company A links together $i, i+n, i+2n, \ldots, i+n^2-n$ in a series and company B links together stations $ni, ni+1, ni+2, \ldots, ni+n-1$. This gives a total of $n^2 - n$ cable cars for each company. Figure 6 shows the case for $n = 4$, with cars for A in bold, and cars for B dashed. It is clear that no car is linked by both companies: since any two cars linked

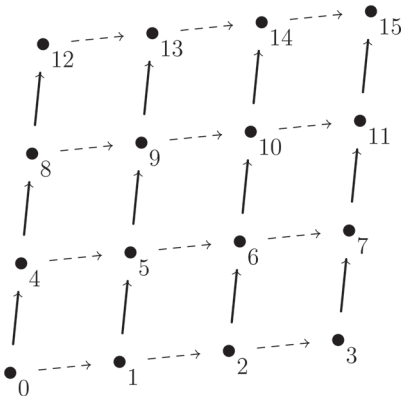

Figure 6 The case for $n = 4$ in Problem 4.

by A have indices differing by at least n, while any two cars linked by B have indices differing by at most $n-1$.

Finally, we prove that $k = n^2 - n + 1$ suffices. In the earlier proof of the lemma, we saw that a path from a vertex i to a vertex j must in fact pass through strictly increasing indices. This implies that G_A and G_B are acyclic — i.e., they are forests.

Now since G_A has n^2 vertices and k edges but no cycles, the number of connected components in G_A is exactly $n^2 - k = n^2 - (n^2 - n + 1) = n - 1$. By the pigeonhole principle, some connected component S of G_A has at least $\left\lceil \frac{n^2}{n-1} \right\rceil = n + 1$ vertices. On the other hand, G_B also has exactly $n-1$ connected components. So by the pigeonhole principle again, there are two vertices in S which lie in the same connected component of G_B. These two stations are therefore linked by both companies.

Problem 5 *Proposed by Oleg Košik, Estonia.* A deck of $n > 1$ cards is given. A positive integer is written on each card. The deck has the property that the arithmetic mean

of the numbers on each pair of cards is also the geometric mean of the numbers on some collection of one or more cards. For which n does it follow that the numbers on the cards are all equal?

Solution by Pravalika Putalapattu, 10th grade, Thomas Jefferson High School for Science and Technology, Alexandria, VA. We will prove that this assertion is true for all n.

Proceeding indirectly, let us assume that there exists some positive integer n and a set of cards labeled $a_1, a_2, \ldots, a_n$ that satisfy the above property, but are not all equal. We may assume without loss of generality that our cards are in decreasing order of their labels: $a_1 \geq a_2 \geq \cdots \geq a_n$. Note that multiplying all card values by some constant will multiply all arithmetic and geometric means by the same value. Thus, the property is preserved if we replace each label a_i with a_i/d, where $d = \gcd(a_1, a_2, \ldots, a_n)$. Therefore, we may assume without loss of generality that the n labels are relatively prime.

If $a_1 = 1$, then all a_i must equal 1, violating our assumption that not all a_i are equal. Thus, $a_1 \geq 2$. Let p be a prime divisor of a_1. Since $\gcd(a_1, a_2, \ldots, a_n) = 1$, there must be some a_i not divisible by p. Let k be the smallest index such that p does not divide a_k. Note that $a_k < a_1$.

Consider the arithmetic mean of a_1 and a_k, which we know is greater than a_k. This must equal some geometric mean, and thus $\frac{a_1+a_k}{2} = \sqrt[m]{a_{i_1} \cdots a_{i_m}}$ for some positive integer m and indices $i_1, \ldots, i_m$. In particular, $\sqrt[m]{a_{i_1} \cdots a_{i_m}} > a_k$.

Next, observe that since a_k is not divisible by p, none of $a_{i_1}, \ldots, a_{i_m}$ can be divisible by p either. Since k is the smallest index such that p does not divide a_k, each of $i_1, \ldots, i_m$ must be at least k, and therefore each of $a_{i_1}, \ldots, a_{i_m}$ must be at most a_k. But then their geometric mean is also at most a_k, resulting in a contradiction, as desired.

Problem 6 *Proposed by Ting-Feng Lin and Hung-Hsun Hans Yu, Taiwan.* Consider an integer $n > 1$ and a set $\mathcal{S}$ of n points in the plane such that the distance between any two different points in $\mathcal{S}$ is at least 1. Prove that there is a line ℓ separating $\mathcal{S}$ such that the distance from any point of $\mathcal{S}$ to ℓ is at least $cn^{-1/3}$ for some positive constant c. (A line ℓ separates a set of points S if some segment joining two points in $\mathcal{S}$ crosses ℓ.)

Solution by Gopal Krishna Goel, 11th grade, Krishna Homeschool, Portland, OR, and Jaedon Whyte, 10th grade, Archimedean Upper Conservatory, Miami, FL. We will show that there exists a line ℓ separating $\mathcal{S}$ such that the distance from any point in $\mathcal{S}$ to ℓ is at least $0.01 \cdot n^{-1/3}$.

Let $[\mathcal{P}]$ denote the area of a region $\mathcal{P}$ in the plane. We will need the following lemma.

Lemma. *Let $\mathcal{R}$ be an $a \times b$ rectangle in the plane, where $a, b \geq \frac{1}{2}$. Then $|\mathcal{S} \cap \mathcal{R}| \leq 20[\mathcal{R}]$.*

Proof. For each point P, let $\mathcal{D}_P$ denote the open disk of radius $\frac{1}{2}$ centered at P. Since $PQ \geq 1$ for all distinct $P, Q \in \mathcal{S}$, their respective disks $\mathcal{D}_P$ and $\mathcal{D}_Q$ cannot intersect.

Now, for any $P \in \mathcal{S} \cap \mathcal{R}$, we see that $\mathcal{D}_P \subseteq \mathcal{R}'$, where $\mathcal{R}'$ is an $(a+1) \times (b+1)$ rectangle with each side of $\mathcal{R}'$ a distance exactly $1/2$ from a side of $\mathcal{R}$. For the total area covered by the disks, we have

$$\sum_{P \in \mathcal{S} \cap \mathcal{R}} [\mathcal{D}_P] \leq [\mathcal{R}'] = |\mathcal{S} \cap \mathcal{R}| \cdot \frac{\pi}{4} = (a+1)(b+1).$$

Since $a, b \geq \frac{1}{2}$, we see that

$$\frac{(a+1)(b+1)}{ab} = \left(1+\frac{1}{a}\right)\left(1+\frac{1}{b}\right) \leq 3 \cdot 3 = 9.$$

Therefore,

$$|\mathcal{S} \cap \mathcal{R}| \leq \frac{4}{\pi}(a+1)(b+1) \leq \frac{36}{\pi}ab < 20[\mathcal{R}],$$

as desired. ■

Let A and B denote the two points in $\mathcal{S}$ such that AB is maximized (if there are multiple pairs, pick one arbitrarily), and let $r = AB$ be this maximum value. Let $\mathcal{T}$ denote the set of points P in the plane such that $\max(AP, BP) \leq r$. We see that $\mathcal{T}$ is simply the intersection of the disk centered at A with radius r and the disk centered at B with radius r, as shown in Figure 7. By definition, we must have $\mathcal{S} \subseteq \mathcal{T}$.

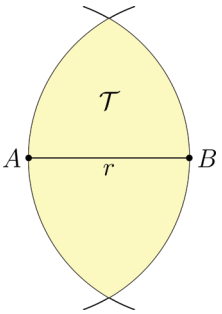

Figure 7 The set $\mathcal{T}$, highlighted in yellow.

We will first resolve the case $r \geq n^{2/3}$. Project all the points of $\mathcal{S}$ onto AB, and suppose they are $A = P_1, P_2, P_3, \ldots, P_n = B$, appearing in that order (it is possible that we may have $P_i = P_{i+1}$ for some values of i). Now, since

$$P_1P_2 + P_2P_3 + \cdots + P_{n-1}P_n = r,$$

we see that there exists some i such that

$$P_iP_{i+1} \geq \frac{r}{n-1} > r/n \geq n^{-1/3}.$$

Take ℓ to be the perpendicular bisector of P_iP_{i+1}. We see that the distance from any point $P \in \mathcal{S}$ to ℓ is simply the distance from the projection of P onto AB to the midpoint of P_iP_{i+1}, which is at least $\frac{1}{2}P_iP_{i+1} > \frac{1}{2}n^{-1/3}$, as desired. This resolves the case $r \geq n^{2/3}$.

We now turn our attention to the case $r < n^{2/3}$. Let XY be a chord of the circle centered at B with radius r such that $XY \perp AB$ and the distance from A to XY is $\frac{1}{2}$. Let M be its midpoint. Since $r = AB \geq 1$, we see that X and Y are on the arc of the circle centered at B with radius r that is a part of $\mathcal{T}$. The line XY divides $\mathcal{T}$ into two parts; let $\mathcal{T}'$ be the part containing A (see Figure 8). Note that $\mathcal{T}'$ can be contained in a rectangle of size $\frac{1}{2} \times XY$. By the Pythagorean theorem on $\triangle XMB$, we have

$$XY = 2\sqrt{r^2 - \left(r - \frac{1}{2}\right)^2} = 2\sqrt{r - \frac{1}{4}} < 2\sqrt{r} < 2n^{1/3},$$

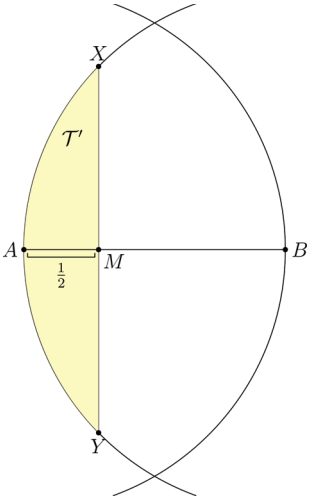

Figure 8 The set $\mathcal{T}'$ highlighted in yellow.

so by the lemma above, we see that

$$|\mathcal{T}' \cap \mathcal{S}| \leq 20 \cdot \frac{1}{2} \cdot |XY| < 20n^{1/3}.$$

Similar to before, let $Q_1 = A, Q_2, Q_3, \ldots, Q_{|\mathcal{T}' \cap \mathcal{S}|}$ denote the projections of the points of $\mathcal{T}' \cap \mathcal{S}$ onto segment AB, in that order.

If A is the only point of S in $\mathcal{T}'$, then we take our line as the perpendicular bisector of line AM. So assume $|\mathcal{T}' \cap \mathcal{S}| \geq 2$. Since all points Q_i lie in a segment of length $\frac{1}{2}$, there must be some i such that

$$Q_i Q_{i+1} \geq \frac{\frac{1}{2}}{|\mathcal{T}' \cap \mathcal{S}| - 1} > \frac{1}{2|\mathcal{T}' \cap \mathcal{S}|} > \frac{1}{40} n^{-1/3}.$$

We may now take ℓ to be the perpendicular bisector of $Q_i Q_{i+1}$, and as before, the distance from any point of $\mathcal{S}$ to ℓ is at least $\frac{1}{80} n^{-1/3} > 0.01 n^{-1/3}$, as desired. This completes the solution.

Summary. We present the problems and solutions to the 61st Annual International Mathematical Olympiad.

BÉLA BAJNOK (MR Author ID: 314851) is a professor of mathematics at Gettysburg College, Gettysburg, PA. He is the Director of the American Mathematics Competitions program of the MAA.

EVAN CHEN (MR Author ID: 1158569) is a graduate student at the Massachusetts Institute of Technology, Cambridge, MA. He is the Assistant Academic Director of the Math Olympiad Program of the MAA.

The Sum of the Reciprocals of Pandigital Numbers

EDUARDO SÁENZ DE CABEZÓN
Universidad de La Rioja
26006 Logroño, Spain
eduardo.saenz-de-cabezon@unirioja.es

JUAN LUIS VARONA
Universidad de La Rioja
26006 Logroño, Spain
jvarona@unirioja.es

It is well known that the harmonic series

$$\sum_{n=1}^{\infty} \frac{1}{n} = 1 + \frac{1}{2} + \frac{1}{3} + \frac{1}{4} + \cdots$$

diverges. In 1914, A. J. Kempner [3] proved that if the denominators include only those numbers which do not contain the digit 9, then the series converges. (Of course, the same can be done with any other digit, and using a base different from ten.) This is somewhat surprising because Kempner's series seems to have most of the summands of the harmonic series. Thus, at first sight, Kempner's series should be also divergent.

However, the demonstration of its convergence is simple: there are 8 one-digit numbers not containing the digit 9, the smallest of which is 1; $8 \cdot 9$ two-digit numbers not containing the digit 9, the smallest of which is 10; $8 \cdot 9^2$ three digit numbers not containing the digit 9, the smallest of which is 100; and so on. Therefore, the sum of the reciprocals of the positive integers not containing the digit 9 is less than

$$8 \cdot 1 + \frac{8 \cdot 9}{10} + \frac{8 \cdot 9^2}{10^2} + \cdots = \frac{8}{1 - \frac{9}{10}} = 80.$$

A more precise estimation for the sum of Kempner's series can be found in [1].

In a given base of numeration, a pandigital number is an integer in which any digit used in the base appears at least once. At the first sight, and without further reflection, our patterns with small numbers in the usual base ten says that very few numbers are pandigital, and thus that the series of the reciprocals of pandigital numbers

$$\sum_{p \text{ pandigital}} \frac{1}{p} \tag{1}$$

should also be convergent.

But, again, our first intuition fails (it is worth recalling the "strong law of small numbers," see Guy [2], that can be formulated as "there aren't enough small numbers to meet the many demands made of them," which describes the problem of determining if a mathematical pattern observed for small positive integers will persist). Actually, the divergence of (1) can be proved as a consequence of the convergence of Kempner's series.

Math. Mag. **94** (2021) 213–214. doi:10.1080/0025570X.2021.1926878
MSC: 40A05

Let us take W_j (for $j = 0, 1, \ldots, 9$, if we use base ten) the set of positive integers without digit j. If n is not a pandigital number, then $n \in W_j$ for some j. Then,

$$\sum_{n \text{ not-pandigital}} \frac{1}{n} \leq \sum_{n \in W_0} \frac{1}{n} + \sum_{n \in W_1} \frac{1}{n} + \cdots + \sum_{n \in W_9} \frac{1}{n} < \infty$$

due to the convergence of Kempner's series, and thus (1) diverges.

We can also give an easy proof of the divergence of (1) that is independent of Kempner's result. In base ten, take $a = 1{,}234{,}567{,}890$. Then, all the numbers

$$n = 10^{10} r + a,$$

with $r \in \mathbb{N} \cup \{0\}$, are pandigital. Consequently, and because $a/10^{10} \leq 1$,

$$\begin{aligned} \sum_{n \text{ pandigital}} \frac{1}{n} &\geq \sum_{r=0}^{\infty} \frac{1}{10^{10} r + a} \\ &= \frac{1}{10^{10}} \sum_{r=0}^{\infty} \frac{1}{r + a/10^{10}} \\ &\geq \frac{1}{10^{10}} \sum_{r=0}^{\infty} \frac{1}{r+1} = \infty. \end{aligned}$$

The same proof applies in any base b taking the corresponding a and using 10^{10} with its meaning b^b in base b.

REFERENCES

[1] Baillie, R. (1979). Sums of reciprocals of integers missing a given digit. *Amer. Math. Monthly.* 86(5): 372–374. doi.org/10.1080/00029890.1979.11994810

[2] Guy, R. K. (1988). The strong law of small numbers. *Amer. Math. Monthly*. 95(8): 697–712. doi.org/10.1080/00029890.1988.11972074

[3] Kempner, A. J. (1914). A curious convergent series. *Amer. Math. Monthly.* 21(2): 48–50. doi.org/10.1080/00029890.1914.11998004

Summary. We show that the sum of the reciprocals of pandigital numbers is divergent.

EDUARDO SÁENZ DE CABEZÓN (MR Author ID: 875028) received his Ph.D. from the Universidad de La Rioja (Spain) in 2008 and is an associate professor at the university. He combines research in computer algebra with an intense work in mathematics popularization. Has written several popular math books, runs the YouTube channel "Derivando" and is the conductor of the national television science show *Órbita Laika*.

JUAN LUIS VARONA (MR Author ID: 260232) received his degree in mathematical sciences from the Universidad de Zaragoza in 1985 and his Ph.D. from the Universidad de Cantabria (Spain) in 1988. He is a full professor at the Universidad de La Rioja (Spain), a region that is known for its wines. He enjoys TEX/LATEX and currently he serves as editor-in-chief of *La Gaceta de la Real Sociedad Matemática Española*.

PROOFS WITHOUT WORDS

Pythagorean Triples and $\pi/4$

ROGER B. NELSEN
Lewis & Clark College
Portland, OR 97219
nelsen@lclark.edu

Theorem 1. *If a, b, and c are positive real numbers such that $a^2 + b^2 = c^2$, then*

$$\frac{\pi}{4} = \arctan\left(\frac{a}{b+c}\right) + \arctan\left(\frac{b}{a+c}\right).$$

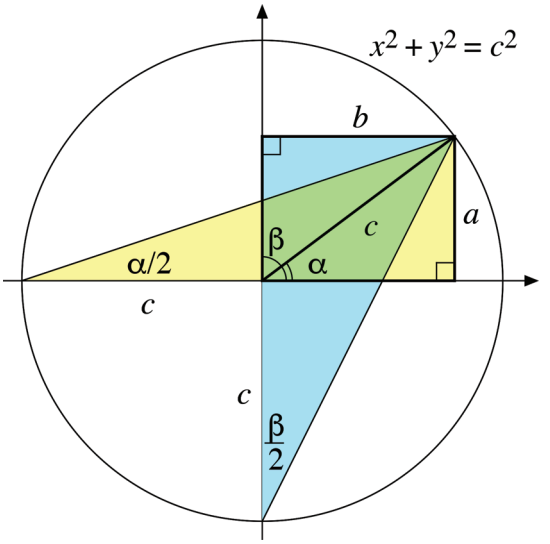

Proof.

$$\frac{\alpha}{2} = \arctan\left(\frac{a}{b+c}\right) \qquad \frac{\beta}{2} = \arctan\left(\frac{b}{a+c}\right),$$

$$\alpha + \beta = \frac{\pi}{2} \Longrightarrow \arctan\left(\frac{a}{b+c}\right) + \arctan\left(\frac{b}{a+c}\right) = \frac{\pi}{4}.$$

■

When a, b, and c are positive integers, (a, b, c) is a *Pythagorean triple*, and hence the theorem relates the triples to $\pi/4$.

Math. Mag. **94** (2021) 225–226. doi:10.1080/0025570X.2021.1908787

Examples

$$(a, b, c) = (3, 4, 5): \qquad \frac{\pi}{4} = \arctan\frac{1}{2} + \arctan\frac{1}{3}.$$

Visual proofs of this result have been previously published by Harris [1] and Wu [4,5].

$$(a, b, c) = (5, 12, 13): \qquad \frac{\pi}{4} = \arctan\frac{2}{3} + \arctan\frac{1}{5};$$

$$(a, b, c) = (8, 15, 17): \qquad \frac{\pi}{4} = \arctan\frac{1}{4} + \arctan\frac{3}{5};$$

$$(a, b, c) = (12, 35, 37): \qquad \frac{\pi}{4} = \arctan\frac{1}{6} + \arctan\frac{5}{7};$$

$$(a, b, c) = (20, 21, 29): \qquad \frac{\pi}{4} = \arctan\frac{2}{5} + \arctan\frac{3}{7}.$$

Exercise Observe that in each of the examples, the expression for $\pi/4$ has the form

$$\frac{\pi}{4} = \arctan\left(\frac{m}{n}\right) + \arctan\left(\frac{n-m}{n+m}\right)$$

for appropriate positive integers m and n. Show that this is always the case. [Hint: Use Euclid's formula for Pythagorean triples.] Visual proofs of this expression for $\pi/4$ appear in Kandall [2] and Nelsen [3].

Acknowledgment The author wishes to thank an anonymous reviewer and the Editor for helpful comments and suggestions on an earlier draft of this note.

REFERENCES

[1] Harris, E. M. (1987). Behold! Sums of arctan. *College Math. J.* 18(2): 141. doi.org/10.1080/07468342.1987.11973025
[2] Kandall, A. K. (2002). Mathematics without words. *College Math. J.* 33(1): 13.
[3] Nelsen, R. B. (2003). Mathematics without words. *College Math. J.* 34(1): 10.
[4] Wu, R. H. (2004). Arctangent identities. *College Math. J.* 34(2): 115, 138.
[5] Wu, R. H. (2004). Proof without words: Euler's arctangent identity. *Math. Mag.* 77(3): 189. doi.org/10.1080/0025570X.2004.11953249

Summary. We use the arctangent function and Pythagorean triples to derive expressions for $\frac{\pi}{4}$.

ROGER B. NELSEN (MR Author ID 237909) is a professor emeritus at Lewis & Clark College, where he taught mathematics and statistics for 40 years.

Three Segments on the Diagonal of a Square

VICTOR OXMAN
Western Galilee College
Acre, Israel
victor.oxman@gmail.com

MOSHE STUPEL
Shaanan Academic College
Haifa, Israel
stupel@bezeqint.net

Theorem 1. *Suppose that F and E lie on the diagonal BD of a square $ABCD$ and that $\angle FAE = 45°$. Then $BF^2 + ED^2 = FE^2$.*

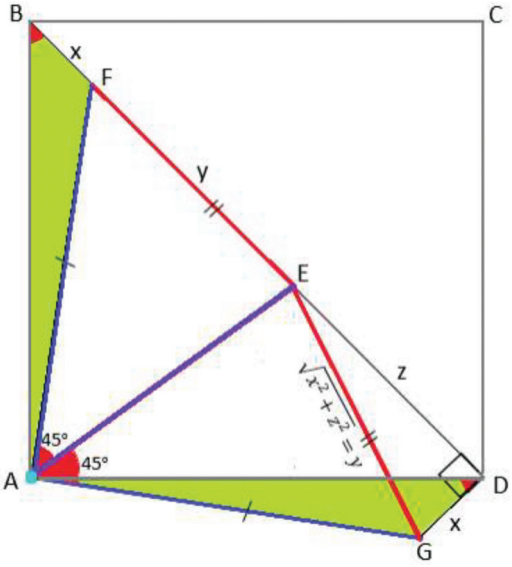

Triangle ADG is obtained from triangle ABF by a 90° clockwise rotation around A (implying that $B \to D$ and $F \to G$). Since $\angle EAG = \angle EAF = 45°$, then triangles FAE and GAE are congruent.

Summary. We present a visual proof for an elegant property of three segments on the diagonal of a square.

VICTOR OXMAN (MR Author ID 756975) is a professor of mathematics and mathematical education at Western Galilee College, Acre, Israel. His areas of research includes the geometry of the triangle, geometric inequalities, approaches in the teaching of mathematics, and using investigative potentialities of dynamic geometry environments (DGEs).

MOSHE STUPEL (MR Author ID: 1028564) is a professor of mathematical education at Gordon College and Shaanan College, Haifa, Israel. His research deals with the existing attributes of different geometric shapes. He has extensive experience in the study of dynamic properties using computers. He also deals with finding different solutions to the same problem by combining different mathematical tools.

Math. Mag. **94** (2021) 227. doi:10.1080/0025570X.2021.1908786

PROBLEMS

LES REID, *Editor*
Missouri State University

EUGEN J. IONAŞCU, *Proposals Editor*
Columbus State University

RICHARD BELSHOFF, Missouri State University; *MAHYA GHANDEHARI*, University of Delaware; *EYVINDUR ARI PALSSON*, Virginia Tech; *GAIL RATCLIFF*, Eastern Carolina University; *ROGELIO VALDEZ*, Centro de Investigación en Ciencias, UAEM, Mexico; *Assistant Editors*

Proposals

To be considered for publication, solutions should be received by November 1, 2021.

2121. *Proposed by Seán M. Stewart, Bomaderry, Australia.*

Evaluate

$$\int_0^{\frac{1}{2}} \frac{\arctan(x)}{x^2 - x - 1}\, dx.$$

2122. *Proposed by Ahmad Sabihi, Isfahan, Iran.*

Let

$$G(m, k) = \max\{\gcd((n+1)^m + k, n^m + k) | n \in \mathbb{N}\}.$$

Compute $G(2, k)$ and $G(3, k)$.

2123. *Proposed by Albert Natian, Los Angeles Valley College, Valley Glen, CA.*

An urn contains n balls. Each ball is labeled with exactly one number from the set

$$\{a_1, a_2, \cdots, a_n\}, \qquad a_1 > a_2 > \cdots > a_n,$$

(so no two balls have the same number). Balls are randomly selected from the urn and discarded. At each turn, if the number on the ball drawn was the largest number remaining in the urn, you win the dollar amount of that ball. Otherwise, you win nothing. Find the expected value of your total winnings after n draws.

Math. Mag. **94** (2021) 228–238. doi:10.1080/0025570X.2021.1909344

We invite readers to submit original problems appealing to students and teachers of advanced undergraduate mathematics. Proposals must always be accompanied by a solution and any relevant bibliographical information that will assist the editors and referees. A problem submitted as a Quickie should have an unexpected, succinct solution. Submitted problems should not be under consideration for publication elsewhere.

Proposals and solutions should be written in a style appropriate for this MAGAZINE.

Authors of proposals and solutions should send their contributions using the Magazine's submissions system hosted at `http://mathematicsmagazine.submittable.com`. *More detailed instructions are available there. We encourage submissions in PDF format, ideally accompanied by LaTeX source. General inquiries to the editors should be sent to* `mathmagproblems@maa.org`.

2124. *Proposed by Mircea Merca, University of Craiova, Craiova, Romania.*

For a positive integer n, prove that

$$\sum_{\substack{\lambda_1+\lambda_2+\cdots+\lambda_k=n \\ \lambda_1\geqslant\lambda_2\geqslant\ldots\geqslant\lambda_k>0}} (-1)^{n-\lambda_1} \frac{\binom{\lambda_1}{\lambda_2}\binom{\lambda_2}{\lambda_3}\cdots\binom{\lambda_k}{0}}{1^{\lambda_1}2^{\lambda_2}\cdots k^{\lambda_k}} = \frac{1}{n!},$$

where the sum runs over all the partitions of n.

2125. *Proposed by Freddy Barrera, Colombia Aprendiendo, and Bernardo Recamán, Universidad Sergio Arboleda, Bogotá, Colombia.*

Given a collection of positive integers, not necessarily distinct, a graph is formed as follows. The vertices are these integers and two vertices are connected if and only if they have a common divisor greater than 1. Find an assignment of ten positive integers totaling 100 that results in the graph shown below.

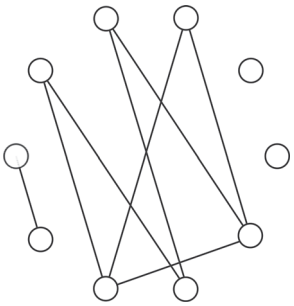

Quickies

1111. *Proposed by George Stoica, Saint John, NB, Canada.*

Prove that for $A, B \in M_2(\mathbb{C})$, the following conditions are equivalent:

(i) $|\det(A+\lambda B)| = |\det(A-\lambda B)|$ for all $\lambda \in \mathbb{C}$

(ii) $\operatorname{tr}(AB) = \operatorname{tr}(A)\cdot\operatorname{tr}(B)$ or $\det A = \det B = 0$.

1112. *Proposed by Lokman Gökçe, Istanbul, Turkey.*

Let $\triangle ABC$ be any triangle with $m\angle BAC = 150^\circ$. Let $\triangle ABE$ and $\triangle ACD$ be equilateral triangles whose interiors lie in the exterior of $\triangle ABC$. Denote the intersection of the segments $\overline{BD}$ and $\overline{CE}$ by F. Prove that $FA + FE + FD = BC$.

Solutions

The number of isosceles triangles in various polytopes — June 2020

2096. *Proposed by H. A. ShahAli, Tehran, Iran.*

Any three distinct vertices of a polytope P form a triangle. How many of these triangles are isosceles if P is (a) a regular n-gon? (b) one of the Platonic solids? (c) an n-dimensional cube?

Solution by Robert Calcaterra, University of Wisconsin-Platteville, Platteville, WI.
Let m denote the number of vertices of P. For a fixed vertex A of P, let $F(P)$ denote the number of unordered triplets of distinct vertices A, B, and C of P for which $AB = AC$, $G(P)$ is the number of such triplets for which $AB = AC = BC$, and $I(P)$ the number of isosceles triangles that can be formed using the vertices of P. Note that since all of the polytopes under consideration are uniform, $F(P)$ and $G(P)$ do not depend on A. Since each equilateral triangle is counted in $F(P)$ for three different choices of A,

$$I(P) = m\left(F(P) - G(P)\right) + \frac{m}{3}G(P) = mF(P) - \frac{2}{3}mG(P).$$

(a) If P is a regular n-gon, then $F(P) = \lfloor (n-1)/2 \rfloor$. Moreover, $G(P) = 1$ if n is a multiple of 3 and $G(P) = 0$ if not. Therefore,

$$I(P) = \begin{cases} n\left\lfloor \frac{n-1}{2} \right\rfloor & \text{if } 3 \nmid n \\ n\left\lfloor \frac{n-1}{2} \right\rfloor - \frac{2n}{3} & \text{if } 3 | n \end{cases}$$

(b) Let P be a Platonic solid. If A and B are vertices of P, the minimum number of edges of the solid that must be traversed to get from A to B will be called the span from A to B. For the Platonic solids, the spans for two pairs of vertices are the same if and only if the Euclidean distances are the same.

- If P is a tetrahedron, every triplet of distinct vertices forms an isosceles (in fact, equilateral) triangle. Therefore $I(P) = \binom{4}{3} = 4$.
- If P is a cube, then the numbers of vertices with spans 1, 2, and 3 from the fixed vertex A are 3, 3, and 1, respectively. Therefore, $F(P) = \binom{3}{2} + \binom{3}{2} = 6$. Moreover, 0 pairs of the vertices with span 1 from A have span 1 from each other, and 3 pairs with span 2 from A have span 2 from each other. Thus $G(P) = 3$ and $I(P) = 8 \cdot 6 - \frac{2}{3} \cdot 8 \cdot 3 = 32$. (This also follows from part (c) below).
- If P is an octahedron, every triplet of distinct vertices forms an isosceles triangle. Therefore $I(P) = \binom{6}{3} = 20$.
- If P is an icosahedron, then the numbers of vertices with spans 1, 2, and 3 from the fixed vertex A are 5, 5, and 1, respectively. Therefore, $F(P) = \binom{5}{2} + \binom{5}{2} = 20$. Moreover, 5 pairs of the vertices with span 1 from A have span 1 from each other, and 5 pairs with span 2 from A have span 2 from each other; thus $G(P) = 10$ and $I(P) = 12 \cdot 20 - \frac{2}{3} \cdot 12 \cdot 10 = 160$.
- If P is a dodecahedron, then the numbers of vertices with spans 1, 2, 3, 4, and 5 from A are 3, 6, 6, 3, and 1, respectively. So, $F(P) = \binom{3}{2} + \binom{6}{2} + \binom{6}{2} + \binom{3}{2} = 36$. Moreover, 0 pairs of vertices with span 1 from A have span 1 from each other, 3 pairs with span 2 from A have span 2 from each other, 6 pairs

with span 3 from A have span 3 from each other, and 0 pairs with span 4 from A have span 4 from each other; thus, $G(P) = 9$ and $I(P) = 20 \cdot 36 - \frac{2}{3} \cdot 20 \cdot 9 = 600$.

(c) Let P be a cube in $\mathbb{R}^n$. We may view the vertices of P as binary n-tuples, so that the distance between two vertices is the square root of the number of components at which they differ. The number of vertices of P at distance $\sqrt{k}$ from A is $\binom{n}{k}$ for $k = 0, 1, \ldots, n$. Recall that

$$\sum_{k=0}^{n} \binom{n}{k} = 2^n \text{ and } \sum_{k=0}^{n} \binom{n}{k}^2 = \binom{2n}{n}.$$

Therefore,

$$\begin{aligned} F(P) &= \sum_{k=1}^{n-1} \frac{1}{2}\binom{n}{k}\left(\binom{n}{k} - 1\right) = \frac{1}{2}\left(\sum_{k=1}^{n-1}\binom{n}{k}^2 - \sum_{k=1}^{n-1}\binom{n}{k}\right) \\ &= \frac{1}{2}\left(\left(\binom{2n}{n} - 2\right) - (2^n - 2)\right) \\ &= \frac{1}{2}\left(\binom{2n}{n} - 2^n\right) \end{aligned}$$

For the vertices A, B, and C to form an equilateral triangle with sides of length $\sqrt{k}$, three disjoint subsets, say X, Y, and Z, must be chosen from $\{1, 2 \ldots, n\}$ in such a way that the components of A differ from those of B at precisely the positions in $X \cup Y$, the components of A differ from those of C at precisely the positions in $X \cup Z$, and the components of B differ from those of C at precisely the positions in $Y \cup Z$. This forces $|X \cup Y| = |X \cup Z| = |Y \cup Z| = k$, which yields $|X| = |Y| = |Z| = \ell$ and $k = 2\ell$. There will be $n - 3\ell$ positions at which the components of A, B, and C all agree (the positions in the complement of $X \cup Y \cup Z$). Note that each equilateral triangle will be generated twice using this procedure because interchanging Y and Z will reverse the roles of B and C. Therefore (using multinomial coefficients), we have

$$G(P) = \frac{1}{2}\sum_{\ell=1}^{\lfloor n/3 \rfloor} \binom{n}{n-3\ell, \ell, \ell, \ell} \text{ and}$$

$$I(P) = 2^{n-1}\left(\binom{2n}{n} - 2^n\right) - \frac{2^n}{3}\sum_{\ell=1}^{\lfloor n/3 \rfloor} \binom{n}{n-3\ell, \ell, \ell, \ell}$$

Also solved by Allen J. Schwenk, Albert Stadler (Switzerland), and the proposer. There were two incomplete or incorrect solutions.

A series involving the floor, ceiling, and round functions **June 2020**

2097. *Proposed by Omran Kouba, Higher Institute for Applied Sciences and Technology, Damascus, Syria.*

For a real number $x \notin \frac{1}{2} + \mathbb{Z}$, denote the nearest integer to x by $\langle x \rangle$. For any real number x, denote the largest integer smaller than or equal to x and the smallest integer

larger than or equal to x by $\lfloor x \rfloor$ and $\lceil x \rceil$, respectively. For a positive integer n let

$$a_n = \frac{2}{\langle \sqrt{n} \rangle} - \frac{1}{\lfloor \sqrt{n} \rfloor} - \frac{1}{\lceil \sqrt{n} \rceil}.$$

(a) Prove that the series $\sum_{n=1}^{\infty} a_n$ is convergent and find its sum L.

(b) Prove that the set

$$\left\{ \sqrt{n}\left(\sum_{k=1}^{n} a_k - L\right) : n \geq 1 \right\}$$

is dense in $[0, 1]$.

Solution by Hongwei Chen, Christopher Newport University, Newport News, VA.

(a) We show that the sum converges to zero. To see this, first, we can easily check the following facts:

$$\langle \sqrt{n} \rangle = k, \text{for } n \in [k(k-1)+1, k(k+1)],$$
$$\lfloor \sqrt{n} \rfloor = k, \text{for } n \in [k^2, (k+1)^2),$$
$$\lceil \sqrt{n} \rceil = k+1, \text{for } n \in (k^2, (k+1)^2].$$

These imply that $a_{k^2} = 0$ and

$$a_n = \frac{2}{k} - \frac{1}{k} - \frac{1}{k+1} = \frac{1}{k(k+1)}, \text{ for } n \in (k^2, k(k+1)],$$
$$a_n = \frac{2}{k+1} - \frac{1}{k} - \frac{1}{k+1} = -\frac{1}{k(k+1)}, \text{ for } n \in (k(k+1), (k+1)^2).$$

Therefore, for $k^2 \leq n \leq (k+1)^2$, we have $\sum_{m=1}^{k^2} a_m = 0$ and

$$0 \leq \sum_{m=1}^{n} a_m \leq \frac{1}{k(k+1)} \cdot [k(k+1) - k^2] = \frac{1}{k+1}$$

As $n \to \infty$, we have $k \to \infty$ and so

$$\sum_{n=1}^{\infty} a_n = \lim_{n\to\infty} \sum_{m=1}^{n} a_m = 0.$$

(b) Let $x \in [0, 1]$. We show that there exists a subsequence from the set $\{\sqrt{n} \sum_{m=1}^{n} a_m\}$, which converges to x. Notice that there exist two integer sequences p_k and q_k with $0 \leq p_k \leq q_k$ such that $p_k/q_k \to x$, as $k \to \infty$. Let $n_k = q_k^2 + p_k$. Then

$$q_k^2 \leq n_k \leq q_k^2 + q_k < \left(q_k + \frac{1}{2}\right)^2.$$

This implies that

$$\langle \sqrt{n_k} \rangle = q_k, \ \lfloor \sqrt{n_k} \rfloor = q_k, \ \lceil \sqrt{n_k} \rceil = q_k + 1.$$

Therefore, as $k \to \infty$, we have

$$\sqrt{n_k} \sum_{m=1}^{n_k} a_m = \sqrt{n_k} \cdot \frac{n_k - q_k^2}{q_k(q_k+1)} = \frac{p_k}{q_k} \cdot \frac{\sqrt{n_k}}{q_k+1} \to x.$$

This proves that the set $\{\sqrt{n} \sum_{m=1}^{n} a_m\}$ is dense in $[0, 1]$.

Also solved by Elton Bojaxhiu (Germany) & Enkel Hysnelaj (Australia), Brian Bradie, Robert Calcaterra, Dmitry Fleischman, Maxim Galushka (UK), GWstat Problem Solving Group, Eugene A. Herman, Walter Janous (Austria), Donald E. Knuth, Sushanth Sathish Kumar, Elias Lampakis (Greece), Shing Hin Jimmy Pa (Canada), Allen Schwenk, Albert Stadler (Switzerland), and the proposer. There was one incorrect or incomplete solution.

A zigzag sequence of random variables **June 2020**

2098. *Proposed by Albert Natian, Los Angeles Valley College, Valley Glen, CA.*

Let $Z_0 = 0$, $Z_1 = 1$, and recursively define random variables $Z_2, Z_3, \ldots$, taking values in $[0, 1]$ as follows: For each positive integer k, Z_{2k} is chosen uniformly in $[Z_{2k-2}, Z_{2k-1}]$, and Z_{2k+1} is chosen uniformly in $[Z_{2k}, Z_{2k-1}]$.

Prove that, with probability 1, the limit $Z^* = \lim_{n\to\infty} Z_n$ exists and find its distribution.

Solution by Northwestern University Math Problem Solving Group, Northwestern University, Evanston, IL.

We will prove:

1. The limit Z^* exists.
2. The limit Z^* has probability density $f(x) = 2x$ on $[0, 1]$.

Proof of 1. We have that $[Z_0, Z_1] \supseteq [Z_2, Z_1] \supseteq [Z_2, Z_3] \supseteq [Z_4, Z_3] \supseteq \ldots$ is a sequence of nested closed intervals. By the nested interval theorem, their intersection will be non-empty, and will consist of a unique point precisely if the sequence of lengths of the nested intervals tends to zero. We prove that this happens with probability 1.

Let I_n ($n = 0, 1, 2, , \ldots$) be the nth interval in the sequence, and L_n = length of I_n, i.e., $L_{2k} = Z_{2k+1} - Z_{2k}$ and $L_{2k+1} = Z_{2k+1} - Z_{2k+2}$. Pick $\delta > 0$. We will prove by induction that the probability of $L_n > \delta$ is $P(L_n > \delta) \le (1-\delta)^n$. Since $P(L_n > 1) = 0$ the result is trivially true for $\delta \ge 1$, so we may assume $1 > \delta > 0$.

Base case: For $n = 0$ the inequality $P(L_0 > \delta) \le (1-\delta)^0$ obviously holds because $L_0 = 1$, hence $P(L_0 > \delta) = P(1 > \delta) = 1$ and $(1-\delta)^0 = 1$.

Induction step: Assume $P(L_n > \delta) \le (1-\delta)^n$. Then

$$P(L_{n+1} > \delta) = P(L_n \le \delta) \cdot P(L_{n+1} > \delta \mid L_n \le \delta) + P(L_n > \delta) \cdot P(L_{n+1} > \delta \mid L_n > \delta).$$

Note that the first term is zero because if $L_n \le \delta$ then $L_{n+1} > \delta$ is impossible. On the other hand, if $L_n > \delta$ then we only have $L_{n+1} > \delta$ if the next endpoint Z_{n+2} is selected at a distance less than $L_n - \delta$ from the right or left (depending on the parity of n) endpoint of I_n. The probability is

$$P(L_{n+1} > \delta \mid L_n > \delta) = \frac{L_n - \delta}{L_n} = 1 - \frac{\delta}{L_n} \le 1 - \delta.$$

Hence

$$P(L_{n+1} > \delta) \le (1-\delta)^n(1-\delta) = (1-\delta)^{n+1},$$

and this completes the induction.

From here we get $\lim_{n\to\infty} P(L_{n+1} > \delta) = 0$ for every $\delta > 0$, hence $L_n \to 0$ as $n \to \infty$ with probability 1.

Proof of 2. For each $n \geq 0$ define the new random variable U_n, chosen between Z_{2n} and Z_{2n+1} with probability density

$$f_{U_n|Z_{2n}=z_n, Z_{2n+1}=z_{2n+1}}(x) = \frac{2(x - z_{2n})}{(z_{2n+1} - z_{2n})^2}$$

on $[z_{2n}, z_{2n+1}]$, where "$U_n|Z_{2n} = z_{2n}, Z_{2n+1} = z_{2n+1}$" means the random variable U_n given $Z_{2n} = z_{2n}$ and $Z_{2n+1} = z_{2n+1}$ (we ignore the case $z_{2n+1} = z_{2n}$ because its probability is zero).

Since U_n is between Z_{2n} and Z_{2n+1}, its limit U^* will coincide with Z^*.

Next, we will prove by induction that for every $n \geq 0$, the probability density of U_n is always the same, namely $f_{U_n}(x) = 2x$ on $[0, 1]$.

Base case: For $n = 0$ we have $Z_0 = 0$, $Z_1 = 1$, hence $f_{U_0}(x) = \dfrac{2(x - 0)}{(1 - 0)^2} = 2x$ on $[0, 1]$.

Induction step: Assume $f_{U_n}(x) = 2x$. Next, note that U_{n+1} is defined like U_n but with starting points Z_2 and Z_3 in place of Z_0 and Z_1. So, U_{n+1} given $Z_2 = z_2$ and $Z_3 = z_3$ is just U_n mapped from $[0, 1]$ to $[z_2, z_3]$ with the transformation $(z_3 - z_2)U_n + z_2$. By induction hypothesis we have $f_{U_n}(x) = 2x$, and its transformation to $[z_2, z_3]$ will have probability density

$$f_{U_{n+1}|Z_2=z_2, Z_3=z_3}(x) = \frac{2(x - z_2)}{(z_3 - z_2)^2}$$

on $[z_2, z_3]$.

The cumulative distribution function of U_{n+1} is $F_{U_{n+1}}(x) = P(U_{n+1} \leq x)$. By definition U_{n+1} must be in the interval $[Z_2, Z_3]$, while x may be in any of two different intervals, namely $[U_{n+1}, Z_3)$ or $[Z_3, 1]$. So, the event $U_{n+1} \leq x$ can be expressed as the union of $Z_2 \leq Z_3 \leq x$ and $Z_2 \leq U_{n+1} \leq x < Z_3$. Since they are disjoint we have

$$P(U_{n+1} \leq x) = P(Z_2 \leq Z_3 \leq x) + P(Z_2 \leq U_{n+1} \leq x < Z_3)\,.$$

We have that X_2 is random uniform on $[0, 1]$, and X_3 is random uniform on $[Z_2, 1]$, so

$$f_{Z_3|Z_2=z_2}(x) = \frac{1}{1 - z_2},$$

hence

$$P(Z_2 \leq Z_3 \leq x) = \int_0^x \frac{x - z_2}{1 - z_2}\, dz_2 = x + (1 - x)\log(1 - x)\,.$$

The second term can be computed as follows:

$$\begin{aligned} P(Z_2 \leq U_{n+1} \leq x < Z_3) &= \int_0^x \int_x^1 \int_{z_2}^x f_{U_{n+1}|Z_2=z_2, Z_3=z_3}(t)\, f_{Z_3|Z_2=z_2}(x)\, dt\, dz_3\, dz_2 \\ &= \int_0^x \int_x^1 \int_{z_2}^x \frac{2(t - z_2)}{(z_3 - z_2)^2} \frac{1}{1 - z_2}\, dt\, dz_3\, dz_2 \\ &= (x - 1)(x + \log(1 - x))\,, \end{aligned}$$

hence

$$F_{U_{2n+1}}(x) = x + (1-x)\log(1-x) + (x-1)(x + \log(1-x)) = x^2\,.$$

Differentiating we get $f_{U_{2n+1}}(x) = 2x$ on $[0, 1]$, and this completes the induction.

Since the distribution of U_n is the same for every n we have that the limit U^* will have the same distribution too. And since $U^* = Z^*$, the same will hold for Z^*, hence $f_{Z^*}(x) = 2x$.

Also solved by Robert A. Agnew, Elton Bojaxhiu (Germany) & Enkel Hysnelaj (Australia), Robert Calcaterra, Shuyang Gao, John C. Kieffer, Omran Kouba (Syria), Kenneth Schilling, and the proposer.

An almost linear functional equation **June 2020**

2099. *Proposed by Russ Gordon, Whitman College, Walla Walla, WA and George Stoica, Saint John, NB, Canada.*

Let r and s be distinct nonzero rational numbers. Find all functions $f : \mathbb{R} \to \mathbb{R}$ that satisfy

$$f\left(\frac{x+y}{r}\right) = \frac{f(x) + f(y)}{s}$$

for all real numbers x and y.

Solution by Eugene A. Herman, Grinnell College, Grinnell, IA.

Clearly the zero function is always a solution and, when $s = 2$, all constant functions are solutions. We show that there are no others. First assume $s \neq 2$. Substituting 0 for both x and y yields $f(0) = 0$. Substituting $y = 0$ and $y = -x$ yield these two identities:

$$f\left(\frac{x}{r}\right) = \frac{f(x)}{s}, \quad f(-x) = -f(x) \quad \text{for all } x \in \mathbb{R}.$$

Given any $x \in \mathbb{R}$, we use induction to show that $f(nx) = nf(x)$ for all $n \in \mathbb{N}$. The base case is a tautology. If $f(nx) = nf(x)$ for some $n \in \mathbb{N}$, then

$$\frac{f((n+1)x)}{s} = f\left(\frac{(n+1)x}{r}\right) = f\left(\frac{nx+x}{r}\right) = \frac{f(nx) + f(x)}{s} = \frac{(n+1)f(x)}{s}$$

and so $f((n+1)x) = (n+1)f(x)$. It follows that $f(x/n) = f(x)/n$ for all $n \in \mathbb{N}$ and hence that $f((m/n)x) = (m/n)f(x)$ for all $m, n \in \mathbb{N}$. Since $f(-x) = -f(x)$, this last statement is also true for m negative. Choose m, n so that $r = n/m$. Therefore

$$\frac{f(x)}{s} = f\left(\frac{x}{r}\right) = \frac{f(x)}{r}$$

and so $f(x) = 0$.

Now assume $s = 2$, and let $t = 2/r$. Thus $t \neq 1$ and

$$f\left(\frac{t}{2}(x+y)\right) = \frac{f(x) + f(y)}{2}, \quad \text{for all } x, y \in \mathbb{R}.$$

Substituting $y = x$ and $y = -x$ yield

$$f(tx) = f(x), \quad \frac{f(x) + f(-x)}{2} = f(0) \quad \text{for all } x \in \mathbb{R}.$$

Thus $f(-x/t) = f(-x)$, and so

$$f\left(\frac{t-1}{2}\,x\right) = f\left(\frac{t}{2}(x - x/t)\right) = \frac{f(x) + f(-x/t)}{2} = \frac{f(x) + f(-x)}{2} = f(0).$$

Therefore f is a constant function.

Also solved by Michel Bataille (France), Elton Bojaxhiu (Germany) & Enkel Hysnelaj (Australia), Paul Budney, Robert Calcaterra, Walther Janous (Austria), Sushanth Sathish Kumar, Omran Kouba (Syria), Elias Lampakis (Greece), Albert Natian, Kangrae Park (South Korea), Kenneth Schilling, Jacob Siehler, Albert Stadler (Switzerland), Michael Vowe (Switzerland), and the proposers.

Two congruent triangles on the sides of an arbitrary triangle **June 2020**

2100. *Proposed by Yevgenya Movshovich and John E. Wetzel, University of Illinois, Urbana, IL.*

Given $\triangle ABC$ and an angle θ, two congruent triangles $\triangle ABP$ and $\triangle QAC$ are constructed as follows: $AQ = AB$, $BP = AC$, $m\angle ABP = m\angle CAQ = \theta$, B and Q are on opposite sides of $\overleftrightarrow{AC}$, and C and P are on opposite sides of $\overleftrightarrow{AB}$, as shown in the figure. Let X, Y, and Z be the midpoints of segments AP, BC, and CQ, respectively.

Show that $\angle XYZ$ is a right angle.

Solution by Sushanth Sathish Kumar (student), Portola High School, Irvine, CA.

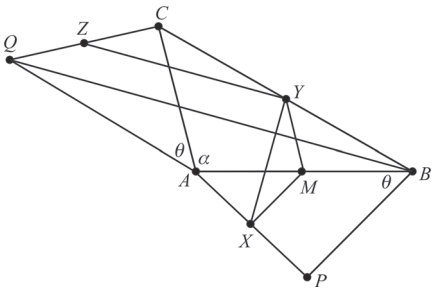

Let M be the midpoint of segment AB. Note that $\overline{YZ}$ is a midline of triangle CBQ, and so $\overleftrightarrow{BQ}$ is parallel to $\overleftrightarrow{YZ}$. Thus, it suffices to show that $\overleftrightarrow{XY}$ is perpendicular to $\overleftrightarrow{BQ}$.

Since $\overline{MX}$ and $\overline{MY}$ are midlines of triangles APB and ABC, we have that $MX = BP/2 = AC/2 = MY$. Hence, triangle MXY is isosceles. Moreover, since $\overleftrightarrow{MX} || \overleftrightarrow{BP}$ and $\overleftrightarrow{MY} || \overleftrightarrow{AC}$, we have

$$m\angle XMY = m\angle XMA + m\angle AMY = \theta + 180^\circ - \alpha,$$

where we set $\alpha = m\angle BAC$. It follows that $m\angle MXY = m\angle XYM = (\alpha - \theta)/2$.

We wish to calculate $m\angle(\overleftrightarrow{XM}, \overleftrightarrow{BQ})$, where $m\angle(\ell_1, \ell_2)$ denotes the measure of the non-obtuse angle between ℓ_1 and ℓ_2. Note that

$$m\angle(\overleftrightarrow{XM}, \overleftrightarrow{BQ}) = m\angle PBQ = m\angle PBA + m\angle ABQ.$$

Since $AB = AQ$ and $m\angle BAQ = \alpha + \theta$, we find that $m\angle ABQ = 90^\circ - (\alpha + \theta)/2$. Thus, $m\angle(\overleftrightarrow{XM}, \overleftrightarrow{BQ}) = 90^\circ - (\alpha - \theta)/2$. But since $m\angle(\overleftrightarrow{MX}, \overleftrightarrow{XY}) = (\alpha - \theta)/2$, we find that $m\angle(\overleftrightarrow{BQ}, \overleftrightarrow{XY}) = 90^\circ$, and we are done.

Also solved by Michel Bataille (France), Elton Bojaxhiu (Germany) & Enkel Hysnelaj (Australia), Robert Calcaterra, Prithwijit De (India), J. Chris Fisher, Dmitry Fleischman, Fresno State Problem Solving Group, Marty Getz & Dixon Jones, Eugene Herman, Walther Janous (Austria), Elias Lampakis (Greece), Kee-Wai Lau (Hong Kong), Graham Lord, Elizabeth Mika, Albert Natian, Celia Schacht, Volkhard Schindler (Germany), Albert Stadler (Switzerland), Michael Vowe (Switzerland) and the proposers.

Answers

Solutions to the Quickies from page 229.

A1111. The implication (ii)⇒(i) follows immediately from

$$\det(A+\lambda B)=\lambda^2\det B+\lambda(\operatorname{tr}A\operatorname{tr}B-\operatorname{tr}(AB))+\det A,\ \lambda\in\mathbb{C}.$$

Conversely, suppose that (i) holds. Let

$$a_\lambda=\lambda^2\det B+\det A\ \text{ and }\ b=\operatorname{tr}A\operatorname{tr}B-\operatorname{tr}(AB).$$

Then (i) can be rewritten as $|a_\lambda+\lambda b|^2=|a_\lambda-\lambda b|^2,\ \lambda\in\mathbb{C}$, which is equivalent to

$$\operatorname{Re}(\lambda b\overline{a_\lambda})=0,\ \lambda\in\mathbb{C}. \tag{1}$$

If we put $\lambda=n, n\in\mathbb{N}$, in (1), we get

$$\operatorname{Re}(nb(n^2\,\overline{\det B}+\overline{\det A}))=0,\ n\in\mathbb{N},$$

that is,

$$\operatorname{Re}(b\,\overline{\det A})=-n^2\operatorname{Re}(b\,\overline{\det B}),\ n\in\mathbb{N},$$

from which it follows that $\operatorname{Re}(b\,\overline{\det B})=0$, and hence $\operatorname{Re}(b\,\overline{\det A})=0$.

If we put $\lambda=in\ n\in\mathbb{N}$, in (1), we get $\operatorname{Re}(inb(-n^2\,\overline{\det B}+\overline{\det A}))=0,\ n\in\mathbb{N}$, that is,

$$\operatorname{Im}(b\,\overline{\det A})=n^2\operatorname{Im}(b\,\overline{\det B}),\ n\in\mathbb{N},$$

from which it follows that $\operatorname{Im}(b\,\overline{\det B})=0$, and hence $\operatorname{Im}(b\,\overline{\det A})=0$.

Consequently, $b\,\overline{\det A}=b\,\overline{\det B}=0$, and therefore $b=0$ or $\det A=\det B=0$, so condition (ii) holds.

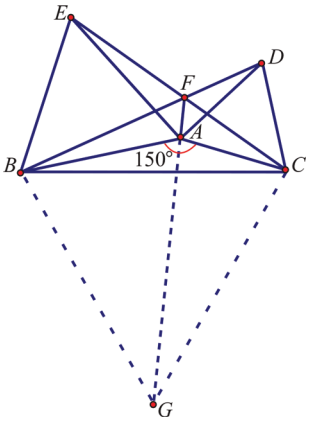

A1112. Construct an equilateral triangle BCG whose interior lies in the exterior of $\triangle ABC$. It is well known that $\overleftrightarrow{AG}$, $\overleftrightarrow{BD}$, and $\overleftrightarrow{CE}$ are concurrent at F and the measure of the angle between any two adjacent lines is $60°$.

Since $m\angle AFE = 120°$, $m\angle ABE = 60°$, $m\angle AFD = 120°$, $m\angle ACD = 60°$, $m\angle BFC = 120°$, and $m\angle BGC = 60°$, we see that $ABEF$, $ACDF$, and $BFCG$ are cyclic quadrilaterals. By Ptolemy's theorem,

$$FE + FA = FB, FD + FA = FC, \quad \text{and} \quad FB + FC = FG = FA + AG.$$

Therefore

$$2FA + FE + FD = FB + FC = FA + AG.$$

Since $2m\angle BAC + m\angle BGC = 360°$, G is the circumcenter of $\triangle ABC$. Hence $AG = GB = BC$. Thus,

$$2FA + FE + FD = FA + BC$$

and we have $FA + FE + FD = BC$ as desired.

Erratum

In the December 2020 issue of this MAGAZINE, we ran a note entitled "When Two Wrongs Make a Right," by Leonard Van Wyk. It has since become clear that the main content of this note had appeared previously in the following publications:

- Brannen, N. S., Ford, B. (2004). Logarithmic Differentiation: Two Wrongs Make a Right. *College Math. J.* 35(5): 388–390.
- Bilodeau, G. E. (1993). An Exponential Rule. *College Math. J.* 24(4): 350–351.

Both Dr. Van Wyk and the Editor offer their sincere apologies to these authors for having been unaware of their work. We thank Gerry Bilodeau for bringing these predecessors to our attention.

Math. Mag. **94** (2021) 238. doi:10.1080/0025570X.2021.1911210

A1112. Construct an equilateral triangle BCG whose interior lies in the exterior of $\triangle ABC$. It is well known that $\overleftrightarrow{AG}$, $\overleftrightarrow{BD}$, and $\overleftrightarrow{CE}$ are concurrent at F and the measure of the angle between any two adjacent lines is $60°$.

Since $m\angle AFE = 120°$, $m\angle ABE = 60°$, $m\angle AFD = 120°$, $m\angle ACD = 60°$, $m\angle BFC = 120°$, and $m\angle BGC = 60°$, we see that $ABEF$, $ACDF$, and $BFCG$ are cyclic quadrilaterals. By Ptolemy's theorem,

$$FE + FA = FB, FD + FA = FC, \quad \text{and} \quad FB + FC = FG = FA + AG.$$

Therefore

$$2FA + FE + FD = FB + FC = FA + AG.$$

Since $2m\angle BAC + m\angle BGC = 360°$, G is the circumcenter of $\triangle ABC$. Hence $AG = GB = BC$. Thus,

$$2FA + FE + FD = FA + BC$$

and we have $FA + FE + FD = BC$ as desired.

Erratum

In the December 2020 issue of this MAGAZINE, we ran a note entitled "When Two Wrongs Make a Right," by Leonard Van Wyk. It has since become clear that the main content of this note had appeared previously in the following publications:

- Brannen, N. S., Ford, B. (2004). Logarithmic Differentiation: Two Wrongs Make a Right. *College Math. J.* 35(5): 388–390.
- Bilodeau, G. E. (1993). An Exponential Rule. *College Math. J.* 24(4): 350–351.

Both Dr. Van Wyk and the Editor offer their sincere apologies to these authors for having been unaware of their work. We thank Gerry Bilodeau for bringing these predecessors to our attention.

Math. Mag. **94** (2021) 238. doi:10.1080/0025570X.2021.1911210

REVIEWS

PAUL J. CAMPBELL, *Editor*
Beloit College

Assistant Editor: Eric S. Rosenthal, West Orange, NJ. Articles, books, and other materials are selected for this section to call attention to interesting mathematical exposition that occurs outside the mainstream of mathematics literature. Readers are invited to suggest items for review to the editors.

Bolker, Ethan D., and Maura B. Mast, *Common Sense Mathematics*, 2nd ed., MAA Press, 2021; xx + 342 pp, $75(P). ISBN 978-1-4704-6134-8.

I wrote a relatively lengthy short review of the first edition (2016) of this book (This Magazine 89 (4) 301). This second edition adds more-recent examples and exercises, derived from "news of the day" involving numerical concepts. Topics include back-of-the-envelope estimation, conversion of units, percentages, inflation, income distribution, reading a credit card bill, climate change, exponential growth, lotteries, coincidences, and disease screening. Arithmetic is applied, spreadsheets are introduced, and no algebra is used. Spreadsheets and extra exercises are available online, as are an instructor's manual and a solutions manual (already available at internet sites that cater to students). The first edition has been used for a quantitative reasoning course at some universities. "Common sense mathematics," with its practical utility for citizenship, is too important to be reserved for college—it needs to be in high school.

Nahin, Paul J., *Hot Molecules, Cold Electrons: From the Mathematics of Heat to the Development of the Trans-Atlantic Telegraph Cable*, Princeton University Press, 2020; xiii + 212 pp, $24.95. ISBN 978-0-691-19172-0.

Author Nahin may be familiar from his previous books, among them *Inside Interesting Integrals* and *Will You Be Alive Ten Years from Now?*, which featured calculations about fascinating problems in mathematics and probability. Here he turns to his background and interests as an electrical engineer. The wonderful key idea in this book, originally due to William Thomson (Lord Kelvin), is that the mathematics for the flow of electricity in a telegraph cable is the same as that of Fourier's equation for the flow of heat. Nahin develops all the Fourier series and other mathematical theory needed in a conversational way, but the reader needs fluency in calculus and—above all—interest in heat diffusion and electrical circuits. A surprise to me was how slow the transmission speed was through the copper wire, unlike the fiber-optic cables today.

The Ramanujan Machine: Using algorithms to discover new mathematics, http://www.ramanujanmachine.com/.

Raayoni, Gal, et al., Generating conjectures on fundamental constants with the Ramanujan Machine, *Nature* 590 (7844) (3 February 2021) 67–73.

Persiflage: The Ramanujan Machine is all hype, https://www.galoisrepresentations.com/2019/07/17/the-ramanujan-machine-is-an-intellectual-fraud/; Ramanujan Machine redux, https://www.galoisrepresentations.com/2021/02/11/ramanujan-machine-redux/.

Researchers at Haifa University have implemented a body of artificial intelligence algorithms, which they call the Ramanujan Machine, that try to discover new mathematical formulas for mathematical constants, such as π, e, and Catalan's constant. The algorithms investigate only continued fraction formulas, do so by matching numerical values to many decimal places, and do not provide proofs. Not all mathematicians are enthusiastic, as evidenced by the blogs by a number theorist objecting to the self-promotion and claiming that nothing new has emerged.

Math. Mag. **94** (2021) 239–240. doi:10.1080/0025570X.2021.1909342

Weltan, Anna, *Supermath: The Power of Numbers for Good and Evil*, Johns Hopkins University Press, 2020; xii + 220 pp, $24.95. ISBN 978-1-4214-3819-1.

This book for a popular audience centers around mathematics involved in attempting to solve the problems of communicating across cultures (New Guinea body counting, Babylonian Plimpton 322, Peruvian quipus), winning games (checkers, Prisoner's Dilemma, altruism in epidemics), eliminating bias in algorithms (recidivism, the secretary problem, voting districts), inequity in mathematics education (Ramanujan, remedial courses), and perceiving beauty in mathematics (Burnside's lemma, the Pythagorean theorem, hyperbolic geometry). The book's title is a little over the top, but the essays are worthwhile reads that are thought-provoking. Equations appear only in a proof of the Pythagorean theorem that relies on similar triangles and algebra, which is dubbed "ugly" in comparison to a visual geometric proof.

Counterman, Elijah D., and Sean D. Lawley, What should patients do if they miss a dose of medication? A probabilistic analysis, https://arxiv.org/pdf/2102.05442.pdf.

Not taking medicine as prescribed causes annually more than 100,000 deaths and $100 billion in avoidable costs in the U.S. This paper devises a mathematical model for drug level in a patient who misses doses, based on the drug half-life t_h, prescribed interval τ between doses, and randomly missed doses. To keep the concentration in the body within therapeutic limits and avoid toxic levels, the conclusions for missing a dose are: If $t_h \ll \tau$, just take the regular dose at the next scheduled time; if $t_h \approx \tau$, take 1.5 doses then; if $t_h \gg \tau$, take the missed dose as soon as possible or else a double dose at the next scheduled time. (Disclaimer: This is not medical advice; consult your doctor. Anyway, do you know the half-life of any of the medicines that you take?) The authors apply the model to hypothyroid patients taking levothyroxine.

Bryan, Kurt, *Differential Equations: A Toolbox For Modeling the World*, Draft Version 0.55, SIMIODE, 2021; 442 pp, $45(PDF). Final release, 15 May 2021. Current version available free for consideration of adoption for use in teaching, from Director@simiode.org.

I have taught differential equations many times, always needing to supplement the textbook with modeling exercises and examples with real data. This textbook-in-progress puts those aspects at the forefront. For example, it begins with modeling Usain Bolt's 2008 Olympic 100-meter sprint, to which it returns several times later as it refines the model. The book draws on a large library of modeling projects available from SIMIODE (Systemic Initiative for Modeling Investigations and Opportunities with Differential Equations), which offers instructors the opportunity to communicate ideas, as well as to contribute and download free class materials, for teaching differential equations. The book features "Reading Exercises" interspersed in the text, with routine exercises at the ends of sections and modeling projects at the ends of chapters. The usual topics are covered: first- and second-order ODEs, numerical methods, Laplace transforms, and systems, with PDEs, Fourier series, and boundary value problems to be added later. Strengths of the book include consideration of nondimensionalization, concentration on parameter estimation, and realism (e.g., determining a drug administration schedule that considers the practicalities of dose denomination and scheduling). With a few exceptions, the situations modeled are from physical science. Solution techniques are practiced enough by exercises; despite the many opportunities offered in the book, students can always use more practice in modeling.

Teixeira, Ricardo V., and Jang-Woo Park, *Mathemagics: A Magical Journey Through Advanced Mathematics*, World Scientific, 2020; xix + 385 pp, $48(P). ISBN 978-981-121-530-8.

This delightful book connects mathematical concepts in a dozen areas to magic tricks. Expositions of the mathematics precede description and analysis of the tricks. The expositions are too short for in-depth learning; the intent is to give sophomores a taste of the content and ideas of later mathematics courses. Each chapter features exercises on the mathematics, and students can have fun practicing the tricks.